Source Apportionment of Carbonaceous Aerosols Using Integrated Multi-Variant and Source Tracer Techniques and a Unique Molecular Marker Data Set

Report Version 4.0

Contract Number 07-333

Principal Investigator:
James J. Schauer
University of Wisconsin-Madison

Co-Principal Investigator:
Costas Sioutas
University of Southern California

May, 2012

Prepared for the
California Air Resources Board and
the California Environmental Protection Agency

DISCLAIMER

The statements and conclusions in this Report are those of the contractor and not necessarily those of the California Air Resources Board. The mention of commercial products, their source, or their use in the connection with material reported herein is not to be construed as actual or implied endorsement of such products.

ACKNOWLEDGEMENT

This report was submitted in fulfillment of ARB Contract number 07-333, Source Apportionment of Carbonaceous Aerosols Using Integrated Multi-Variant and Source Tracer Techniques and a Unique Molecular Marker Data Set by the University of Wisconsin-Madison under the partial sponsorship of the California Air Resources Board. Work was completed on January 15, 2012.

TABLE OF CONTENTS

List of Appendices (Separate Electronic Documents)

LIST OF FIGURES

LIST OF TABLES

ABSTRACT

Four hundred fine particulate matter samples from two sites in the Los Angeles Basin were analyzed for molecular marker source tracers, and the results were used in three source apportionment models to obtain daily, monthly and the annual average source contributions to fine particle organic carbon (OC). Good agreement between the source contribution from mobile sources and biomass burning for the chemical mass balance (CMB) model and the positive matrix factorization (PMF) models were obtained and provide additional weight of evidence that these source apportionment techniques aresufficiently accurate for policy development. However, the CMB model did not quantify primary biogenic emissions, which were quantified by the PMF model, and were included in other sources with secondary organic carbon (SOC) in the CMB model. The PMF apportionment results demonstrate seasonal patterns in the split between SOC and primary organic carbon (POC), which emphasize the biases that can result from previous short term intensive studies used to represent the annual average source contributions as well as source contributions in other seasons than those examined. The PMF model also provided new insight into the differences in composition and impacts of forest fires and high wintertime wood burning events. PMF and a second multi-variant receptor model (UNMIX) were unable to separate source contributions from diesel and gasoline engines. However, a new multi-variant receptor model, Interactive Confirmatory Factor Analysis (ICFA) was able to separate mobile sources into diesel, gasoline and smoking engines.

EXECUTIVE SUMMARY

Background

Molecular marker source apportionment models have been applied in the LA Basin in the past, but only two such studies have been implemented that address the seasonal trends and annual average source contributions to fine particle matter organic carbon (OC) and these studies were based on samples collected in 1982 and 1993. In recent years there has been a number of PM2.5 source apportionment studies conducted in the LA Basin, but most are based on short-term,intensive studies that do not provide a good estimate of seasonal trends and averages. Some of these studies have estimated that secondary organic carbon (SOC) contributes up to 75% of the organic aerosol, which is inconsistent with earlier annual average estimates. Additionally, two multi-year studies conducted in the LA Basin in the mid-2000s were unable to provide reliable estimatesof SOC.

In the past several years, laboratory and pilot studies have been conducted that raise questions about the utility of specific molecular markers and offer new opportunities for molecular marker chemical mass balance (CMB) studies. The current study provides a contemporary assessment of OC sources in the LA Basin and provides a unique data set to further evaluate and test molecular marker CMB apportionment models. It further demonstrates the added information that can be obtained with a molecular marker PMF model.

Methods

As part of this project, daily carbonaceous aerosol measurements were obtained for a full year at a site in Central Los Angeles,whichincludes fine particulate matter (PM2.5), elemental and organic carbon (ECOC), PM2.5 water-soluble organic carbon (WSOC), PM2.5 water-soluble inorganic carbon, PM2.5 water-soluble organic nitrogen (WSON), and 100 particle-phase organic compounds often referred to as molecular markers. Parallel measurements were conductedover the same time period every sixth day at a site in Riverside. The results were used to examine seasonal and spatial trends and were used in four receptor models: CMB, Positive Matrix Factorization (PMF), UNMIX, and Interactive Confirmatory Factor Analysis (ICFA). The comparison of the source apportionment models was focused on the CMB and PMF results. ICFA was used in conjunction with UNMIX to assess its ability to provide a split between emissions from gasoline and diesel engines. The entire measurement data set is provided with this report to allow other researchers to examine additional trends and utilize the data for new and more advanced source apportionment models.

Results

Four hundred fine particulate matter samples from two sites in the LA Basin were analyzed for molecular marker source tracers, and the results were used in four source apportionment models (MM-CMB, MM-PMF, MM-UNMIX, and MM-ICFA) to obtain daily, monthly and annual average source contributions to fine particle organic carbon (OC).

Southern California experiences a number of days with very high OC concentrations that result from local biomass burning, forest fires, and secondary organic aerosols. During the one year sampling program, thirteen days had OC concentrations greater than 8.0 µg per cubic meter of OC, which equates to approximately14-16 µg per cubic meter of organic compounds with an assumed organic mass to organic compound ratio of 1.75-2.0 [*Bae et al.*, 2006]. Of thesethirteen days, eight were determined to be high wood smoke days, three were impacted by forest fires, and only two of these days were not associated with forest fires or high wood smoke events. Although forest fires can be considered outside the scope of local air quality regulation,

the extreme events due to residential wood burning need to be better tracked and mitigatedin Southern California. These occasional emission events can be challenging for speciation models to correctly allocate.

On an annual average, the MM-CMB and MM-PMF models show good agreement for the contribution of mobile sources and biomass smoke to PM2.5 OC of 30% and 10%, respectively. However, the remaining 60% of the OC was distributed differently in the two models. MM-CMB modeling results show that SOC dominates the remaining OC, while on an annual average the MM-PMF model shows 40% of the remaining OC is from SOC and 20% from primary biogenic material (e.g. forest fires and food cooking). It is important to note that the primary biogenic source, which peaks in days with large forest fires, is very different from the biomass burning source. The SOC estimates from the MM-PMF model were in good agreement with non-biomass burning water soluble organic carbon (WSOC), which has been shown to be a robust estimate of SOC. In addition, the MM-CMB model was able to quantify vegetative detritus, which was only a very small component of the primary biogenic source.

Although the total mobile source contribution is similar between both models, the split between gasoline and diesel engine exhaust emissions within the mobile source contribution is important to better understand. A key finding of the DOE Gasoline/Diesel PM Split study (http://www.nrel.gov/vehiclesandfuels/nfti/feat_split_study.html) was that the CMB modeling split between gasoline and diesel engine exhaust emissions is very sensitive to the input profiles used in the CMB model but the total mobile source contribution was reasonably stable. Similar results were seen in the current study and the multi-variant receptor models (MM-CMB and MM-PMF) were used to further investigate the drivers of model sensitivity. In the current study, MM-CMB, MM-PMF and two additional receptor models (MM-UNMIX and MM-ICFA) were investigated as a means to split the mobile source contributions between gasoline and diesel engines. All showed good agreement for contribution from mobile sources but only MM-ICFA was able to differentiate gasoline and diesel emissions. Although it is not possible to fully evaluate the accuracy of the MM-ICFA split between gasoline and diesel emissions at this time, the results demonstrate a potential new strategy to understand the relative contributions of gasoline and diesel emissions to organic aerosol concentrations. Previous MM-CMB models have differentiated tailpipe emissions from diesel engines, gasoline engines and smoking engines with the use of EC, hopanes, steranes and polycyclic aromatic hydrocarbons (PAH) as tracers. The current study demonstrated with principal component analysis (PCA) and MM-PMF that PAH concentrations in the LA Basin are significantly impacted by biomass burning as well as tailpipe emissions.

The PMF model demonstrates a seasonal trend in SOC concentrations, with its maximum contribution to OC in April of about 73% and a minimum in December of approximately 21%. The MM-PMF model identified two SOC sources with different seasonal trends. One of the SOC sources, which had more biogenic components, dominated SOC concentrations in winter and spring. The second SOC source, which had more anthropogenic components, was higher in the late spring and summer. In late spring and summer, the anthropogenic SOC constituted approximately 51-68% of the total SOC and from December through March, it only contributed approximately 17-21% of the total SOC in Central LA. SOC products of isoprene oxidation were much greater in the springtime, which has also been observed in other regions.

Trends in water-soluble organic nitrogen (WSON) at both sites were compared with trends in water-soluble inorganic nitrogen (Nx), OC, WSOC, and source contribution factors derived from the MM-PMF model. WSON typically represented about 20% of the total water-soluble

nitrogen (TN) at both sites but a few events were observed in winter months in which WSON made up more than 50% of the TN. While WSON was significantly correlated with Nx across nearly all seasons at both sites, correlations between the MM-PMF SOC source contribution factors were only significant during summer and winter months, suggesting divergent sources of secondary organic nitrogen may contribute to WSON concentrations.

In summary, the MM-PMF modeling is able to better apportion SOC, and the CMB model is biased as it includes primary biogenic emissions with SOA. The MM-PMF apportionment results demonstrate seasonal patterns in the split between SOC and primary OC, which were not previously shown because of the short-term intensive nature of previous studies. The resultsdemonstratethe importance of this unique year-long data set. The MM-PMF model also provided new insight into the differences in composition and impacts of forest fires and high wintertime wood burning events. However, all the studied receptor models were unable to separate PM source contributions between diesel and gasoline engines.

Overall this study demonstrates: 1) the importance of year-long data sets toaccurately quantify OC emissions and source apportionment, particularly seasonal trends, 2) source apportionment techniques are sufficiently accurate for policy development but model results vary substantially for some source categories, and 3) the diesel and gasoline exhaust PM2.5 split remains difficult to accurately quantify but new models have the potential of improving the split between gasoline and diesel emissions.

Conclusion

The current study provides a comprehensive and updated source apportionment analysis of the organic aerosols in the LA Basin. The study demonstrates that past source apportionment results from short,intensive studies are not able to represent the annual average source contributions and the seasonal trends. This study demonstrates the bias of current molecular marker CMB model estimates of SOC, which result from the inability of the models to accurately represent primary biogenic materials. The PMF results of the study are able to effectively capture a lumped primary biogenic source which includes forest fires. However, additional research is needed to better trace these sources since together they account for approximately20% of the PM2.5 OC in the LA Basin. The three multi-variant models used in the study were unable to separate the mobile source contributions to gasoline/diesel subcategories, but the data generated in the study provide a unique data set to further test new multi-variant receptor models in the future.

PROJECT REPORT

1. Introduction

Historically, source apportionment models for atmospheric particulate matter have been directed at understanding the sources of particle mass to support regulatory compliance efforts [*Kim et al.*, 2010]. The monitoring and modeling efforts of these traditional source apportionment models have been optimized to allow sufficient understanding of the key sources of particulate matter but are not well suited for understanding the source of specific components of atmospheric particulate matter [*Christensen and Schauer*, 2008]. As health studies are demonstrating that carbonaceous particulate matter and specific components of carbonaceous particulate matter concentrations in the atmosphere are linked with adverse health outcomes and adverse health indicators [*Delfino et al.*, 2010a, 2010b; *Janssen et al.*, 2011], there is a need to better understand the sources of organic and elemental carbon in atmospheric particulate matter as well as the specific components of particulate matter carbon that have been linked to adverse health effects.

Molecular markers andparticle-phase organic compounds that have specificity for air pollution source emissions were originally used for source apportionment in the Los Angeles Basin in the 1990s [*Schauer et al.*, 2002, 1996]. These original models relied heavily on Chemical Mass Balance (CMB) models that require source profiles whichshould be representative of local sources. Since their development, the application of molecular marker CMB models has been widely adoptedthroughout the US and in other regions of the world for atmospheric particulate matter source apportionment. They have been used in a number of health studies to apportion personal exposure to particulate matter [*Delfino et al.*, 2010b; *Spira-Cohen et al.*, 2011] and there is a great need to assess the accuracy and identify the limitations of molecular marker usage for source apportionment.

Two concerns about molecular marker CMB models have been raised in the past several years: 1) the source profiles used in the studies are not representative of local sources, and 2) the molecular markers used in the model are not stable enough in the atmosphere to be used as tracers. There have been a number of studies that have partially addressed these concerns,including sensitivity analyses [*Lough and Schauer*, 2007; *Rutter et al.*, 2011; *Sheesley et al.*, 2007] and intercomparison studies [*Bhave et al.*, 2007; *Docherty et al.*, 2008]. Independent laboratory studies suggest some key molecular markers are not sufficiently stable in the atmosphere, while field based assessment of molecular marker source apportionment models suggests that the models are accurate enough to support health studies and the development of control strategies[*Robinson et al.*, 2006a, 2006b, 2006c]. Nonetheless, given the importance of carbonaceous aerosols for human health, climate change and compliance with air quality standards, there is additional need to evaluate molecular markers and their use in source apportionment models.

An important strategy to evaluate molecular marker source apportionment models and the sources and stability of molecular markers is to directly compare molecular marker CMB model results with those from a multi-variant receptor model, utilizing the same molecular marker dataset. This allows a comparison of the sources apportionment results as well as a direct comparison of the sources of key tracers. However, to perform such an analysis, a very large data set of molecular markers is required. The first analysis of this nature was conducted in St. Louis, MO using data obtained from the US EPA Midwest Supersite [*Jaeckels et al.*, 2007]. In

the St. Louis analysis, Positive Matrix Factorization (PMF) was used as the multi-variant source receptor model and demonstrated there were a number of local industrial and point sources of fine particle organic carbon not captured by the CMB analysis and the source profile for resuspended road dust was not representative of local sources. The point sources adversely impacted the source attribution of vegetative detritus, but good agreement between the two models was observed for the apportionment of mobile sources and biomass burning. Given the results in the St. Louis Molecular Marker study, there has been great interest in conducting a similar study in the Los Angeles Basin to confirm the absence of local and industrial sources of organic aerosols, to further study the abilities of molecular marker source apportionment models to quantify mobile sources, biomass smoke, secondary organic aerosol, and to distinguish the contributions from diesel and gasoline engines.

In the past decade, there have been a few source apportionment studies conducted in the Los Angeles Basin that have been directed at understanding the seasonal and annual average sources of fine particulate matter [*Kim et al.*, 2010; *SCAQMD*, 2008], but neither of these studies quantified secondary organic aerosol and therefore provide limited insight into the annual average and seasonal trends in organic aerosols. The current study seeks to advance the use of molecular markers for source apportionment and provide a more contemporary assessment of the source of fine particulate organic matter in the Los Angeles Basin.

2. Materials and Methods

2.1 Sample Collection

Integrated 24-hour PM2.5 samples were collected on an every-day schedule at the Universityof Southern California (USC) in Central Los Angeles and on a 1-in-6 day schedule at the University of California in Riverside (UCR), as a site downwind of the LA Basin, from May 2009 through April 2010. PM2.5 samples were collected on pre-baked 90 mm quartz-fiber filters (Pall Gellman, Ann Arbor, MI) at each site by a URG-3000B medium volume sampler (URG, Chapel Hill, NC) equipped with 92 lpm PM2.5 cyclones. The sites selected for the project have been used for a large number of atmospheric aerosol studies in the past. The Riverside site was located at the Air Pollution Research Center (APRC) on the University of California-Riverside campus (33°58′18.40″N, 117°19′21.41″W), and the Central LA site was located at the Particle Instrumentation Unit (PIU) on the campus of the University of Southern California (34° 1'9.12"N, 118°16'38.41"W).

Samples were collected from midnight to midnight PST. Sampler flow rates were controlled by needle valves and measured before and after sample collection using a calibrated rotameter. After sample collection, samples were shipped in insulated coolers with blue ice to the Wisconsin State Laboratory of Hygiene and stored at or below -5° C until analyzed. Field blanks were collected at both sites by loading filters into the samplers and unloading without sample collection to account for any contamination associated with filter handling. The field blanks were handled and analyzed in the same manner as the samples to allow for blank corrections for all chemical measurements.

2.2 Chemical Analysis

All samples and field blanks were analyzed at the Wisconsin State Laboratory of Hygiene for organic carbon (OC), elemental carbon (EC), water-soluble organic carbon (WSOC), and organic molecular marker compounds by gas chromatography mass spectrometry (GCMS). Organic markers included n-alkanes, cycloalkanes, alkanoic acids, resin acids, aromatic diacids, alkanedioic acids, steranes, hopanes, PAHs, oxy-PAHs, phtalalates, and levoglucosan. In addition, samples collected at the Central LA and the Riverside sites on the 1-in-6 schedule were analyzed for water-soluble nitrogen (TN) and water-soluble inorganic nitrogen (N_x). All data was blank corrected using the measurements from the field blank samples. Uncertainties were estimated using the standard deviation of field blanks and the analytical uncertainty. Details of these methods are provided below.

Water insoluble organic carbon (WIOC) was calculated as the difference between OC and WSOC. Water-soluble organic nitrogen was calculated as the difference between TN and water-soluble inorganic nitrogen, which was estimated as nitrate ion plus ammonium ion.

2.2.1 Elemental and Organic Carbon (ECOC)

Samples and field blanks were analyzed for organic carbon (OC) and elemental carbon (EC) using the ACE-Asia method [*Schauer et al.*, 2003] and a thermal-optical analyzer (Sunset Labs, Tigard, OR). A 1.5 cm^2punch was used for the ECOC analysis.

2.2.2 Water Soluble Carbon and Water Soluble Organic Nitrogen

Samples and blanks were analyzed for water-soluble organic carbon (WSOC) and water-soluble nitrogen (TN) content by extracting a 1.5 cm^2 punch from each filter. Filter punches were placed

in acid-washed centrifuge tubes along with purified water and agitated on a shaker table for two hours at room temperature. Samples were then filtered through an acid-washed, 0.2 μm polypropylene syringe filter and split into 2 aliquots. One aliquot was analyzed for organic carbon and total nitrogen using a Shimadzu TOC-5000A total organic carbon analyzer, which utilizes a high temperature combustion technique [*Wangersky,* 1993] coupled with a Shimadzu TNM-1 chemiluminescence detector and the second aliquot was analyzed for water soluble ions.

2.2.3 Water Soluble Ions

Water-soluble inorganic nitrogenwas measured using a LachatAutoanalyzer (Lachat Instruments, Milwaukee, WI). Water-soluble organic nitrogen (WSON) was calculated as the difference between total water-soluble nitrogen and inorganic nitrogen (WSON = TN – Nx).

2.2.4 Molecular Marker Analysis

Half of each 90mm quartz filter sample and blank filter was placed separately into soxhlet tubes, which were attached to 500mL receiving flasks. Each sample was then spiked with 100μL of internal standard: pyrene-D10, benz(a)anthracene-D12, coronene-D12, cholestane-D4, pentadecane D32, eicosane-D42, tetracosane-D50, triacontane-D62, dotriacontane-D66, hexatriacontane-D74, decanoic acid-D19, tetradecanoic acid-D27, heptadecanoic acid-D33, eicosanoic acid-D39, tetracosanoic acid-D59, and decanedioic acid-D16, andplaced in a 250mL mixture of 50:50 methylene chloride (DCM)/acetone. Samples and field blanks were individually extracted in batches of ten extractionsalong with a lab blank (a clean quartz fiber filter stored in the laboratory) and a spikedsample, which was a blank filter spiked with a known amount of matrix standard. Each batch was extracted for 24 hours with approximately 7 solvent cycles per hour.

After extraction, the samples were rotovapped down to 3-4mL and quantitatively transferred with DCM to a 15mL centrifuge tube. Samples were then blown down under nitrogen to 1-2mL and filtered using a syringe filter. Samples were then further blown down to 0.1mL and transferred into an appropriately labeled auto-sampler vial. The final volume for each sample was adjusted to 100 μLthen split into two aliquotsfor chemical analysis. One aliquot was silylated before analysis and the remainingaliquot was methylated with 50μL of fresh diazomethane derivatization reagent.

The methylated aliquot was analyzedusing gas chromatography electron impact mass spectrometry (GC-EI-MS) using a HP5-MS (30m x .25mm x .25μm) column inside a 6890N GC oven attached to a 5973 inert MSD run in scan mode. The temperature of the inlet and the transfer line was held at 300°C. At injection the oven was held at 65°C for 10 minutes, then ramped to 300°C at 10°C/minute (33.5 minutes ramp time) and then held at 300°C for 26.5 minutes for a run time of one hour.

Calibration curveswere generated for each batch of samples using six point calibration curves for more than 100 organic compounds. Calibration curves for each compound were calculated by normalizing to the appropriate deuterated and carbon-13 labeled reference compounds in the internal standard. Each sample, blank, and spike were then quantified using these calibration curves and the final concentrations were reported in nanograms of compound per filter, accounting for the fact that only half of the filter was analyzed.

Levoglucosan and the secondary organic carbon (SOC) tracers were analyzed using the unmethylated cut of the extract. A 25μL aliquot of the sample was transferred into a labeled

auto-sampler vial then blown down to dryness with nitrogen. Twenty-five µLof pyridine wereadded followed by 50µL of BSTFA (silylating reagent) to each vial, which was then capped. Samples were baked in a 70°C oven for two hours. After baking, the samples were analyzed using gas chromatography positive chemical ionization mass spectrometry (GC-PCI-MS)using an HP5-MS (30m x .25mm x .25µm) column inside a 6890N GC oven attached to a 5973 MSD. The temperature of the inlet was 310°C and the transfer line was 325°C. To attain the proper reaction inside the MS chamber,ultra-high purity (UHP) methane wasset at 20% of the maximum flow for the MSD. At the time of the injection, the oven was held at 90°C for 1 minute. Following this initial hold time, the temperature was ramped up 10°C/minute until 320°C was reached and was held for a total run time of 34 minutes.

Levoglucosan was quantified using C-13 labeled levoglucosan and authentic quantification standards. Because authentic standards are not available for SOC tracers, these compounds were quantified using ketopinic acid (KPA) as the internal standard and pinonic acid as the quantification reference[*Kleindienst et al.*, 2007; *Stone et al.*, 2010]. These concentrations were reported in the same manner as the compounds quantified from the methylated aliquot analysis.

The original extraction methods used for the analysis of molecular markers developed in the 1990s used a solvent mixture of benzene, hexane and isopropyl alcohol [*Schauer et al.*, 1996]. Due to changes in high purity benzene manufacturing in the late 1990s, commercial benzene with suitable purity was no longer available. To avoid the need to distil commercial benzene before extraction and to migrate to a more volatile solvent to improve recoveries of semi-volatile organic compounds, most research groups started using methylene chloride or a solvent mixture of methylene chloride and methanol for molecular marker analysis in the early 2000s. To assure better recovery of polar compounds, the University of Wisconsin-Madison examined the use of methylene chloride and acetone as the mixed solvent for molecular marker analysis and determined this mixture was far superior to the solvents used in the past. Figure 1ab shows a summary of performance measures used to evaluate the DCM and acetone solvent mixture. Given the excellent performance of DCM and acetone mixture, this solvent was used for the present study.

Table 1 lists all of the aerosol components measured for thestudy samples along with the average concentrations and the standard errorsof the concentrations for the Central Los Angeles sampling site.

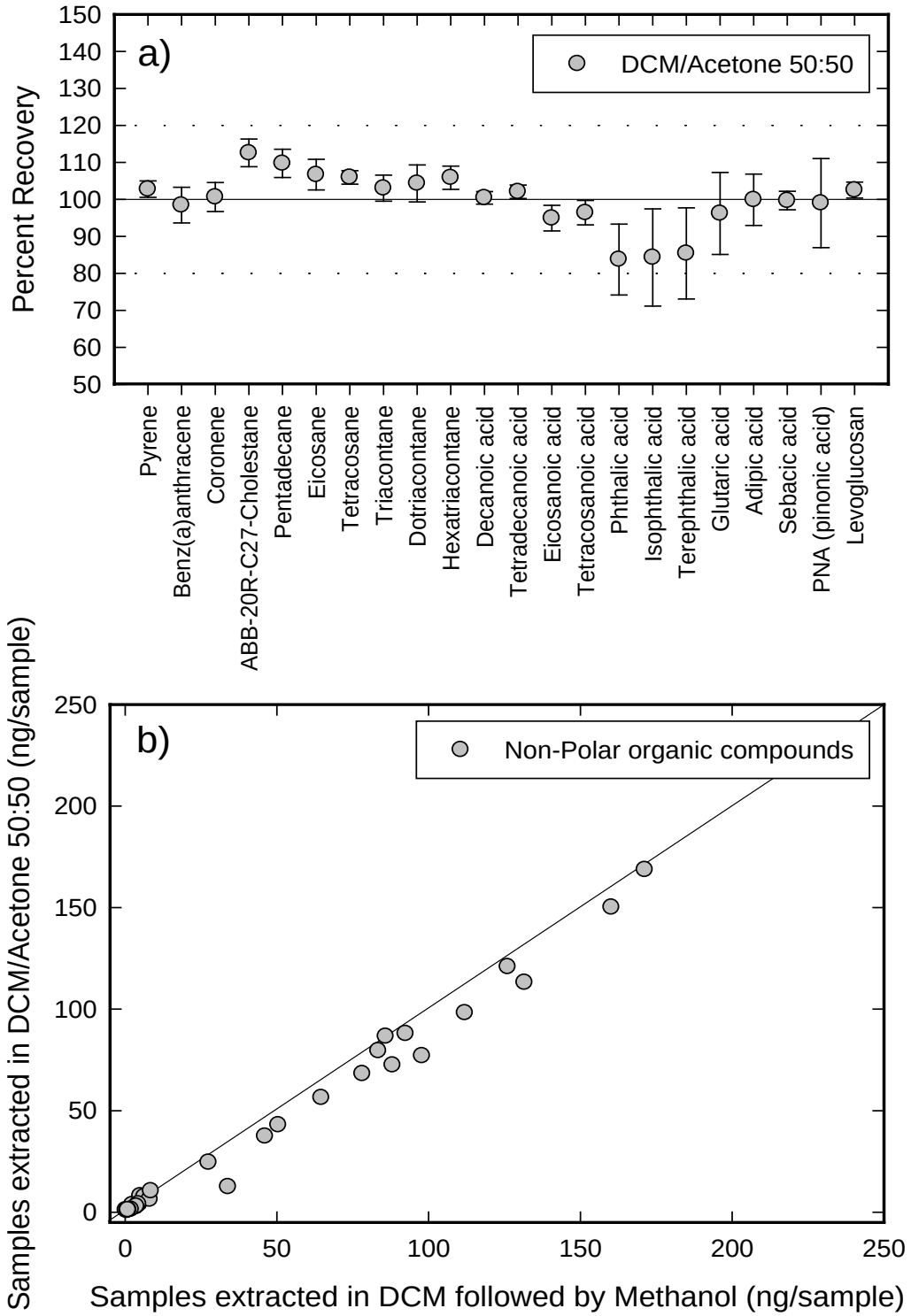

Figure 1ab– Evaluation of the methylene chloride (DCM) and acetone mixed solvent for molecular marker analysis: a) spike recoveries for polar and non-polar compounds and b) results from an intercomparison study of two different solvents for non-polar compounds

2.3 Data Analysis

A total of 345 samples were collected at the Central LA site and 61 samples at the Riverside site, which representsapproximately 95% annual completion at the Central site and 100% completion at the Riverside site. Five additional samples from the Central LA site were deemed invalid after review of the sample collection log sheets. A summary of the samples that were not collected or analyzed isprovidedin Table 21. In addition, due to analytical problems, some of the water-soluble nitrogen samples (collected in May 2009 and some in April of 2010 at the Central LA site) were deemed invalid for WSON and excluded from the analysis.A list of extreme events that were removed from trend averages are shown in Table 2, as noted in the report. EC and WIOC values that were not statistically different from zero are noted in Table 2 and were removed from the analysis that used EC and WIOC data as a denominator in a ratio calculation.

All measured organic molecular markers along with EC and WSOC at the Central LA site were used to investigate the different chemical classes, which share similar source categories by applying Principle Component Analysis (PCA). PCA was conducted using SAS (version 9.2), with varimax rotation and the maximum likelihood extraction method. Significant factors defined as factors with eigenvalues greater than 1.0 are presented in Table 3. Thirteen factors account for 86.5% of the variance in the dataset with 22%, 18%, and 14% accounted for by factor 1, factor 2, and factor 3, respectively. The first factor accounted for 22% of the variance and appears to represent mobile impacts at the Central LA site due to a high correlation with EC and hopanes. The second factor represents 18% of the data set variance and is significantly correlated with levoglucosan and PAHs, indicating biomass burning impacts. In general, heavy PAHs are used as indicators for tailpipe emissions and are used in CMB models to help split mobile source emissions into gasoline and diesel vehicles. However, this PCA-deduced factor indicates that PAHs concentrations are strongly correlated with levoglucosan emitted by biomass smoke, suggesting that the use of PAHs to differentiate gasoline and diesel emissions from mobile sources can lead to a biased estimate in cases when heavy PAH are also associated with biomass burning. The third factor accounted for 14% of the data variance and can be represented by vegetative detritus and other primary biogenic sources, due to its strong correlation with odd-numbered alkane (i.e., nonacosane and hentriacontane) and n-alkanoic acids[*Rogge et al.*, 1993a]. Other minor factors shown in Table 3 can be interpreted based on their correlations with key markers species, including a biogenic related SOC that is associated with isoprene derived methylthrietols (Factor 11), anα-pinene-derived SOC with pinic and pinonic acids (Factor 7), phthalic acid related SOC (Factor 4), and a toluene related SOC (Factor 8). The PCA analysis was largely used as a reference point and consistency check for the source apportionment models discussed below.

2.3.1 Chemical Mass Balance Model

Sources of the PM2.5 OC were apportioned using the publically available CMB software (EPA CMB v8.2) developed by the U.S. Environmental Protection Agency (EPA). The CMB program solves for an effective-variance-least-squares solution to the linear combination of the product of the source contribution and its concentration [*Watson et al.*, 1984]. Molecular marker species employed in this analysis were assumed to be stable during transport from source to receptor and were selected based on previous studies.

The source profiles used in the optimized analysis (as described below) for both sites are as follows: US west coast biomass burning [*Sheesley et al.*, 2007]; natural gas combustion [*Rogge*

et al., 1993b]; diesel exhaust [*Lough et al.*, 2007]; gasoline engines [*Lough et al.*, 2007]; smoking gasoline vehicles [*Lough et al.*, 2007]; and vegetative detritus [*Rogge et al.*, 1998].

The natural gas combustion source profile was not statistically significant in any of the CMB model runs for Riverside and was only statistically significant in a small fraction of the model runs for Central LA. For this reason, natural gas combustion was not included in the model. In the Central LA model runs, the model was able to include all three mobile source profiles (diesel, gasoline and smoking vehicles) with statistical significance. All three profiles were included in the model, but as shown by Lough et al. [*2007*], the gasoline and diesel splits have significant uncertainty and should be viewed as a rough estimate. Although there is uncertainty of the split between gasoline and diesel emissions, the sum of these source contributions, which represent mobile sources, is reasonably stable and is not very sensitive to changes in source profiles (Lough et al. [*2007*]). In the Riverside CMB model, inclusion of all three mobile source profiles led to co-linearity problems. The model was rerun with only diesel engines and smoking vehicles, and the result was not statistically different from the co-linearity cluster of the three mobile source profiles when all three were included in the model. As a result, the mobile source contributions were estimated from the sum of diesel and smoking vehicle source contributions in the model runs that only included these two mobile source profiles, where the smoking vehicle source includes the gasoline vehicle emissions.

2.3.2 Positive Matrix Factorization Model

PMF [*Paatero and Tapper*, 1994] is an advanced factor analysis technique based on a weighted least-squares fit and error estimates of the measured data. Detailed principles and applications have been previously described elsewhere in literature [*Heo et al.*, 2009; *Jaeckels et al.*, 2007]. Briefly, PMF is based on the assumption of mass conservation of atmospheric pollutants from emission sources to receptor sites. A mass balance approach is employed to the analysis of multivariate pollutant data in which non-negativity constraints on the factor computational process can be imposed. Although EPA's versions of PMFs have been well applied in source apportionment studies using organic molecular makers, these versions of PMF still have a very limited error model [*Hopke*, 2010; *Paatero and Hopke*, 2009]. Thus, the two-way factor analytic model PMF2 was used in this study.

Allocating appropriate uncertainties to the observed data is an important part of the analysis because the application of the PMF model depends mainly on the estimated uncertainties. The uncertainties for each organic species analyzedwerecalculated by taking the square root of the sum of squares of the sample values multiplied by the coefficient of variation for the spike data and the maximum of either standard deviation of blanks or analytical detection limit values. Values below the methods detection limits (MDLs) were replaced by half of the MDLs, and their overall uncertainties were set at 5/6 of the MDLs [*Polissar et al.*, 1998]. Several WSOC data points were missing and were replaced by the geometric mean of the measured WSOC as observed values, and associated uncertainties were set at four times the geometric mean [*Polissar et al.*, 1998].

The signal-to-noise (SN) ratio was reviewed for the concentration statistics of each chemical species to determine if any species had high noise that could potentially distort the model fitting [*Paatero and Hopke*, 2003]. In this study, SN ratio was categorized according to three different ranges determined by Jaeckels et al. [2007]. There were no bad or weak species for the current data set and no compounds were down-weighted or removed for poor SN.

The PMF model was run with different numbers of factors to achieve the best solution. Different pseudorandom numbers were examined for the initial values in the iterative fitting process to secure the global optimal PMF solutions. The robust mode was used to reduce the effects of extreme values in the analysis and the FPEAK parameter along with FKEY values [*Paatero et al.*, 2002] were applied to control the rotational ambiguity. In order to address the mass closure issue, the measured OC, EC, and WSOC concentrations were included in the PMF analysis as input variables, then the apportioned OC, EC, and WSOC contributions for each source were calculated according to its temporal variation.

2.3.3 UNMIX Model

UNMIX model is another transformed multivariate receptor model based on the PCA analysis. This modeluses a geometric approach of self-modeling curve resolution technique to derive meaningful factors that obey (to within error) the non-negative constraints on source composition and contributions [*Miller et al.*, 2002]. Uncertainties for each measured chemical species in the data are not considered by UNMIX model, which implicitly assumes a certain standard of accuracy in the data for a good model fit[*Henry*, 2003].

The EPA UNMIX version 6.0 was used to investigate source apportionments of PM2.5 OC and to compare source contributions deduced from UNIMX with those of PMF resolved sources. Like CMB, the user must select which input fitting species are to be used to generate meaningful source profiles and source contribution estimates in the UNMIX model. For this study, UNMIX was run with the same observations and molecular markers as those applied in the PMF model. Although this approach was needed to directly compare the two model's results, there were no feasible solutions provided from UNMIX. As seen in Table 3, organic molecular markers that were considered key markers in source characterization were finally selected and thus provided reasonably stable solutions.

2.3.4 Iterated Confirmatory Factor Analysis

The third multivariate receptor model applied in the study was Iterative Confirmatory Factor Analysis (ICFA). Algorithm and application of the ICFA have been detailed in a previous study [Christensen et al., 2006]. Briefly, if there is knowledge of the source profiles, then the ICFA approach can be solved by integrating aspects of CMB analysis by allocating varying degrees of constraints for each chemical species in the source profiles. In contrast, when there is little knowledge of source profiles or sources with unknown source profiles present, the ICFA method can incorporate aspects of confirmatory factor analysis and exploratory factor analysis. In order to solve the source apportionment matrix problems, ICFA utilizes a Bayesian approach that has a low computational burden. The Bayesian approach can be fit using prior distributions on elements of source profiles and contributions to allow both source profiles and source contributions to be estimated. In earlier work, Moussaoui et al. [2004] applied a Bayesian method with independent Gamma distributions for both source profiles and contributions, and independent and identically normal distribution for error term in order to produce non-negative source profiles and contributions. More recently, Lingwall et al. [2008] investigated a Bayesian method using the Dirichlet distribution as a prior distribution on source profiles with Markov chain Monte Carlo methods (MCMC) and identified greater flexibility of this method in specifying the error structure within the profile. In this study, a Bayesian method is applied to identify source contributions to the PM2.5 OC at the Central

LA site, with the Dirichlet distributions using MCMC on elements of source profiles from CMB model and PMF model.

2.3.5 Potential Source Contribution Function

In order to help interpret and validate the PMF resolved factor contributions and to help identify the source regions of these factor contributions, backward trajectories of air parcels can be ensemble with daily source contributions for each factor to map the source regions for each factor. A relatively simple trajectory analysis, named the Potential Source Contribution Function (PSCF), has been used in the past with PMF model results to further investigate and assess PMF results[*Kim et al.*, 2005; *Lee and Hopke*, 2006; *Zhao and Hopke*, 2006]. In the present study,the PSCF model was applied and evaluated to identify the potential source regions for each of the PMF-resolved OC source factors. Due to the limited data available at the Riverside site, we considered only the daily source contributions at the Central LA site. For the application of the PSCF model, backward trajectories associated with each of the daily source contributions were calculated with the Hybrid Single-Particulate Lagrangian Integrated Trajectory model (HYSPLIT 4.9 version) using EDAS 40 km gridded meteorological data [*Draxler and Rolph, 2012*] from May 2009 through April 2010. Five-day back trajectories arriving at heights of 500 m above ground level at the Central LA site with an every hour interval were calculated using a vertical velocity model for each of the estimates of source contributions. Grid cells of $0.5^o \times 0.5^o$ geographical coordinates (latitude and longitude) representing 2,400 cells were assigned by the daily source contributions along the corresponding back trajectories, in which an average of 46 trajectory endpoints were located. The high PSCF values representing the potential source locations were then calculated with the equation; $PSCF_{ij} = m_{ij}/n_{ij}$, where n_{ij} is the total number of endpoints that pass through the grid cell (i, j), and m_{ij} is the number of endpoints related to the samples that exceed the threshold criterion value in the same grid cell. In this study, an average of each of the source contributions was used as the threshold criterion. Specific grid cells with small numbers of endpoints are often biased in the PSCF analysis.To reduce this bias, the PSCF values were down-weighted using an arbitrary weight function $W(n_{ij})$ [*Polissar et al.*, 2001] for the grid cells which had total endpoints less than three times the average of endpoints per cell.See example below:

$$W(n_{ij}) = \begin{cases} 1.0, & 138 < n_{ij} \\ 0.7, & 46 < n_{ij} \leq 138 \\ 0.4, & 23 < n_{ij} \leq 46 \\ 0.2, & n_{ij} \leq 23 \end{cases}$$

3. Results and Discussion

3.1 Trend Analysis

3.1.1 Carbonaceous Aerosol

Figure 2abcd (EC and EC/OC), Figure 6abcd (WSOC), and Table 4 present the monthly average concentrations of EC, WSOC, WIOC and EC/OC for the two sites. The annual average PM2.5 EC and WIOC concentrations at the Central LA site were approximately 50% higher than the PM2.5 EC and WIOC concentrations at the Riverside site. In contrast, the WSOC levels at the Riverside site were approximately 20% higher than the annual average concentration at the Central LA site. The annual average fractions of OC that were water-soluble were 45% and 60% for the Central LA and the Riverside site, respectively. As seen in Figure 2ab, smooth seasonal trends were observed for the Central LA site but clear trendsappear absent for the Riverside site. This is in part due to the fact that the Central LA site includes daily samples for the entire year, whiletheRiverside site only includes one sixth of the days in the year or about 4-6 days per month. A plot of the one-in-six data from the Central LA sites appears very similar to the daily sampling averages shown in Figure 2a. This suggests that the smoother trends in the Central LA site are not solely due to the frequency of sampling. It appears the monthly average carbonaceous aerosol concentration at the Riverside site is sensitive to daily changes in local emissions and/or meteorology. As seen in Figure 2cd, the annual trends for the EC/OC ratio are similar with minimums in July and August, which are associated with higher SOC and lower impacts from biomass burning.

Figures 3-8 examine trends in the monthly averages and ratios of key source tracers at the Central LA site to provide insight into the trends of POC and SOC sources. The parallel trends for the Riverside site are very sporadic and difficult to interpret, preventing a clear intrepation of the results.Figures 3-5 show monthly and day of the week trends at the Central LA site forthe molecular marker tracers associated with mobile source emissions and biomass burning. Figures 6-8 show monthly trends in Central LA for indicators for SOC.

PM2.5 hopanes concentrations in the LA Basin are dominated by emissions from mobile sources. The monthly trends in the dominant hopanes are presented in Figure 3a and show a summertime minimum and a wintertime maximum. Some researchers have interpreted these trends to indicate hopanes are undergoing enhanced oxidation in the summer months and suggest that these compounds degrade rapidly in the atmosphere[*Robinson et al.*, 2006a; *Subramanian et al.*, 2006]. Figure 3bcd shows the monthly average ratio of hopanes to EC, OC and WIOC. It is interesting to note that these ratios are fairly constant across all months and suggest that the trends observed for hopane concentrations are due to meteorological dispersion and not chemical oxidation. Although researchers have shown that in laboratory smog chambers, hopanes can be oxidized reasonablyquickly, the data presented in Figure 3abcd suggests that these laboratory experiments are likely not representative of the atmosphere in Los Angeles. To further examine the stability of the hopanes in the LA atmosphere, Figure 4ab examines the annual averages of EC and the hopanes/EC ratios calculated by six different one-in-six day measurements for the Central LA site. Since measurements were made every day during the year, the data allow six representations of the one-in-six average. As can been seen by these figures, the averages are the same and there is no evidence that extreme events are dominating the averages. Along these lines, Figure 4cd shows the same averages for the day of the week. Although the averages for Monday through Friday are very similar, the weekend averages are very different, which suggest

the hopane-to-EC ratios are largely controlled by changes in emissions and not chemical oxidation as suggested by other researchers.

Figure 5abcd presents the monthly average concentrations for levoglucosan, hopanes, and polycyclic aromatic hydrocarbons (PAH) for the Central LA site. Levoglucosan is a key tracer for biomass smoke and makes up approximately 20% of particulate matter from biomass combustion. As seen in Figure 5a, there is a very strong seasonal pattern for biomass smoke with much higher concentrations of levoglucosan in winter than during summer months. As discussed above, fine particle hopanes in the LA basin are tracers for mobile sources. PAH are generic tracers for combustion and are largely from mobile sources and biomass burning in the LA basin. Peak winter concentrations of hopanes were approximately twice the concentration observed in the summer, while levoglucosan levels were more than ten times higher in winter than summer months. PAH levels in the winter were also approximately 5-10 times higher in winter than summer, suggesting the importance of the contribution of biomass burning to PAH concentrations.

The dominant sources of WSOC in PM2.5 are biomass smoke and SOC[*Snyder et al.*, 2009]. Figure 6abcd presents the trends in WSOC and non-biomass burning WSOC for the Central LA and Riverside sites. Non-biomass burning WSOC is calculated by subtracting the WSOC associated with biomass burning using the atmospheric concentration of levoglucosan and the ratio of levoglucosan to WSOC in biomass smoke [*Snyder et al.*, 2009]. Comparing the trends in WSOC and non-biomass burning WSOC, WSOC in the Los Angeles basin is dominated by SOCdue to only minor differences in these graphs. It is important to note that the WSOC and non-biomass burning WSOC concentrations at the Riverside site have sharp peaks in August and September, which are absent in Central Los Angeles site. The annual average WSOC concentration was1.71 µg m^{-3}at the Central LA site and 2.05 µg m^{-3}at the Riverside site. Excluding the extreme peaks in WSOC during August and September, the WSOC levels at both sites are very similar.

A number of tracers and indicators for SOC and specific sources of SOC have been proposed in the past and include methylthreitrols, aromatic diacids, n-alkanoic acids and low molecular weight diacids. Figures 7abcd and 8abcd show the monthly average trends in these potential SOC indicators and tracers for the Central LA and Riverside sites, respectively. Most importantly, none of these tracers show the pattern observed for non-biomass burning SOC shown in Figure 6d for the Riverside site. The lack of association suggests that these tracers are not good indicators of the SOC impacting Riverside during the peak SOC season, or these compounds are formed on a different time scale than the SOC in Riverside in August and September. Another important feature of the trends in Figures 7abcd and 8abcd is the peak of the methylthreitrols in late spring and early summer at both sites and very low levels in late summer when SOC peaks in Riverside. These compounds are largely believed to be derived from the oxidation of isoprene and suggest isoprene-derived SOC does not have a maximum during periods of maximum SOC. Figure 9abcd examines the relationship of some of these potential SOC tracers with non-biomass burning WSOC. There is very poor correlation amongst these components as indicated from the different trends in the methylthreitrols and non-biomass burning SOC. In contrast, there is a moderate correlation between the non-biomass burning SOC and adipic acid and phthalic acid that seems to be similar for both sites.

Table 1.List of compounds available for possible use in the receptor models for the Central LA site

Compound name	Data summary		Used in receptor model			
	Mean	Standard Error	CMB	PMF	UNMIX	ICFA
OC	3.92	0.11	Yes	Yes	Yes	Yes
EC	0.81	0.03	Yes	Yes	Yes	Yes
fWSOC	1.77	0.05	No	Yes	Yes	Yes
Fluoranthene	75.4	3	No	No	No	No
Acephenanthrylene	3.9	0.7	No	No	No	No
Pyrene	67.1	3.5	No	No	No	No
Benzo(ghi)fluoranthene	82.2	3.7	No	No	No	No
Cyclopenta(cd)pyrene	4.7	1.1	No	No	No	No
Benz(a)anthracene	47.1	3.4	No	No	No	No
Chrysene	121.1	5.7	No	No	No	No
1-Methylchrysene	8.4	1.2	No	No	No	No
Retene	97.9	15	No	No	No	No
Benzo(b)fluoranthene	160.9	9.2	Yes	Yes	Yes	Yes
Benzo(k)fluoranthene	98.3	7	Yes	Yes	Yes	Yes
Benzo(j)fluoranthene	8.5	1.3	No	Yes	No	Yes
Benzo(e)pyrene	147.4	8.4	Yes	Yes	Yes	Yes
Benzo(a)pyrene	44.8	4.2	No	Yes	No	Yes
Indeno(1,2,3-cd)pyrene	127.6	7.6	Yes	Yes	Yes	Yes
Benzo(ghi)perylene	260	12.3	Yes	Yes	Yes	Yes
Dibenz(ah)anthracene	4.4	1.1	No	No	No	No
Picene	2.4	1	No	No	No	No
Coronene	136.9	6.1	No	Yes	Yes	Yes
Dibenzo(ae)pyrene	0.9	0.7	No	No	No	No
17α(H)-22,29,30-Trisnorhopane	49.8	2.3	Yes	Yes	No	Yes
17β(H)-21α(H)-30-Norhopane	200	7.1	Yes	Yes	Yes	Yes
17α(H)-21β(H)-Hopane	169.7	5.5	Yes	Yes	Yes	Yes
22S-Homohopane	110.4	3.7	No	Yes	Yes	Yes
22R-Homohopane	91.3	3.1	No	Yes	Yes	Yes
22S-Bishomohopane	46.8	3	No	Yes	Yes	Yes
22R-Bishomohopane	35.6	2.3	No	Yes	Yes	Yes
22S-Trishomohopane	9.5	1.6	No	Yes	No	Yes
22R-Trishomohopane	6.9	1.2	No	Yes	No	Yes
αββ-20R-C27-Cholestane	35.5	2.2	Yes	Yes	Yes	Yes
αββ-20S-C27-Cholestane	42.8	2.6	Yes	Yes	Yes	Yes
ααα-20S-C27-Cholestane	52.7	3.2	No	Yes	No	Yes
αββ-20R-C28-Ergostane	8.7	1.1	No	Yes	No	Yes
αββ-20S-C28-Ergostane	9.9	1.3	No	Yes	No	Yes
αββ-20R-C29-Sitostane	42.4	2.3	Yes	Yes	No	Yes
αββ-20S-C29-Sitostane	44.1	2.4	Yes	Yes	No	Yes
Undecane	ND	ND	No	No	No	No
Dodecane	ND	ND	No	No	No	No
Tridecane	ND	ND	No	No	No	No
Tetradecane	ND	ND	No	No	No	No
Pentadecane	ND	ND	No	No	No	No
Hexadecane	20.3	5.9	No	No	No	No
Norpristane	ND	ND	No	No	No	No
Heptadecane	87	11.9	No	No	No	No
Pristane	ND	ND	No	No	No	No

Table 1 (continued)

Compound name	Data summary		Used in receptor model			
	Mean	Standard Error	CMB	PMF	UNMIX	ICFA
Octadecane	27.8	4.6	No	No	No	No
Phytane	0.4	0.4	No	No	No	No
Nonadecane	207.6	14.9	No	No	No	No
Eicosane	479.2	27.6	No	No	No	No
Heneicosane	565.8	31.9	No	No	No	No
Docosane	1023	39.1	No	No	No	No
Tricosane	1640.6	61.7	No	No	No	No
Tetracosane	1680.8	74.8	No	Yes	No	Yes
Pentacosane	1871.1	78	Yes	Yes	No	Yes
Hexacosane	1718.9	79.9	Yes	Yes	No	Yes
Heptacosane	1863.9	82.9	Yes	Yes	No	Yes
Octacosane	1335.5	60.8	Yes	Yes	No	Yes
Nonacosane	2060.5	126.7	Yes	Yes	Yes	Yes
Triacontane	1116.3	45.4	Yes	Yes	No	Yes
Hentriacontane	1713	66.4	Yes	Yes	Yes	Yes
Dotriacontane	794.7	35	Yes	Yes	No	Yes
Tritriacontane	973.5	39	Yes	Yes	Yes	Yes
Tetratriacontane	557	26.4	Yes	Yes	No	Yes
Pentatriacontane	474.4	19.7	Yes	Yes	No	Yes
Hexatriacontane	338.4	20.9	Yes	Yes	No	Yes
Heptatriacontane	79.1	12.4	No	Yes	No	Yes
Octatriacontane	59.3	12.2	No	No	No	No
Nonatriacontane	ND	ND	No	No	No	No
Tetracontane	ND	ND	No	No	No	No
Decylcyclohexane	ND	ND	No	No	No	No
Pentadecylcyclohexane	ND	ND	No	No	No	No
Hexadecylcyclohexane	ND	ND	No	No	No	No
Heptadecylcyclohexane	ND	ND	No	No	No	No
Octadecylcyclohexane	ND	ND	No	No	No	No
Nonadecylcyclohexane	41.5	3.5	No	No	No	No
Squalane	ND	ND	No	No	No	No
Octanoic acid	573.9	100.9	No	No	No	No
Decanoic acid	427.1	36.4	No	No	No	No
Dodecanoic acid	1834.3	81.9	No	No	No	No
Tetradecanoic acid	5010.5	139.3	No	No	No	No
Pentadecanoic acid	2108.6	54.1	No	No	No	No
Hexadecanoic acid	51814.6	1873.1	No	No	No	No
Heptadecanoic acid	2171.6	142.1	No	No	No	No
Octadecanoic acid	27850	1185.4	No	Yes	Yes	Yes
Nonadecanoic acid	286.7	13.6	No	Yes	No	Yes
Pinonic acid	2631.9	97.9	No	Yes	Yes	Yes
Palmitoleic acid	249.3	43.9	No	Yes	No	Yes
Oleic acid	7154	792	No	Yes	No	Yes
Linoleic acid	4276.9	495.9	No	Yes	No	Yes
Linolenic acid	319.3	43.8	No	Yes	No	Yes
Eicosanoic acid	1524	79.7	No	Yes	No	Yes
Heneicosanoic acid	491.6	25.9	No	Yes	No	Yes
Docosanoic acid	2170.4	163.3	No	Yes	Yes	Yes

Table 1 (continued)

Compound name	Data summary		Used in receptor model			
	Mean	Standard Error	CMB	PMF	UNMIX	ICFA
Tricosanoic acid	707.6	50.2	No	Yes	Yes	Yes
Tetracosanoic acid	2371.1	200.3	No	Yes	Yes	Yes
Pentacosanoic acid	454.7	22.8	No	Yes	Yes	Yes
Hexacosanoic acid	1123.8	79.6	No	Yes	Yes	Yes
Heptacosanoic acid	281.1	17.3	No	Yes	No	Yes
Octacosanoic acid	1067	72.3	No	Yes	Yes	Yes
Nonacosanoic acid	315.8	21.2	No	Yes	Yes	Yes
Triacontanoic acid	873.5	66.6	No	Yes	Yes	Yes
Phthalic acid	10322.4	404.6	No	Yes	Yes	Yes
Isophthalic acid	1386.4	44.9	No	Yes	No	Yes
Terephthalic acid	3151.3	366.6	No	Yes	No	Yes
1,2,4-Benzenetricarboxylic acid	3397.4	144.4	No	No	No	No
1,2,3-Benzenetricarboxylic acid	102.9	9.3	No	No	No	No
Methylphthalic acid	3032.7	96.7	No	Yes	Yes	Yes
Succinic acid	11653.8	581.8	No	Yes	No	Yes
Glutaric acid	4994.5	189.7	No	Yes	No	Yes
Adipic acid	2559.2	75.7	No	Yes	No	Yes
Pimelic acid	1289.6	50	No	Yes	No	Yes
Suberic acid	1823.9	49	No	Yes	No	Yes
Azelaic acid	9782.1	240.7	No	Yes	No	Yes
Sebacic acid	907.1	37.1	No	Yes	No	Yes
I-1 (2-methylglyceric acid)	16.9	16.9	No	No	No	No
T-3 (2,3-dihydroxy-4-oxopentanoic acid)	1050.3	105.2	No	Yes	No	Yes
PNA (pinonic acid)	2710.6	125.9	No	Yes	Yes	Yes
I-2 (2-methylthreitol)	157.8	26.4	No	Yes	No	Yes
I-3 (2-methylthreitol)	318.8	43.8	No	Yes	No	Yes
A-5 (3-hydroxyglutaric acid)	5331.1	383.9	No	Yes	Yes	Yes
PA (pinic acid)	249	29.9	No	Yes	No	Yes
A-6 (2-hydroxy-4,4-dimethylglutaric acid	1254.2	114.7	No	Yes	No	Yes
A-4 (3-acetyl hexanedioic acid)	2141	126.7	No	Yes	No	Yes
A-3 (2-hydroxy-4-ispropyladipic acid)	5149	220.9	No	Yes	No	Yes
C-1 (β-carophyllinic acid)	306.9	37.1	No	Yes	No	Yes
Levoglucosan	51876.8	5277.8	Yes	Yes	Yes	Yes

- Unit for OC, EC, and WSOC is microgram per cubic meters. Unit for other compounds is picogram per cubic meters
- ND represents that a compound was not detected in the sample or was below the detection limits

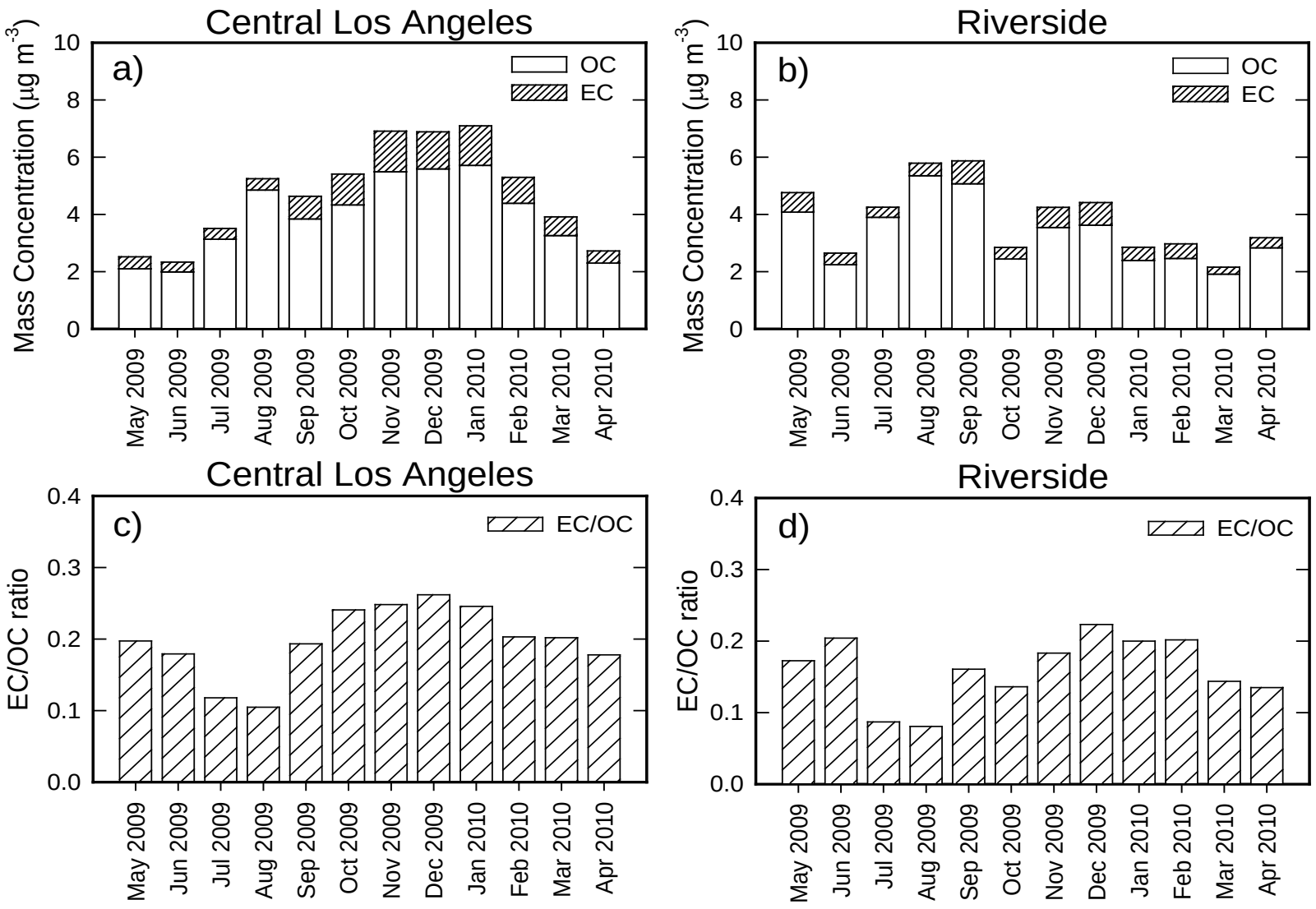

Figure 2abcd – Monthly trends in PM2.5 organic carbon (OC), elemental carbon (EC), and EC/OC for the Central LA and Riverside sites

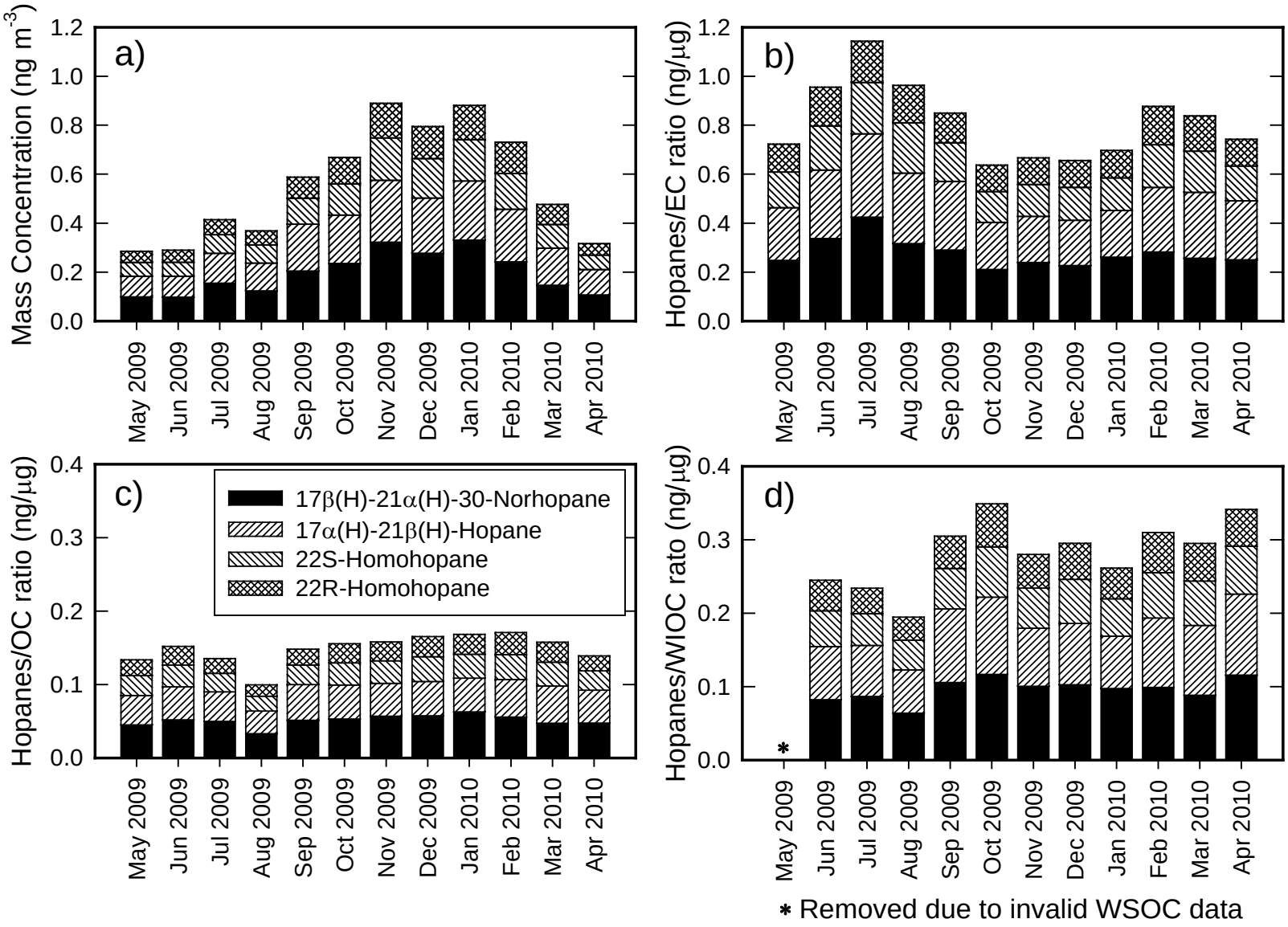

Figure 3abcd – Monthly trends in PM2.5 hopane concentrations and normalized hopane concentrations at Central LA site

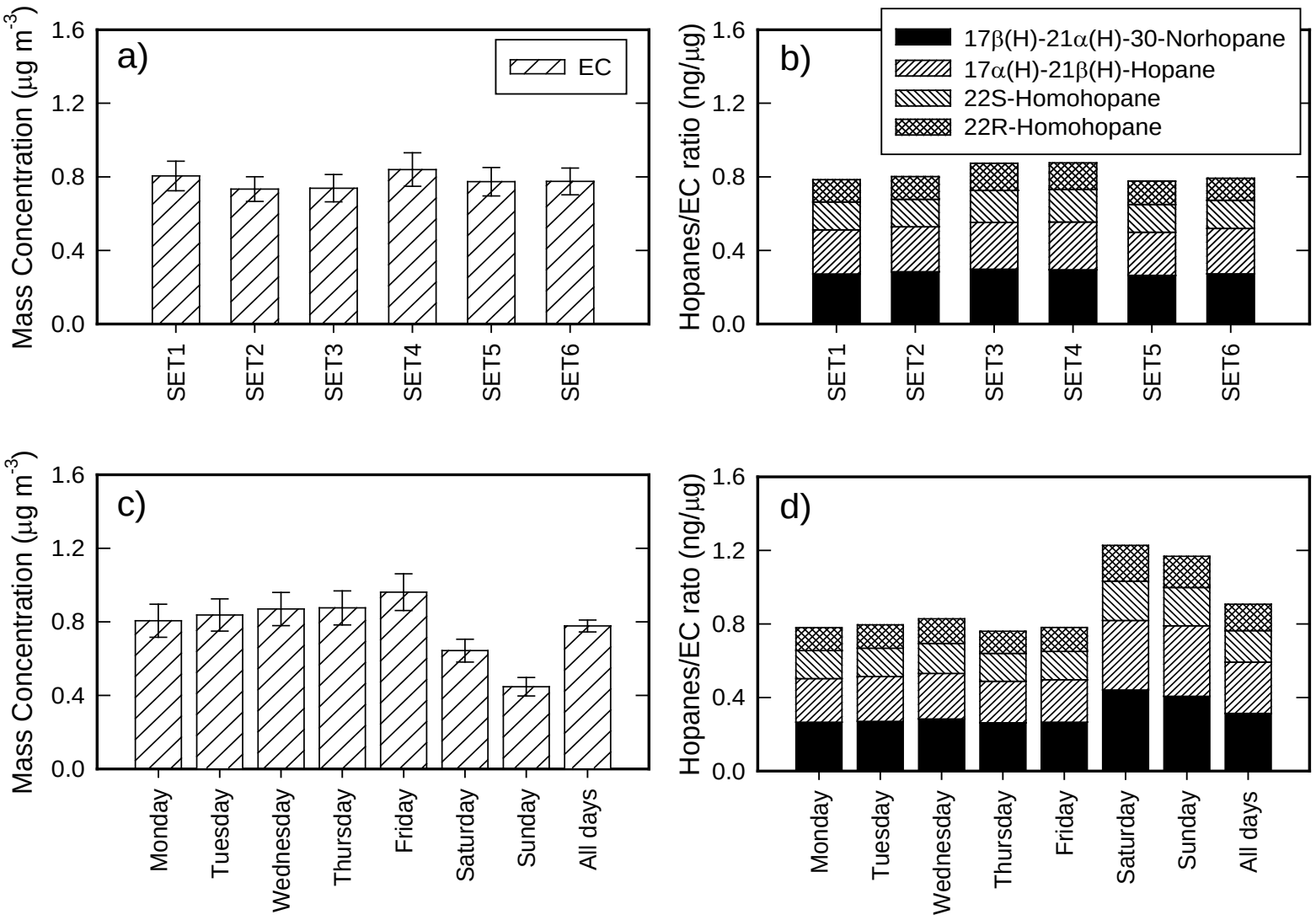

Figure 4abcd –Comparison of one-in-six day annual averaged and day of the week trends in PM2.5 EC and the PM2.5 hopanes to EC ratio at the Central LA site.

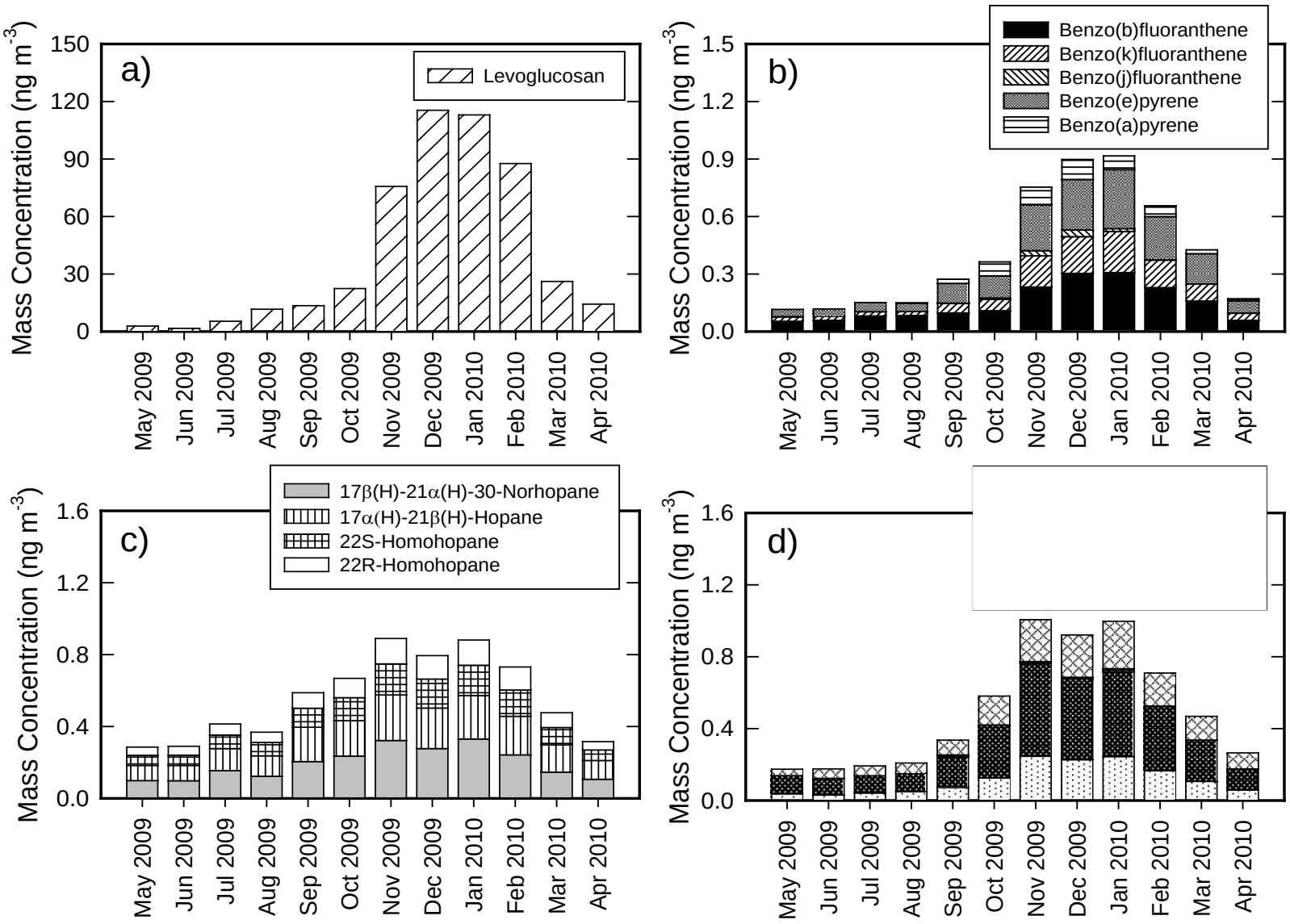

Figure 5abcd –Trends in the monthly average concentration of key PM2.5 molecular marker tracers at the Central LA site

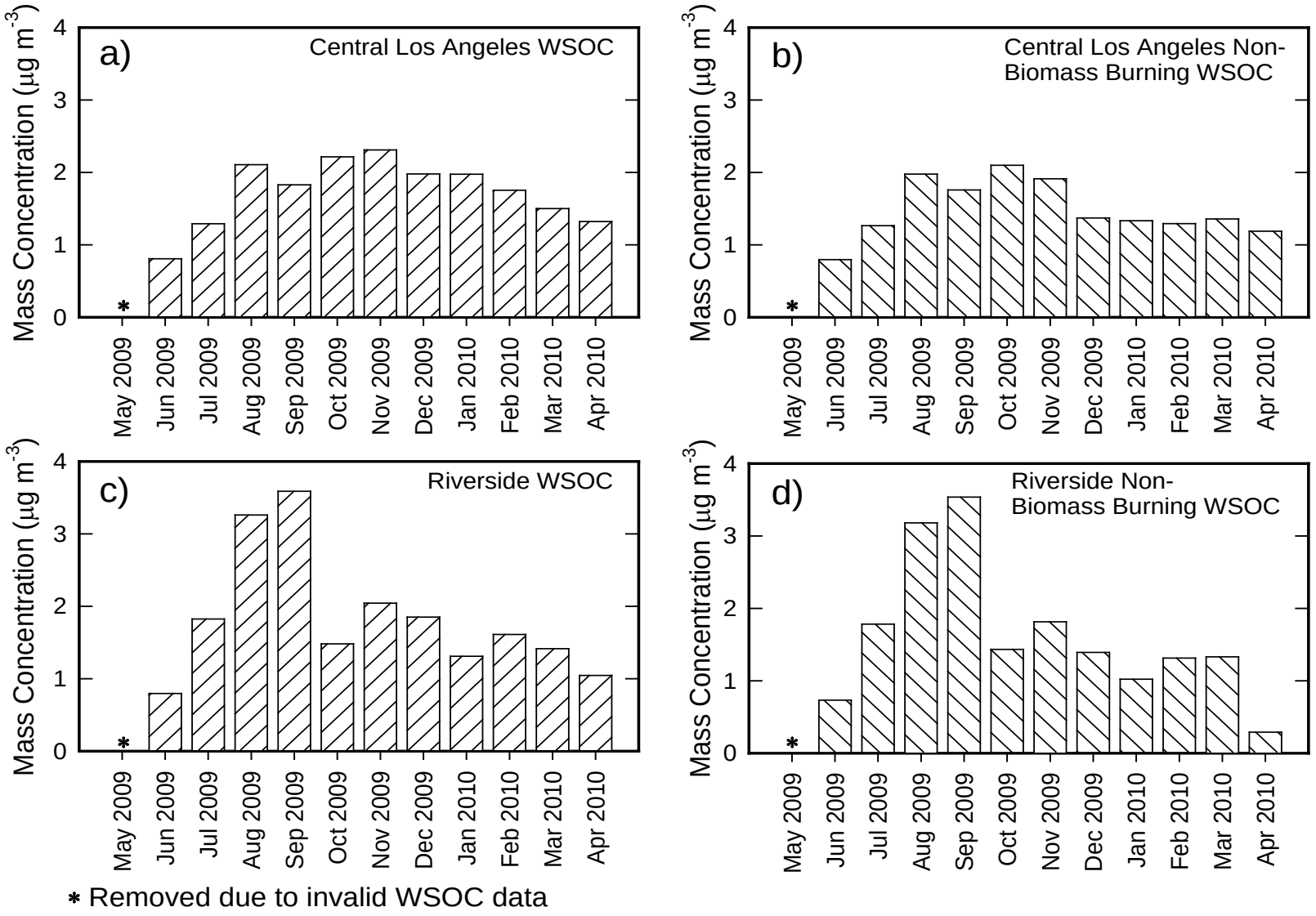

Figure 6abcd –Monthly trends in PM2.5 water soluble organic carbon (WSOC) and non-biomass burning PM2.5 WSOC at the Central LA and Riverside sites

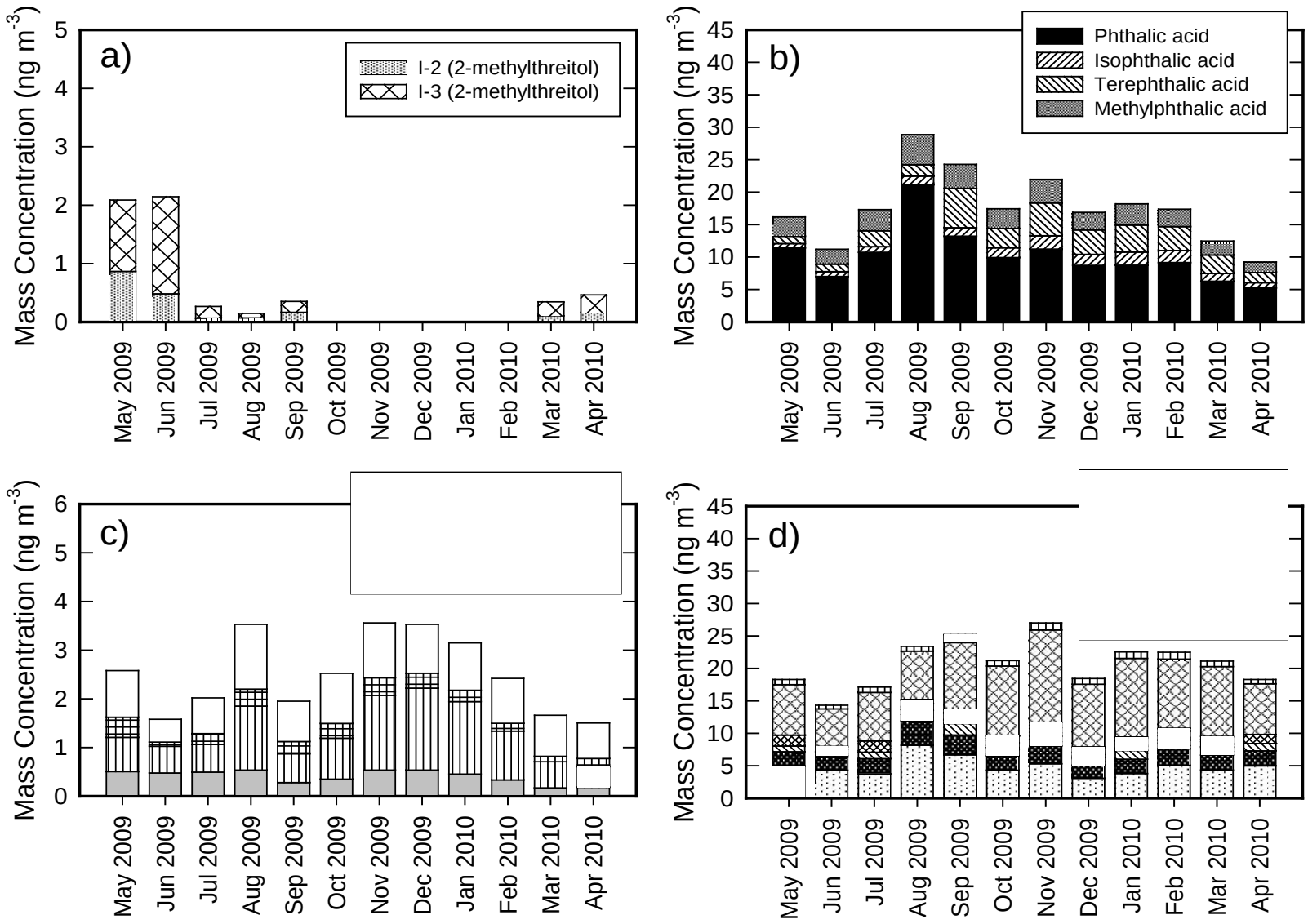

Figure 7abcd –Monthly trends in PM2.5 polar organic compounds at the Central LA site

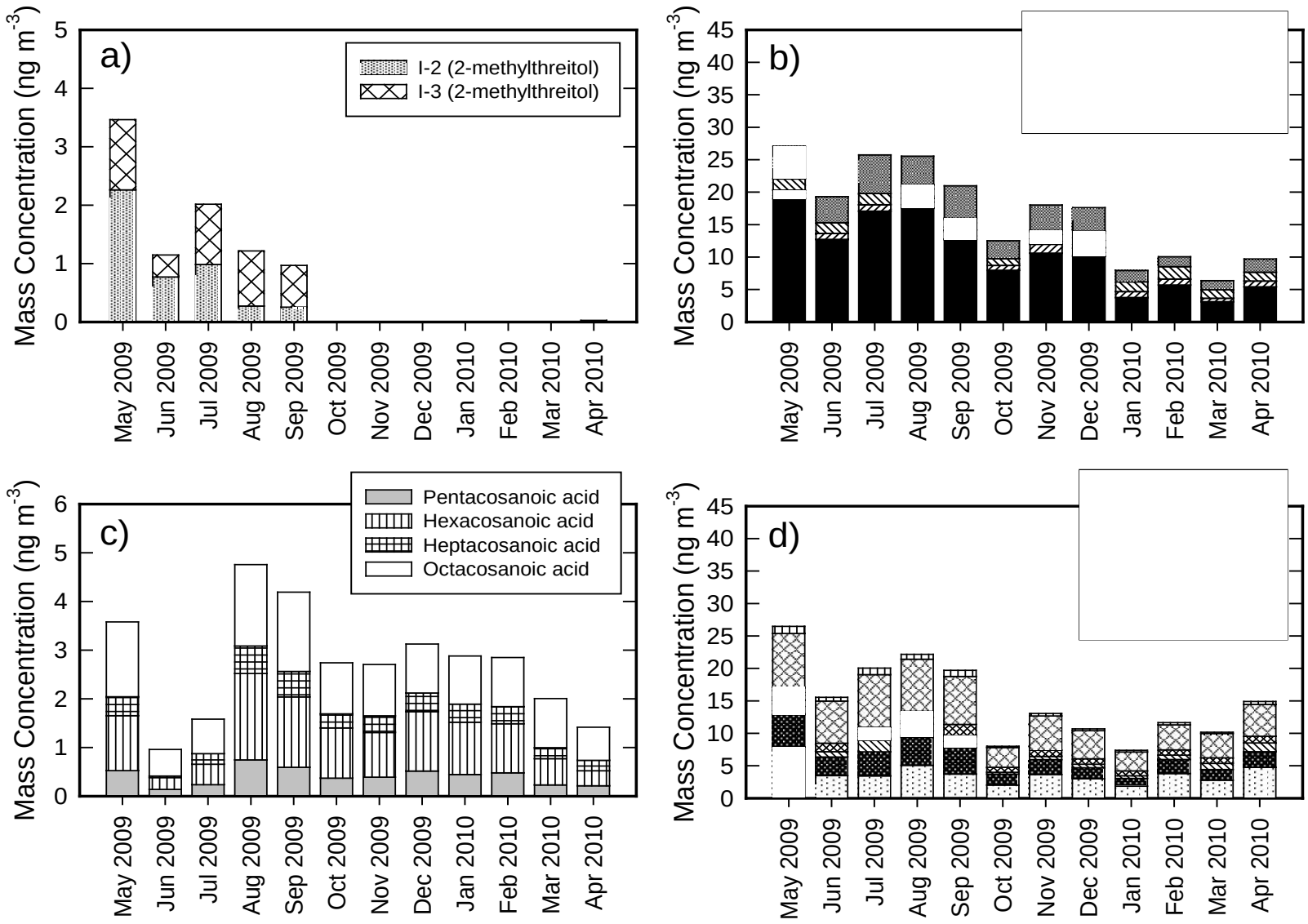

Figure 8abcd –Monthly trends in PM2.5 polar organic compounds at the Riverside site

Table 2. Summary of invalid samples and data removed for select trend analysis

Site	Invalid data and data removed	Date
Central LA	WSOC measurement invalid	All of May 2009 samples
	Extreme sample events[a)]	August 25-31 2009. December 23-28 30-31, 2009. January 1-2 2010.
	WIOC not statistically significant	May 19, 25 2009. July 31 2009. August 6 2009. September 14 2009. October 10 2009. April 12 2009.
	EC not statistically significant	July 4-5 2009. October 4 2009. April 4, 10-11 2010.
	Samples Not Collected or Analyzed	May 7, 22, 24 2009. June 21, 29 2009. October 18-19 2009. November 9-11 2009. December 3, 29 2009. January 15, 17, 19, 21 2010. February 5 2010. March 10-11, 14-15, 19 2010. April 6, 14, 24 2010.
Riverside	WSOC measurement invalid	All of May 2009 samples
	WSOC measurements invalid	April 8, 14, 20, 26 2010.
	Extreme sample events [a)]	January 2 2010. August 29 2009. December 27 2009.
	WIOC not statistically significant	June 6 2009. September 22 2009. October 4 2009.

a) Represent possible forest fires events and high wood smoke days

Table 3.Varimaxrotated factor analysis results for the Central LA site

Chemical species	Factor													Communalities
	1	2	3	4	5	6	7	8	9	10	11	12	13	
EC	0.81	0.42	0.21	0.04	0.10	-0.01	0.00	0.01	0.05	0.06	-0.04	0.03	0.00	0.89
WSOC	0.32	0.33	0.50	0.51	0.12	0.00	0.12	0.05	0.16	0.15	-0.12	0.03	0.03	0.82
Fluoranthene	0.63	0.67	0.11	-0.03	0.07	0.02	0.15	0.00	0.01	-0.10	-0.01	0.02	0.01	0.89
Pyrene	0.64	0.67	0.12	-0.04	0.06	0.00	0.14	0.01	0.00	-0.09	-0.04	0.00	-0.01	0.91
Benzo(ghi)fluoranthene	0.67	0.62	0.04	-0.07	0.03	0.01	0.18	-0.02	0.01	-0.05	-0.06	-0.06	0.02	0.88
Benz(a)anthracene	0.38	0.85	0.12	0.01	0.08	0.05	0.04	-0.01	0.02	-0.07	-0.01	0.06	0.05	0.91
Chrysene	0.52	0.76	0.13	-0.02	0.07	0.06	0.12	-0.07	0.07	0.00	-0.04	-0.05	0.04	0.90
Retene	-0.03	0.88	0.14	0.02	0.07	0.10	0.06	-0.04	0.08	-0.06	-0.01	0.13	-0.01	0.85
Benzo(b)fluoranthene	0.32	0.86	0.19	0.07	0.13	0.08	-0.05	-0.11	0.08	0.08	-0.02	0.01	0.16	0.95
Benzo(k)fluoranthene	0.34	0.85	0.18	0.03	0.12	0.06	-0.03	-0.10	0.07	0.12	0.01	-0.07	0.20	0.96
Benzo(e)pyrene	0.47	0.77	0.19	0.02	0.13	0.06	-0.03	-0.12	0.09	0.14	-0.02	-0.09	0.20	0.96
Benzo(a)pyrene	0.32	0.78	0.26	-0.03	0.07	0.06	0.07	0.03	0.02	-0.01	-0.04	0.05	0.09	0.80
Indeno(1,2,3-cd)pyrene	0.41	0.77	0.26	-0.02	0.10	0.03	-0.06	-0.12	0.05	0.15	0.00	-0.12	0.13	0.92
Benzo(ghi)perylene	0.65	0.64	0.18	-0.03	0.10	0.01	-0.03	-0.09	0.02	0.16	-0.02	-0.10	0.06	0.92
Coronene	0.65	0.66	0.14	-0.04	0.12	0.04	0.06	-0.10	0.05	0.13	-0.06	-0.03	0.02	0.94
17α(H)-22,29,30-Trisnorhopane	0.72	0.45	0.20	-0.05	0.10	0.15	0.19	-0.11	0.09	-0.09	-0.06	0.02	-0.10	0.87
17β(H)-21α(H)-30-Norhopane	0.88	0.28	0.16	0.01	0.16	0.05	0.03	-0.06	0.10	0.02	0.00	0.07	-0.02	0.93
17α(H)-21β(H)-Hopane	0.89	0.24	0.16	0.02	0.11	0.13	0.01	-0.03	0.14	0.01	-0.03	0.04	0.04	0.93
22S-Homohopane	0.88	0.32	0.12	0.04	0.13	0.11	-0.02	-0.01	0.07	0.01	-0.04	0.04	0.04	0.93
22R-Homohopane	0.85	0.34	0.13	0.04	0.13	0.10	0.00	0.00	0.10	0.02	-0.05	0.05	0.05	0.90
22S-Bishomohopane	0.90	0.24	0.01	0.01	0.09	0.07	-0.03	-0.02	0.05	0.02	-0.05	-0.02	0.04	0.89
22R-Bishomohopane	0.88	0.23	0.01	0.03	0.11	0.11	-0.02	-0.03	0.05	0.04	-0.04	-0.03	0.05	0.87
αββ-20R-C27-Cholestane	0.84	0.21	0.04	-0.04	0.11	0.04	0.20	-0.08	0.06	0.03	-0.06	-0.03	0.06	0.82
αββ-20S-C27-Cholestane	0.86	0.20	0.03	-0.04	0.06	0.02	0.17	-0.08	0.06	0.01	-0.06	-0.02	0.05	0.84
ααα-20S-C27-Cholestane	0.85	0.16	0.07	-0.03	0.07	0.04	0.17	-0.10	0.10	0.02	-0.06	-0.03	0.06	0.82
αββ-20R-C29-Sitostane	0.86	0.26	0.07	-0.02	0.08	0.13	0.04	-0.07	0.07	0.07	-0.08	-0.05	0.05	0.86
αββ-20S-C29-Sitostane	0.87	0.26	0.05	-0.02	0.08	0.18	0.08	-0.08	0.08	0.05	-0.06	-0.05	0.04	0.89
Nonadecane	0.55	0.59	0.05	-0.10	0.04	0.08	0.34	-0.05	-0.06	-0.07	-0.04	-0.04	-0.06	0.80
Eicosane	0.51	0.54	0.15	-0.09	0.05	0.21	0.34	-0.07	0.02	-0.10	-0.04	0.01	-0.01	0.76
Heneicosane	0.44	0.68	0.09	-0.11	0.09	0.11	0.36	0.02	0.00	-0.19	-0.01	0.10	-0.05	0.88
Docosane	0.55	0.41	0.08	-0.19	0.00	0.31	0.41	-0.01	0.01	-0.15	0.00	-0.06	-0.01	0.80
Tricosane	0.49	0.57	0.12	0.00	0.12	0.38	0.29	-0.07	0.10	-0.09	-0.03	0.07	0.01	0.85
Tetracosane	0.58	0.35	0.09	-0.01	0.13	0.60	0.08	-0.07	0.01	-0.07	-0.02	0.00	-0.07	0.87

Table 3 (continued)

Chemical species	Factor													Communalities
	1	2	3	4	5	6	7	8	9	10	11	12	13	
Pentacosane	0.63	0.24	0.16	0.01	0.16	0.64	-0.01	-0.09	0.07	0.01	0.03	-0.03	-0.04	0.94
Hexacosane	0.57	0.20	0.13	0.02	0.21	0.72	-0.07	-0.06	0.06	0.07	0.02	-0.05	-0.01	0.96
Heptacosane	0.55	0.14	0.45	0.03	0.23	0.60	-0.02	-0.03	0.07	0.08	0.00	-0.02	0.03	0.96
Octacosane	0.55	0.21	0.23	0.04	0.33	0.63	-0.07	-0.06	0.08	0.12	-0.01	-0.07	0.04	0.94
Nonacosane	0.31	0.01	0.84	-0.01	0.09	0.29	0.15	0.00	0.05	0.08	-0.04	0.02	0.09	0.93
Triacontane	0.55	0.27	0.25	0.09	0.50	0.46	-0.05	-0.04	0.09	0.12	-0.04	-0.04	0.07	0.94
Hentriacontane	0.54	0.19	0.67	0.06	0.30	0.22	0.11	-0.02	0.06	0.15	-0.04	0.02	0.06	0.95
Dotriacontane	0.44	0.33	0.22	0.12	0.71	0.27	-0.01	-0.04	0.08	0.06	-0.07	0.00	0.02	0.96
Tritriacontane	0.51	0.28	0.45	0.12	0.59	0.16	0.07	-0.05	0.07	0.09	-0.07	-0.01	0.04	0.96
Tetratriacontane	0.38	0.33	0.12	0.11	0.77	0.15	0.03	-0.07	0.07	-0.01	-0.08	-0.03	0.04	0.92
Pentatriacontane	0.37	0.17	0.15	0.11	0.81	0.12	0.03	-0.01	0.06	0.01	-0.02	0.04	0.05	0.89
Hexatriacontane	0.04	0.29	0.09	0.12	0.83	0.02	0.14	-0.02	0.11	-0.07	-0.09	0.12	0.09	0.87
Nonadecylcyclohexane	0.52	0.53	0.01	0.03	0.03	0.07	0.15	-0.12	-0.03	0.13	-0.04	-0.04	-0.01	0.62
Decanoic acid	-0.14	-0.09	0.12	0.04	0.03	-0.11	0.02	-0.02	-0.04	0.03	0.30	0.64	-0.03	0.56
Dodecanoic acid	0.34	0.60	0.16	0.01	0.16	0.05	0.42	-0.17	0.08	0.01	-0.01	0.32	-0.01	0.85
Tetradecanoic acid	0.55	0.57	0.10	0.09	0.19	0.10	0.25	-0.20	0.08	0.19	0.08	0.16	-0.11	0.88
Pentadecanoic acid	0.42	0.58	0.21	0.14	0.23	0.03	0.14	-0.08	0.01	0.18	0.19	0.34	-0.13	0.87
Hexadecanoic acid	0.49	0.74	0.16	0.07	0.18	0.10	0.06	-0.13	0.15	0.19	-0.03	0.02	-0.05	0.94
Heptadecanoic acid	0.27	0.26	0.10	0.02	0.09	0.03	0.04	0.00	0.85	-0.06	-0.01	-0.05	-0.04	0.89
Octadecanoic acid	0.40	0.77	0.16	0.06	0.18	0.14	-0.03	-0.14	0.13	0.21	-0.03	-0.04	-0.04	0.93
Nonadecanoic acid	0.16	0.42	0.66	0.11	0.22	-0.10	-0.22	-0.05	0.03	0.04	0.11	0.03	-0.16	0.80
Pinonic acid	0.33	0.33	0.09	0.04	0.09	-0.08	0.75	-0.15	0.02	0.02	-0.02	-0.03	-0.10	0.84
Palmitoleic acid	0.02	0.32	0.08	0.05	0.05	0.03	-0.04	0.00	0.05	0.00	-0.08	0.70	-0.04	0.62
Oleic acid	0.28	0.81	0.07	-0.02	0.16	0.03	0.18	0.06	0.06	-0.09	-0.05	0.16	-0.10	0.85
Linoleic acid	0.27	0.79	0.06	-0.03	0.15	0.03	0.17	0.09	0.06	-0.14	-0.06	0.18	-0.09	0.83
Eicosanoic acid	0.22	0.53	0.61	0.15	0.12	0.00	-0.15	0.01	0.07	0.06	-0.03	-0.09	-0.15	0.80
Heneicosanoic acid	0.03	0.26	0.85	0.16	0.11	-0.08	-0.15	0.03	0.23	-0.07	0.05	0.02	-0.09	0.93
Docosanoic acid	0.07	0.37	0.88	0.14	0.05	0.02	-0.06	-0.02	0.04	0.01	-0.05	-0.08	-0.06	0.95
Tricosanoic acid	0.03	0.22	0.95	0.10	0.06	-0.01	-0.06	-0.01	0.02	0.01	0.01	0.01	-0.02	0.97
Tetracosanoic acid	0.05	0.34	0.89	0.13	0.04	0.03	-0.03	-0.04	0.05	0.01	-0.06	-0.05	-0.03	0.93
Pentacosanoic acid	0.00	0.21	0.92	0.11	0.11	-0.01	-0.07	0.02	0.02	0.00	0.12	0.08	-0.03	0.95
Hexacosanoic acid	0.07	0.39	0.89	0.09	0.05	0.04	-0.01	-0.05	0.01	0.05	-0.02	-0.01	-0.02	0.97
Heptacosanoic acid	0.07	-0.03	0.91	0.10	0.09	0.01	0.02	0.07	0.11	-0.06	0.07	0.13	0.03	0.89

Table 3 (continued)

Chemical species	Factor													Communalities
	1	2	3	4	5	6	7	8	9	10	11	12	13	
Octacosanoic acid	0.08	0.01	0.95	0.05	-0.03	0.09	0.14	0.02	0.04	0.00	-0.02	0.08	0.06	0.96
Nonacosanoic acid	0.19	-0.03	0.89	0.11	0.00	0.09	0.15	0.01	0.06	0.00	-0.09	0.00	0.09	0.89
Triacontanoic acid	0.10	-0.07	0.93	0.06	-0.02	0.10	0.18	0.03	0.04	-0.02	-0.05	0.10	0.09	0.94
Phthalic acid	0.03	-0.09	0.23	0.86	0.11	-0.06	-0.10	0.21	-0.01	-0.07	-0.01	-0.01	-0.03	0.87
Isophthalic acid	0.66	0.42	0.21	0.40	0.17	-0.02	-0.06	0.00	0.14	0.15	-0.06	-0.01	0.07	0.91
Terephthalic acid	0.19	0.16	0.03	0.08	0.13	-0.04	-0.08	0.01	0.02	-0.02	0.03	-0.06	0.86	0.84
1,2,4-Benzenetricarboxylic acid	0.43	-0.01	0.19	0.64	0.22	-0.07	-0.20	0.12	0.11	0.17	-0.09	-0.10	0.07	0.80
Methylphthalic acid	0.30	-0.04	0.27	0.74	0.20	-0.12	-0.11	0.21	0.03	0.03	0.05	0.00	-0.04	0.84
Succinic acid	-0.23	-0.07	0.04	0.85	-0.02	0.08	0.06	0.15	-0.05	0.00	0.07	-0.05	0.03	0.82
Glutaric acid	-0.19	0.04	0.09	0.91	-0.02	0.09	0.12	0.09	0.04	0.02	0.00	0.03	0.03	0.92
Adipic acid	-0.03	0.14	0.20	0.83	0.07	0.05	0.05	0.06	0.26	0.07	-0.03	0.19	0.09	0.89
Pimelic acid	0.12	0.18	0.34	0.52	0.09	0.08	0.14	0.00	0.55	0.04	-0.19	0.12	0.11	0.84
Suberic acid	0.25	0.14	0.28	0.40	0.18	0.03	-0.06	-0.03	0.59	0.32	0.07	0.15	0.07	0.84
Azelaic acid	0.58	0.16	0.27	0.30	0.17	0.01	-0.02	-0.14	0.21	0.53	0.04	-0.01	0.02	0.90
Sebacic acid	0.28	0.05	0.27	0.13	0.09	0.07	-0.03	-0.03	0.81	0.10	0.05	-0.02	0.02	0.85
T-3 (2,3-dihydroxy-4-oxopentanoic acid)	-0.22	-0.13	0.01	0.33	-0.07	0.00	-0.10	0.72	0.03	0.17	0.04	0.04	0.10	0.75
PNA (pinonic acid)	0.30	0.36	0.00	-0.02	0.09	-0.05	0.76	-0.11	-0.01	0.09	-0.03	-0.03	-0.05	0.84
I-2 (2-methylthreitol)	-0.17	-0.06	0.00	0.06	-0.08	0.04	0.02	-0.02	0.04	0.00	0.76	0.18	0.05	0.65
I-3 (2-methylthreitol)	-0.20	-0.05	-0.06	-0.12	-0.11	-0.03	-0.07	0.25	-0.03	0.02	0.78	-0.05	-0.05	0.75
A-5 (3-hydroxyglutaric acid)	-0.15	-0.22	0.17	0.51	0.02	-0.13	-0.17	0.62	0.04	0.00	-0.07	0.04	0.10	0.81
PA (pinic acid)	-0.09	0.09	-0.08	-0.01	-0.09	0.19	0.26	0.29	0.07	0.54	-0.26	0.01	0.06	0.59
A-6 (2-hydroxy-4,4-dimethylglutaric acid	-0.25	-0.14	0.03	0.43	-0.05	-0.08	-0.16	0.67	-0.03	-0.05	0.06	-0.05	-0.10	0.78
A-4 (3-acetyl hexanedioic acid)	-0.10	-0.15	-0.02	0.22	-0.03	-0.04	0.03	0.73	-0.07	0.22	0.21	-0.06	0.01	0.72
A-3 (2-hydroxy-4-ispropyladipic acid)	0.26	0.02	0.03	0.05	0.00	-0.07	-0.08	0.36	0.05	0.67	0.36	0.05	-0.06	0.79
C-1 (β-carophyllinic acid)	0.17	0.05	-0.07	0.32	0.08	0.08	-0.07	0.29	0.04	0.46	-0.15	-0.02	0.50	0.73
Levoglucosan	0.06	0.81	0.42	0.06	0.09	0.12	-0.04	-0.14	0.10	0.15	-0.03	-0.07	0.06	0.93
Eigenvalue	20.7	17.3	12.7	6.0	4.3	3.3	2.9	2.8	2.6	2.1	1.8	1.6	1.4	
% of Variance	22.5	18.8	13.8	6.6	4.7	3.5	3.2	3.0	2.8	2.3	2.0	1.7	1.6	
Cumulative %	22.5	41.4	55.1	61.7	66.4	69.9	73.1	76.1	79.0	81.2	83.2	84.9	86.5	

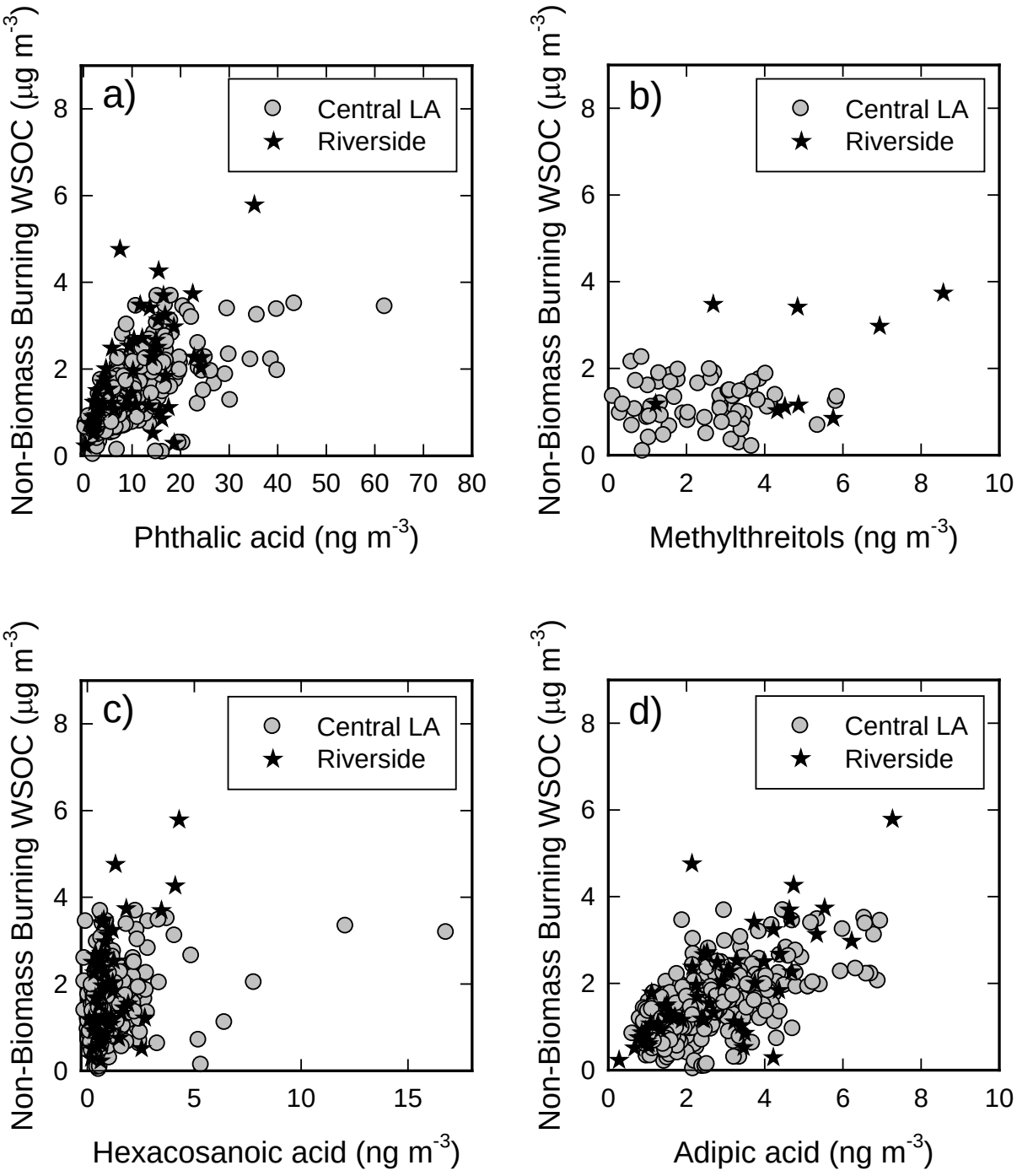

Figure 9abcd –Comparison of non-biomass burning WSOC and potential PM2.5 secondary organic carbon (SOC)indicators

Table 4. Summary of data in Figures 2-5 including key source tracers

Site	Chemical Species	May 2009	Jun 2009	Jul 2009	Aug 2009	Sep 2009	Oct 2009	Nov 2009	Dec 2009	Jan 2010	Feb 2010	Mar 2010	Apr 2010
Riverside	EC[a)]	0.680	0.407	0.348	0.437	0.798	0.403	0.705	0.794	0.459	0.509	0.245	0.352
	WSOC[a)]	*	0.795	1.824	3.375	3.587	1.481	2.043	1.982	1.218	1.611	1.413	1.791
	WIOC[a)]	*	1.447	2.073	1.975	1.481	0.960	1.497	1.640	1.167	0.851	0.501	2.470
Central LA	EC[a)]	0.415	0.342	0.378	0.396	0.790	1.078	1.417	1.294	1.382	0.901	0.652	0.423
	WSOC[a)]	*	0.806	1.291	2.102	1.828	2.215	2.310	1.978	1.975	1.754	1.499	1.312
	WIOC[a)]	*	1.183	1.836	1.837	2.013	2.117	3.183	2.827	3.669	2.632	1.760	1.038
	Levoglucosan[b)]	2.819	1.626	5.325	11.629	13.465	22.388	75.646	115.417	112.999	87.592	26.137	14.259
	17β(H)-21α(H)-30-Norhopane[b)]	0.099	0.098	0.154	0.123	0.205	0.235	0.322	0.277	0.330	0.242	0.146	0.106
	17α(H)-21β(H)-Hopane[b)]	0.084	0.086	0.122	0.114	0.191	0.198	0.253	0.226	0.242	0.215	0.152	0.104
	22S-Homohopane[b)]	0.057	0.057	0.076	0.075	0.106	0.128	0.173	0.161	0.169	0.146	0.097	0.059
	22R-Homohopane[b)]	0.046	0.050	0.061	0.057	0.086	0.108	0.141	0.131	0.140	0.128	0.082	0.047
	Benzo(b)fluoranthene[b)]	0.053	0.058	0.081	0.084	0.097	0.108	0.232	0.304	0.307	0.229	0.159	0.058
	Benzo(k)fluoranthene[b)]	0.023	0.021	0.022	0.020	0.049	0.060	0.163	0.191	0.215	0.144	0.089	0.037
	Benzo(j)fluoranthene[b)]	0.001	nd	nd	nd	0.002	0.007	0.027	0.036	0.015	0.003	nd	0.002
	Benzo(e)pyrene[b)]	0.038	0.038	0.048	0.045	0.103	0.115	0.239	0.263	0.308	0.224	0.158	0.063
	Benzo(a)pyrene[b)]	nd[c)]	nd	nd	0.001	0.022	0.073	0.092	0.105	0.072	0.056	0.020	0.011
	Indeno(1,2,3-cd)pyrene[b)]	0.037	0.030	0.042	0.049	0.071	0.124	0.246	0.226	0.244	0.165	0.106	0.058
	Benzo(ghi)perylene[b)]	0.102	0.093	0.096	0.104	0.171	0.296	0.517	0.451	0.472	0.358	0.230	0.117
	Dibenz(ah)anthracene[b)]	nd	nd	nd	nd	0.006	nd	0.006	0.008	0.009	0.002	nd	nd
	Picene[b)]	nd	nd	nd	nd	0.006	nd	0.004	nd	0.009	nd	nd	nd
	Coronene[b)]	0.035	0.052	0.055	0.055	0.082	0.161	0.233	0.236	0.264	0.184	0.132	0.089

a) Unit of microgram per cubic meters, b) Unit of nanogram per cubic meters, c) Compounds was not detected or was below detection limits, * Represents invalid data.

Table 5. Summary of previous source apportionment results for the Los Angeles Basin

	Annual Average Studies				Late Summer Studies		
	Schauer et al. (1996)		Hannigan et al. (2005)	MATES III - App VII (2008)*	Schauer et al. (2002)		Docherty et al. (2008)
Time Period	1982	1982	1993	2004-06	1993	1993	2005
Apportionment Method	CMB	CMB	CMB	CMB	CMB	CMB	AMS-PMF
Location	Central LA	Rubidoux	Basin AVG	Central LA	Central LA	Claremont	Riverside
Contributions to OC							
Mobile Sources (%)	49	34.7	13.7	59.4	34.7	22.3	na
Biomass Smoke (%)	12.2	0	8.9	4.1	0	0	na
Other Primary Sources (%)	25.5	12.7	42.7	36.5	12.7	10.8	na
Secondary Organic Aerosol (%)	13.3	52.6	34.9	0	52.6	66.9	74
Apportioned Primary OC (%)	86.7	47.4	65.1	100	47.4	33.1	26
Secondary OC (%)	13.3	52.6	34.9	0	52.6	66.9	74

* Calculated from PM2.5 mass apportionment and source profiles

3.2 Source Apportionment Models

Although there have been many intercomparisons of source apportionment models, very few intercomparisons utilize consistent data sets and consistent apportionment objectives. As a result, it is difficult to assess how well the methods agree. In the current study, the same set of molecular markers have been used in a molecular marker CMB model, a molecular marker PMF model, and a molecular marker UNMIX model to help assess the agreement of these models and to elucidate potential shortcoming of both source apportionment approaches for quantifying the sources of carbonaceous aerosols.

Table 5 summarizes some of the key source apportionment studies in the LA Basin that are used to represent sources of organic aerosols. As can be seen from these results, very inconsistent results are obtained from the different studies that were conducted using multiple methodologies at different times over the past 20 years. One key feature of several of these studies is the use of cholesterol to trace meat smoke. Since these apportionment studies, there have been a number of research projects that have demonstrated that cholesterol levels in the atmosphere in urban and remote locations are too high to be uniquely from meat cooking operations and that it is not a good tracer for meat smoke[*Dutton et al.*, 2010]. As a result, cholesterol is not used as a tracer for meat smoke in the current study. Likewise, Rutter et al. [2011] has shown that the use of trace elements to apportion the organic carbon associated with resuspended soil has considerable uncertainty due to the variability in the organic carbon in soils across urban areas. As a result, the current source apportionment model seeks to use only carbonaceous components of particulate matter to apportion OC.

3.2.1 Chemical Mass Balance Model

The molecular marker CMB model was used to apportion the source of fine particle OC for each sample day that had valid measurements. The source apportionment results were averaged to obtain monthly average source contributions that are presented in Figure 10ab and Table 6 for both sites. Six sources were quantified that contribute to PM2.5 OC at the Central LA site including diesel engines, gasoline engines, smoking engines, wood smoke, vegetative detritus and other sources. Due to co-linearity problems between the mobile sources in Riverside, only diesel engines and smoking vehicles mobile source profiles could be included in the model.. The presented smoking vehiclesshould be considered a combination of gasoline engines and smoking vehicles for the Riverside apportionment due to the removal of the gasoline vehicle profile, which was collinear with the smoking vehicle profile in the CMB model. As expected from the graphs previously discussed addressing the OC, EC and tracer trends, there is a smooth seasonal pattern in the source contribution at the Central LA site, which is not seen at the Riverside site. Nonetheless, the patterns in wood smoke are very similar at both sites, with higher winter contributions and a peak source contribution in December. Figure 11 shows the peak wood smoke events around the Christmas and New Year Holidays with very high wood smoke contributions compared to other periods of the year. Clearly, these individual events are important for the 24-hour fine particle mass standard.

To better relate the source apportionment results from the two sites, which are based on different sampling strategies, Figure 12ab compares the monthly average source apportionment results for both sites using only data from days in which samples were collected at the Riverside site (one-in-six). Though Figure 12a only has one sixth of the sample days that areshown in Figure 10a, the results are very similar to each other with the exception of December, which has very high

wood smoke on only a few days as shows on Figure 11. These results demonstrate that there are significant differences in source contributions and trends in Central LA and Riverside.

Figure 13a presents the six versions of the one-in-six day annual source apportionment averages for the Central LA site and indicates that the one-in-six representation of the annual average is in good agreement with the daily annual average. Figure 13b shows the same data averaged by day of the week. There are clear trends in biomass smoke that peak on Friday and Saturday and clear trends in mobile source emissions that reach a minimum on Sunday.

Forest fires in the LA basin reported during this study period are summarized in Table 7. Removing these days, the monthly average source apportionment results were recalculated and presented in Figure 14ab and Figure 15ab along with the averages that include the forest fires for Central LA and Riverside, respectively. Very little differences were observed in the monthly averages by removing forest fires. To better understand the impact of forest fires and how they related to the CMB results, see the PMF source apportionment section of this report.

Wintertime events with very high wood smoke were observed as indicated in Figure 11. These days represent some of the highest OC concentrations and are associated with these extreme wood smoke events. Thirteen days had OC concentrations greater than 8.0 µg per cubic meter,which is approximately 14-15 µg per cubic meter of organic compound mass. Of the 13 days, five were the very high wood smoke days, three had high wood smoke concentrations, three were impacted by forest fires, and only two of these days were not impacted by forest fires or high wood smoke events. Figure 16ab and Figure 17ab compare the monthly average OC apportionments with and without the extreme wood smoke events and emphasize the improvements to reducing high OC concentrations days and the seasonal average OC concentrations that could be achieved by winter wood burning regulations.

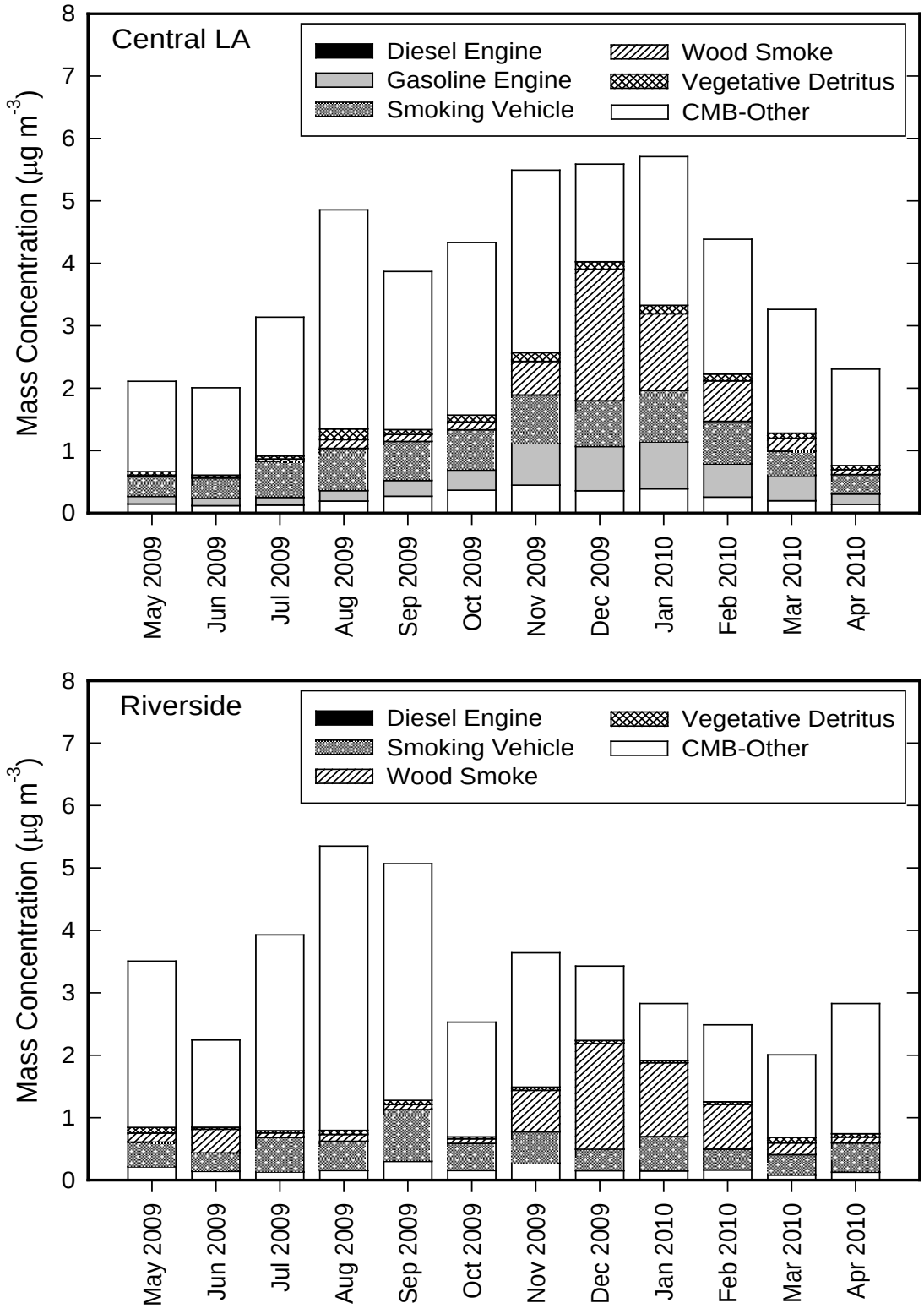

Figure 10– Monthly average OC apportionment for Central LA and Riverside from the CMB Model

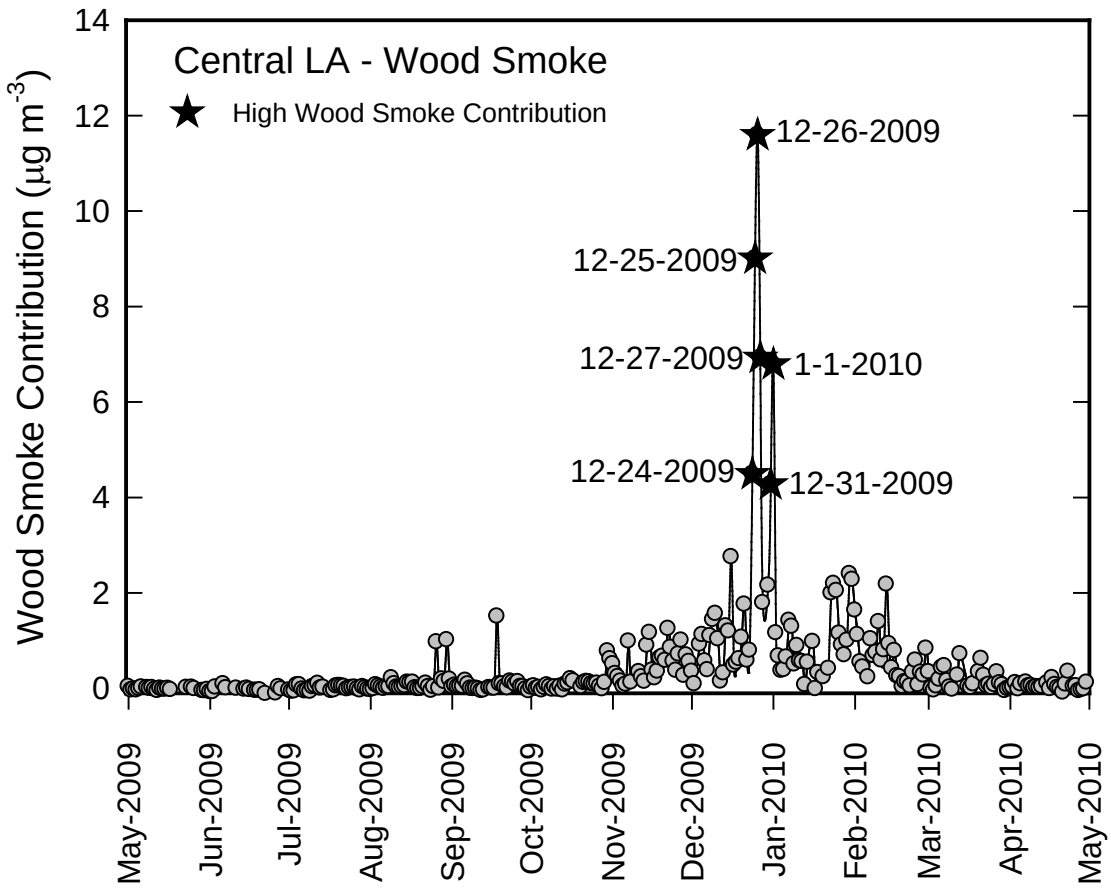

Figure 11– Time series of biomass burning at the Central LA site from the CMB Model

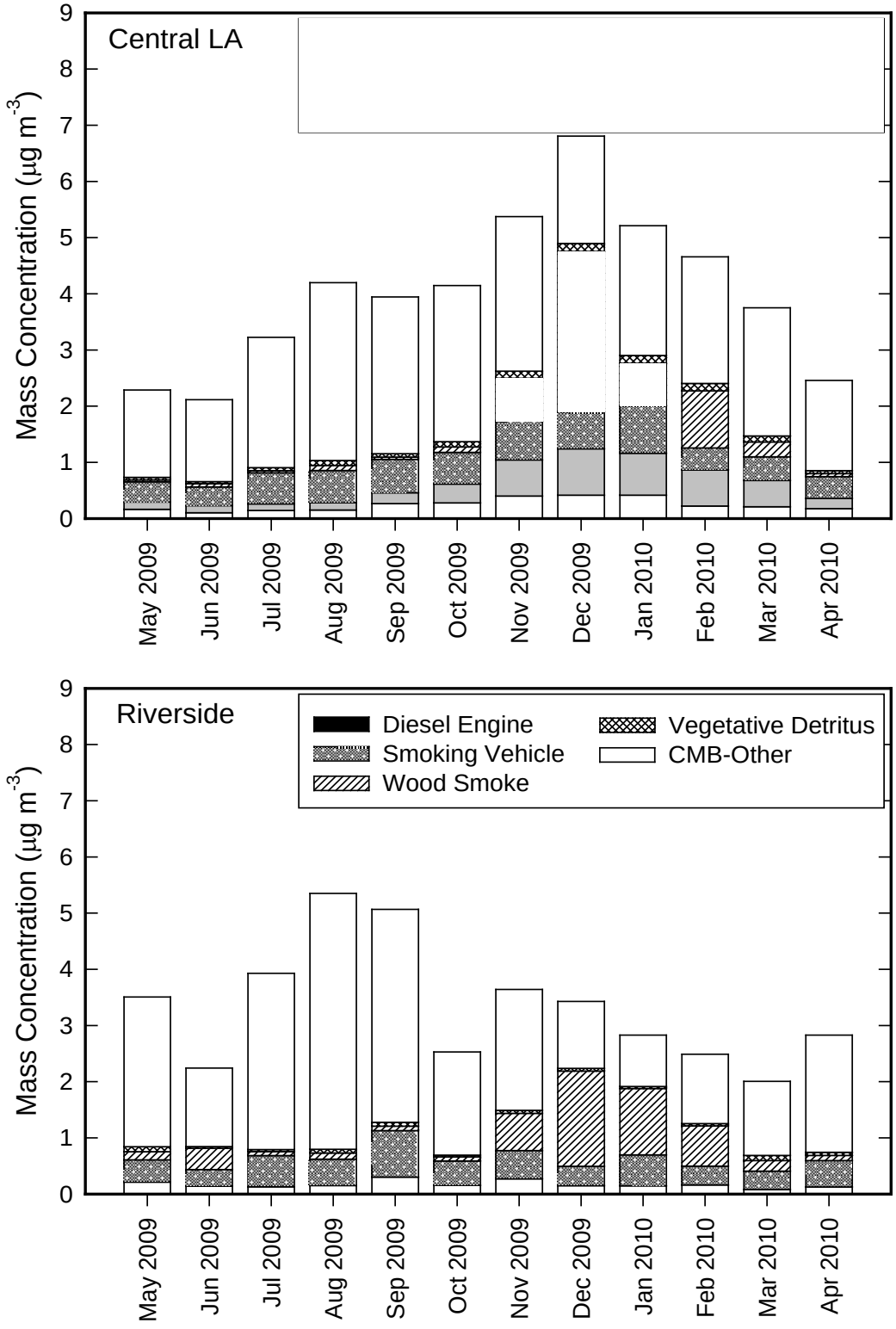

Figure 12– Monthly trends in the CMB apportionment for the 1-in-6 sampling days for both sampling sites

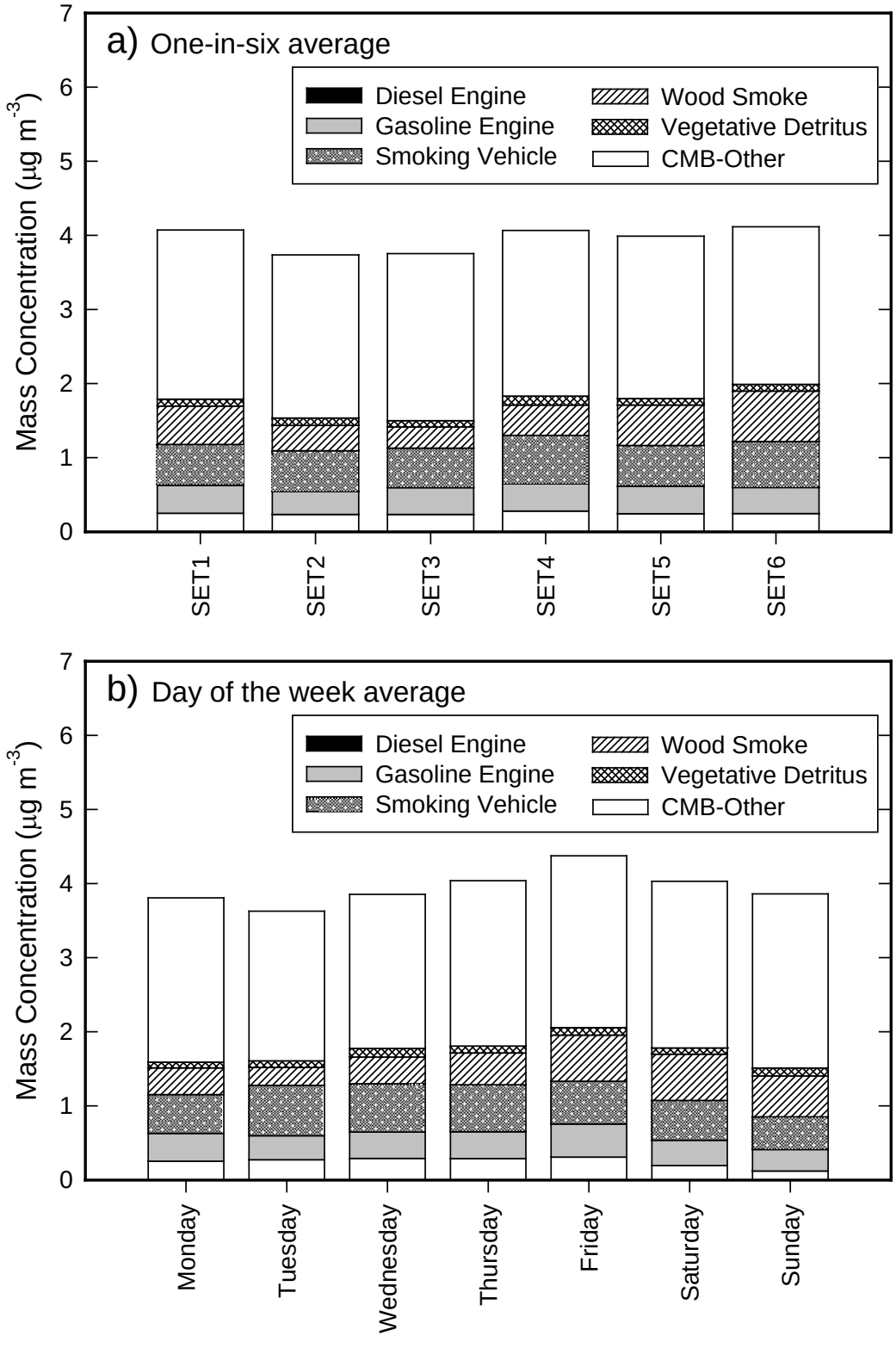

Figure 13ab – Comparison of the 1-in-6day PM2.5 OC source apportionment averages and the day of the week PM2.5 OC source apportionment averages for the Central LA site

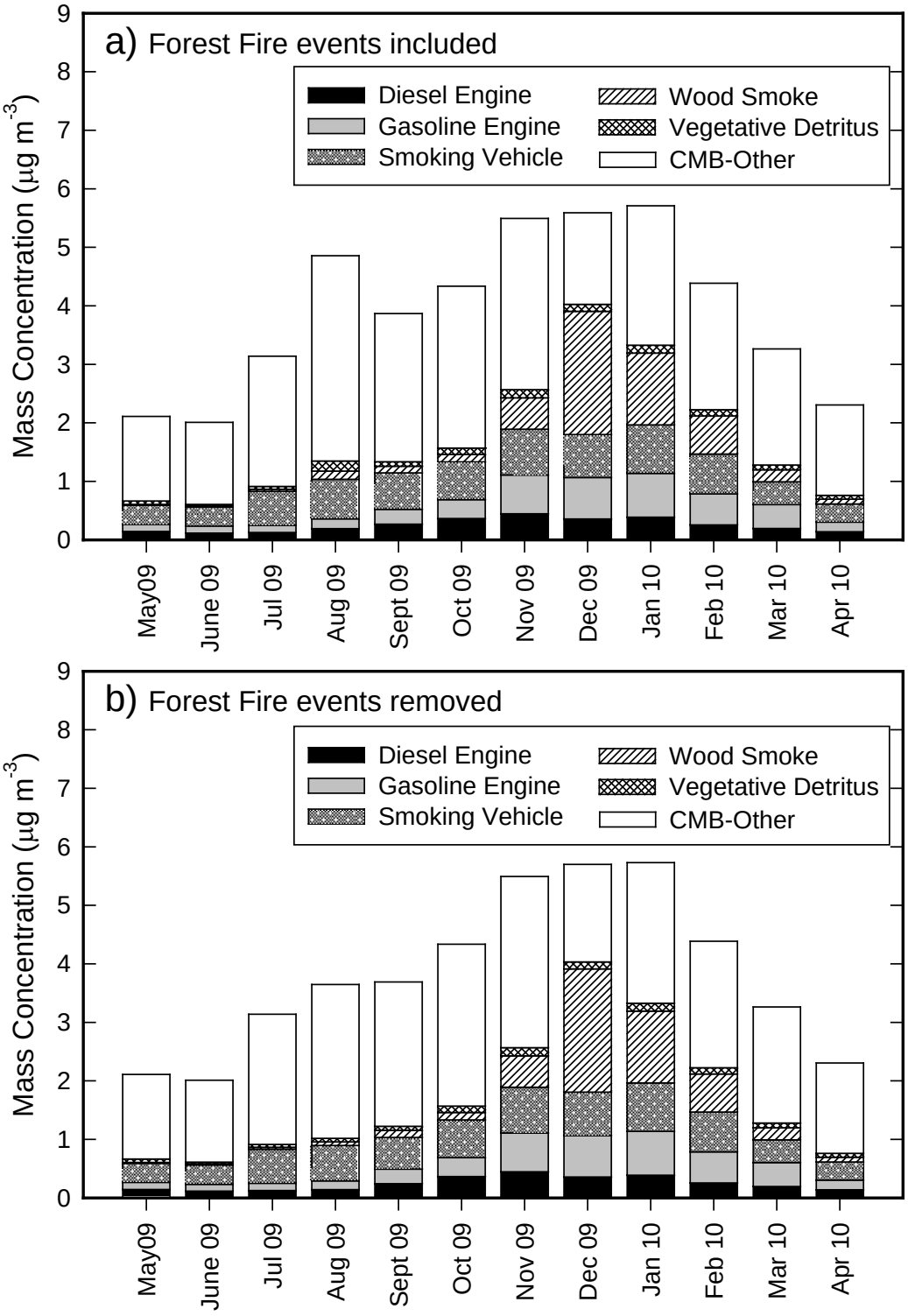

Figure 14ab –Monthly trends of PM2.5 OC apportionment with and without forest fires for the Central LA site

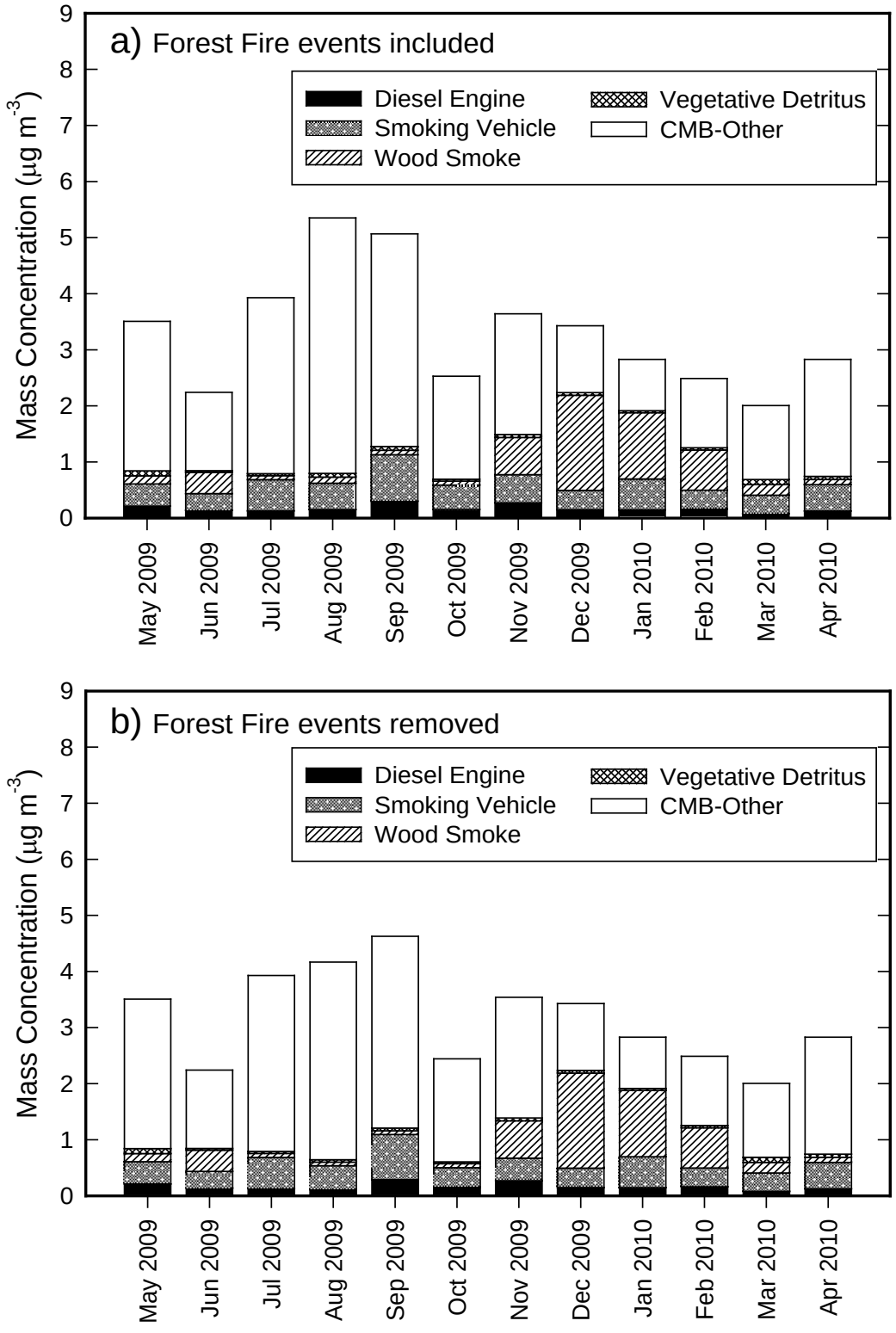

Figure 15ab –Monthly trends of PM2.5 OC apportionment with and without forest fires for the Riverside site

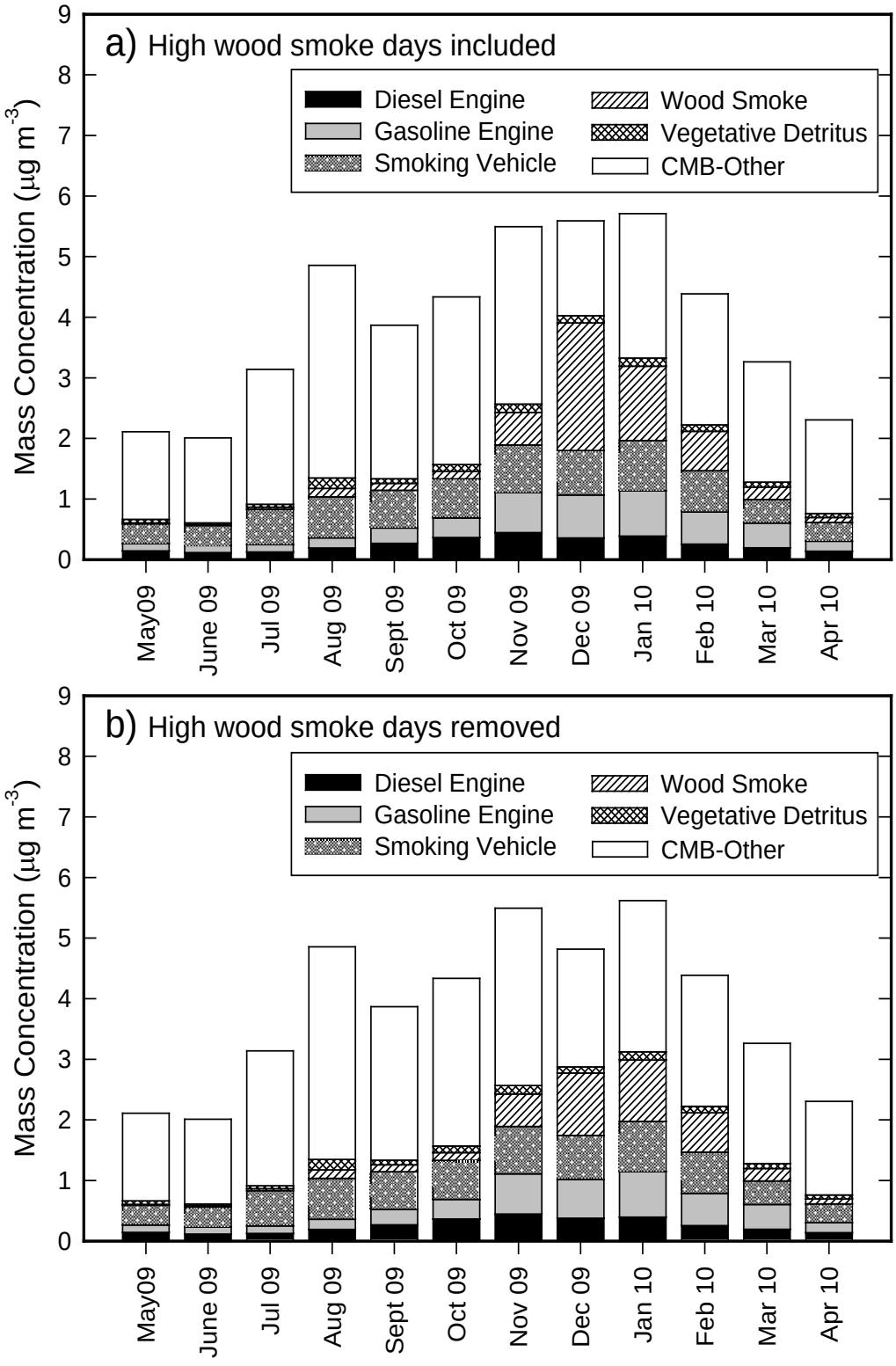

Figure 16ab –Monthly trends of PM2.5 OC apportionment with and without high wood smoke days for the Central LAsite

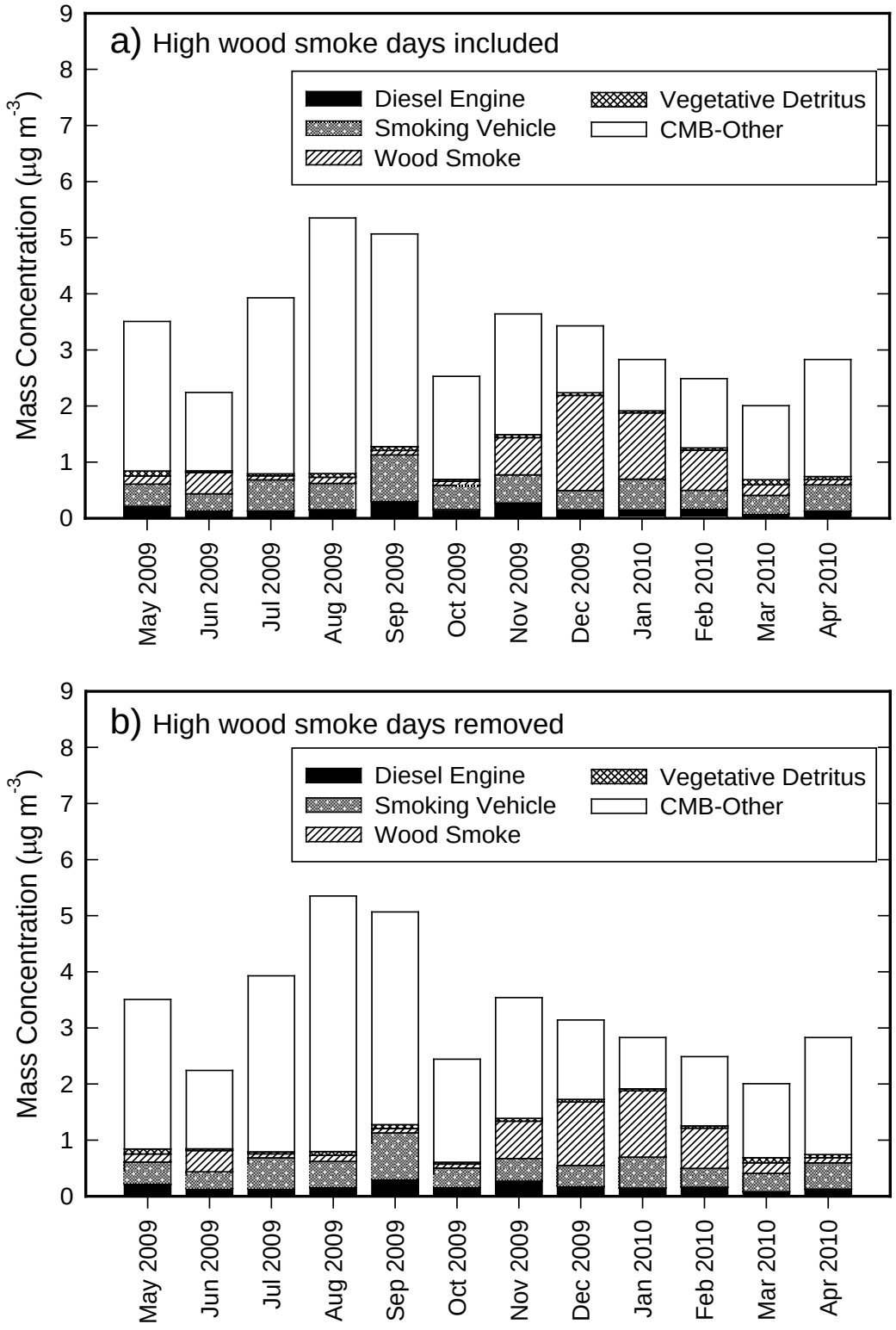

Figure 17ab –Monthly trends of PM2.5 OC apportionment with and without high wood smoke days for the Riverside site

Table 6.Summary of monthly PM2.5 OC CMB results for the Central LA and Riverside sites [value; mean (+- standard error), unit; microgram per cubic meters]

Site	Month	Samples	Total OC	Vegetative Detritus	Wood Smoke	Diesel Vehicles	Gasoline Vehicles	Smoking Vehicles	CMB-Other
Central LA	May-09	28	2.10 (+- 0.12)	0.06 (+- 0.01)	0.02 (+- 0.00)	0.14 (+- 0.01)	0.12 (+- 0.01)	0.32 (+- 0.03)	1.45 (+- 0.09)
	Jun-09	28	1.99 (+- 0.11)	0.03 (+- 0.00)	0.02 (+- 0.01)	0.12 (+- 0.01)	0.12 (+- 0.01)	0.33 (+- 0.03)	1.40 (+- 0.10)
	Jul-09	31	3.13 (+- 0.14)	0.05 (+- 0.00)	0.03 (+- 0.01)	0.13 (+- 0.01)	0.12 (+- 0.01)	0.58 (+- 0.03)	2.22 (+- 0.11)
	Aug-09	31	4.85 (+- 0.45)	0.17 (+- 0.06)	0.14 (+- 0.04)	0.19 (+- 0.03)	0.17 (+- 0.02)	0.68 (+- 0.10)	3.51 (+- 0.31)
	Sep-09	30	3.84 (+- 0.27)	0.08 (+- 0.01)	0.11 (+- 0.05)	0.27 (+- 0.04)	0.25 (+- 0.07)	0.62 (+- 0.06)	2.53 (+- 0.18)
	Oct-09	29	4.33 (+- 0.38)	0.11 (+- 0.01)	0.13 (+- 0.03)	0.36 (+- 0.04)	0.32 (+- 0.05)	0.65 (+- 0.08)	2.77 (+- 0.25)
	Nov-09	28	5.49 (+- 0.27)	0.14 (+- 0.01)	0.54 (+- 0.06)	0.44 (+- 0.05)	0.66 (+- 0.06)	0.78 (+- 0.07)	2.93 (+- 0.14)
	Dec-09	29	5.59 (+- 0.44)	0.12 (+- 0.01)	2.11 (+- 0.51)	0.36 (+- 0.03)	0.71 (+- 0.06)	0.74 (+- 0.07)	1.67 (+- 0.19)
	Jan-10	27	5.71 (+- 0.37)	0.13 (+- 0.01)	1.23 (+- 0.25)	0.39 (+- 0.04)	0.75 (+- 0.06)	0.83 (+- 0.06)	2.40 (+- 0.25)
	Feb-10	27	4.39 (+- 0.37)	0.11 (+- 0.01)	0.65 (+- 0.10)	0.25 (+- 0.03)	0.53 (+- 0.06)	0.68 (+- 0.07)	2.16 (+- 0.21)
	Mar-10	26	3.26 (+- 0.25)	0.08 (+- 0.01)	0.21 (+- 0.04)	0.20 (+- 0.02)	0.41 (+- 0.04)	0.39 (+- 0.05)	1.98 (+- 0.17)
	Apr-10	27	2.30 (+- 0.17)	0.06 (+- 0.01)	0.08 (+- 0.02)	0.14 (+- 0.02)	0.17 (+- 0.02)	0.31 (+- 0.03)	1.54 (+- 0.12)
	All study period	341	3.92 (+- 0.11)	0.10 (+- 0.01)	0.46 (+- 0.06)	0.25 (+- 0.01)	0.36 (+- 0.02)	0.58 (+- 0.02)	2.23 (+- 0.06)
Riverside	May-09	4	3.85 (+- 0.46)	0.09 (+- 0.05)	0.11 (+- 0.09)	0.25 (+- 0.06)		0.64 (+- 0.13)	3.09 (+- 0.32)
	Jun-09	5	2.65 (+- 0.57)	0.03 (+- 0.01)	0.05 (+- 0.33)	0.14 (+- 0.05)		0.24 (+- 0.10)	0.93 (+- 0.48)
	Jul-09	5	3.64 (+- 0.37)	0.04 (+- 0.01)	0.05 (+- 0.02)	0.14 (+- 0.02)		0.54 (+- 0.09)	3.12 (+- 0.32)
	Aug-09	5	5.91 (+- 0.92)	0.05 (+- 0.01)	0.11 (+- 0.03)	0.16 (+- 0.03)		0.40 (+- 0.08)	5.36 (+- 0.86)
	Sep-09	5	5.18 (+- 0.59)	0.05 (+- 0.02)	0.08 (+- 0.02)	0.31 (+- 0.04)		0.76 (+- 0.16)	3.60 (+- 0.52)
	Oct-09	5	2.51 (+- 0.69)	0.03 (+- 0.01)	0.06 (+- 0.03)	0.18 (+- 0.07)		0.36 (+- 0.12)	1.75 (+- 0.55)
	Nov-09	5	3.49 (+- 0.62)	0.05 (+- 0.01)	0.78 (+- 0.08)	0.13 (+- 0.11)		0.21 (+- 0.18)	2.14 (+- 0.48)
	Dec-09	4	3.47 (+- 0.73)	0.05 (+- 0.01)	1.22 (+- 0.57)	0.14 (+- 0.03)		0.25 (+- 0.14)	0.68 (+- 0.56)
	Jan-10	4	2.81 (+- 0.97)	0.04 (+- 0.01)	0.82 (+- 0.60)	0.15 (+- 0.06)		0.57 (+- 0.11)	0.52 (+- 0.47)
	Feb-10	5	2.32 (+- 0.53)	0.04 (+- 0.01)	0.59 (+- 0.20)	0.17 (+- 0.04)		0.33 (+- 0.09)	1.05 (+- 0.26)
	Mar-10	5	1.64 (+- 0.45)	0.04 (+- 0.04)	0.15 (+- 0.07)	0.09 (+- 0.01)		0.33 (+- 0.09)	0.96 (+- 0.38)
	Apr-10	5	2.31 (+- 0.64)	0.05 (+- 0.01)	0.09 (+- 0.03)	0.11 (+- 0.01)		0.45 (+- 0.12)	1.83 (+- 0.50)
	All study period	57	3.29 (+- 0.22)	0.04 (+- 0.01)	0.13 (+- 0.09)	0.14 (+- 0.02)		0.40 (+- 0.04)	2.12 (+- 0.20)

Table 7.Five reported large wildfires in California that occurred during the study

Fire Name	County	Location	Loss Cost	Acreage	Fire Duration	Date Started
Backbone	Trinity County	Trinity Alps Wilderness	$16,897,750	6,324	20 days	July 7 2009
Big meadow	Mariposa County	Foresta Community	$16,947,244	7,418	25 days	August 26 2009
Knight	Tuolumne County	10 miles north of Twain Harte, near Mount Knight on the Middle Fork of the Stanislaus River	$12,122,452	6,130	25 days	July 26 2009
La Brea	Santa Barbara County	21 miles east of Santa Maria	$34,888,910	89,489	44 days	August 8 2009
Station	Los Angeles County	Hwy 2, 1.5 miles north of USFS Angeles Crest Station	$94,739,316	160,577	41 days	August 26 2009

Sources;1) Large Fire Cost Review for FY 2009 (US Forest Service; Secretary of Agriculture's Independent Large Cost Fire Review Panel)
2) California Department of Forestry and Fire Protection (http://bof.fire.ca.gov/incidents/incidents_archived)
*From the beginning of July through late November, 63 wildfires were activated in the California during the year 2009

3.2.2 Positive Matrix Factorization Model

Determination of the optimal number of factors is the critical step in PMF model whose result depends on the input number of factors and the imposed control values of rotation. Although mathematical diagnostics for the goodness of model fit and change of Q-values can be used as a criterion to investigate the optimal number of factors, the criterion for selecting the optimal solution should be determined by the interpretability of the PMF model results. Rotational ambiguity is a potential problem with the PMF procedure and can lead to errors in the identified source factors, and must be addressed to assure an optimal solution is obtained.

In the current study, PMF was first performed using the Central LA site data to determine an optimal solution and then the model was used to analyze the Riverside data, which contained considerably less observations than the Central LA data set. For the Central LA data, factors from 4 through 13 were explored and the results of 5, 6, and 7 factors led to physically reasonable sources in regards to the nature of the profiles and source contributions. Each of the extracted factors, which were very similar in the different solutions, had a distinctive group of associated molecular markers,which were related to a specific source category. The main difference between each of 5 and 6 factor models was splitting of the mobile factor in the five-factor model into two different mobile factors in the six-factor models. Although the second mobile factorwas characterized by EC and hopanes, it was not clear that this factor could be clearly dominated by a single mobile source. In the seven-factor model, the additional factor that emerged was second biomass smoke, whose key chemical species was oleic acid, linoleic acid, and linolenic acid. This source profile could not be adequately associated with a specific component of biomass burning. For this reason, the five-factor model was chosen as the optimal solution for the Central LAdata set. To investigate rotational ambiguity of the Central LA-PMF result, the FPEAK parameter was applied using different ranges of values from -1.0 to 1.0 and the results were compared to the base case solution. EC consistently contributed to the two SOC factors and was interpreted as an error in the derived source profiles. To pull down EC concentrations in the profiles, the FKEY matrix was examined by adjusting values from 3 through 7. EC in the anthropogenic SOC (SOC1) was completely pulled down without any other significant changesin the source profiles and source contributions, but the EC in the biogenic SOC (SOC2) factor was not impacted by the FKEY. The final solution for the Central LA-PMF model included the following five factors: mobile source, wood smoke, primary biogenic emissions, SOC1, and SOC2. The PMF derived source contributions of each factor are shown in Figure 18. Figures 19 and 20 present the source profiles derived from the PMF model for the five factors in the optimized PMF model.

The PMF model was also applied to investigate sources of the Riverside organic compounds using the same procedure as the Central LA-PMF. Because there was less precision and strength of the measurements at Riverside,PM2.5 OC contributions from four, five, and six factor PMF solutions were explored. The five factor model and the value of FPEAK=0.0 provided physically reasonable solutions. Molecular markers characterizing of each factor in the Riverside profiles were very similar to those of the Central LA-PMF profiles and are compared in Figures 21-22.

Mobile Factor

Annually, the mobile factor is characterized by high concentrations of hopanes, steranes and EC in both downtown and downwind LA. The resolved mobile source profile containslarger molecular PAHs, especially benzo(ghi)perylene, which are common in emissions from gasoline

powered engines. Due to the fact that EC and other molecular markers such as hopanes and steranes are associated with gas and diesel emission from internal combustion engines [*Schauer et al.*, 1996], these molecular markers have been used as indicatorsfor mobile sources in numerous CMB model studies. Moreover, the separated molecular markers group, that has far less EC and much higher hopanes and heavy-PAHs, has been used as an indicator to split different types of mobile emissions in the factor analysis based model because EC is more likely to be dominated by diesel emissions. But in this study, the separated mobile profiles are insufficient to draw distinctive characterization of mobile emissions.

The mobile factor contributes 31% and 33% to the ambient OC in Central LA and Riverside, respectively (Figures 23-24 and Table 8), and also describes 51% and 14% to the apportioned EC and WSOC, respectively, in the downtown LA area (Figure 25). The average source contributions to OC from this mobile factor are compared between weekday and weekend in Figures 23-25. The high weekday/weekend ratio indicates that this mobile factor is dominated from mobile source emissions primarily operating on weekdays. The seasonal patterns for the absolute mass fraction of this factor are different between Central LA and Riverside.

Wood Smoke Factor

The wood smoke factor is characterized by high contribution of levoglucosan in both sites. Levoglucosan was identified as a specific and general molecular marker indicator for wood burning [*Simoneit et al.*, 1999]. It has been applied as a unique marker in source profiles for many source apportionment studies using the CMB model, and has been used as an indicator for the wood smoke source in PMF model studies [*Jaeckels et al.*, 2007; *Shrivastava et al.*, 2007; *Zhang et al.*, 2009]. This factor has a strong seasonal pattern at both sites with very high contributions occurring in November through February and very low contributions during the remaining months (Figures23-24). Comparison of observed levoglucosan as an indicator of wood smoke and OC contributions from wood smoke in Central LA and Riverside are plotted in Figure 26. The temporal patterns of the observed levoglucosan concentrations in Central LA and Riverside agree fairly well but the correlation of the PMF resolved source contributions is moderate, suggesting the limited number of observations of wood smoke events at the Riverside site may be influencing the PMF model and may be insufficient to draw conclusion about daily wood smoke contributions at the Riverside site.

Annually, the wood smoke factor contributes 9% and 9% to the ambient OC in Central LA and Riverside, respectively, and contributes 10% and 9% to the ambient EC and WSOC, respectively, in Central LA area.

Primary Biogenic Source

Several wildfires were observed in the LA air basin during this study period, including the Station fire that was the largest wildfire during the fire season[*Wonaschütz et al.*, 2011]. The primary biogenic source factor concentration correlated with reported wildfires. These extreme events can have a significant impact on the PMF model and impact the stability of related factors. In order to investigate the effect of these extreme observations, the sensitivity of the PMF model to these events was evaluated by removing these events from the model. When the forest fires events were removed from the PMF model, the resolved source profiles and average source contributions did not change except for the removal of theevent contributions. Although this factor is clearly impacted by the forest fires, the source profile has very little levoglucosan and has significant contributions on days when wildfires were not observed. For this reason, this

factor is likely to be impacted by several sources, such as vegetative detritus and meat cooking, and is combined in this factor because it is characterized by high contributions of n-alkane and n-alkanoic acid, especially odd-alkane and odd-alkanonic acid.

Annually, the primary biogenic emissions factor contributes 19% and 18% to the ambient OC in Central LA and Riverside, respectively, and contributes to 16% and 20% to the apportioned EC and WSOC, respectively, at the Central LA site.

Secondary Organic Aerosols Factor

Two factors of secondary organic aerosols were identified at both sites. The first SOC factor has large summer contributions and is characterized by high concentrations of phthalic acid, succinic acid, glutaric acid, 2,3-dihydroxy-4-oxopentanoic acid, 3-hydroxyglutaric acid and 2-hydroxy-4,4-dimethylglutaric acid. In contrast, the second SOC factor had peak contributions in spring and is characterized by high concentrations of pinonic acid, pinic acid andmethylthreitols. The temporal trends of source contributions are very similar between two sites. Pinonic acid and methylthreitols, which are formed in the atmosphere from the oxidation of biogenic precursor such as α-pinene and isoprene, are used as indicators for biogenic secondary organic aerosols. In contrast, 2,3-dihydroxy-4-oxopentanoic acid and phthalic acid are proposed as indicators of anthropogenic secondary organic aerosols[*Kleindienst et al.*, 2007; *Sheesley et al.*, 2004]. Thus SOC1 is identified as anthropogenic SOC, and SOC2 indicates biogenic SOC.

The total annual average SOC factors contribute approximately 41% and 40% to the ambient fine OC in Central LA and Riverside, respectively. The SOC factors also account for 16% and 57% of the apportioned EC and WSOC respectively, in Central LA site.

Figure 27 shows the comparison of OC source contributions using the molecular marker PMF and CMB for Central LA and Riverside. Although the year-long average contribution to OC is very similar between the two sites, the correlation of daily PMF source contributions is only moderate. Figure 28ashows a strong agreement between the monthly average contribution of OC from SOC calculated by the PMF model and the monthly average non-biomass burning WSOC. Figure 28b compares the unapportioned OC from the CMB model minus the biogenic source derived by the PMF model with non-biomass burning WSOC. Good agreement is observed for all months except August and December, which are the months impacted by forest fires and extreme wood smoke events.

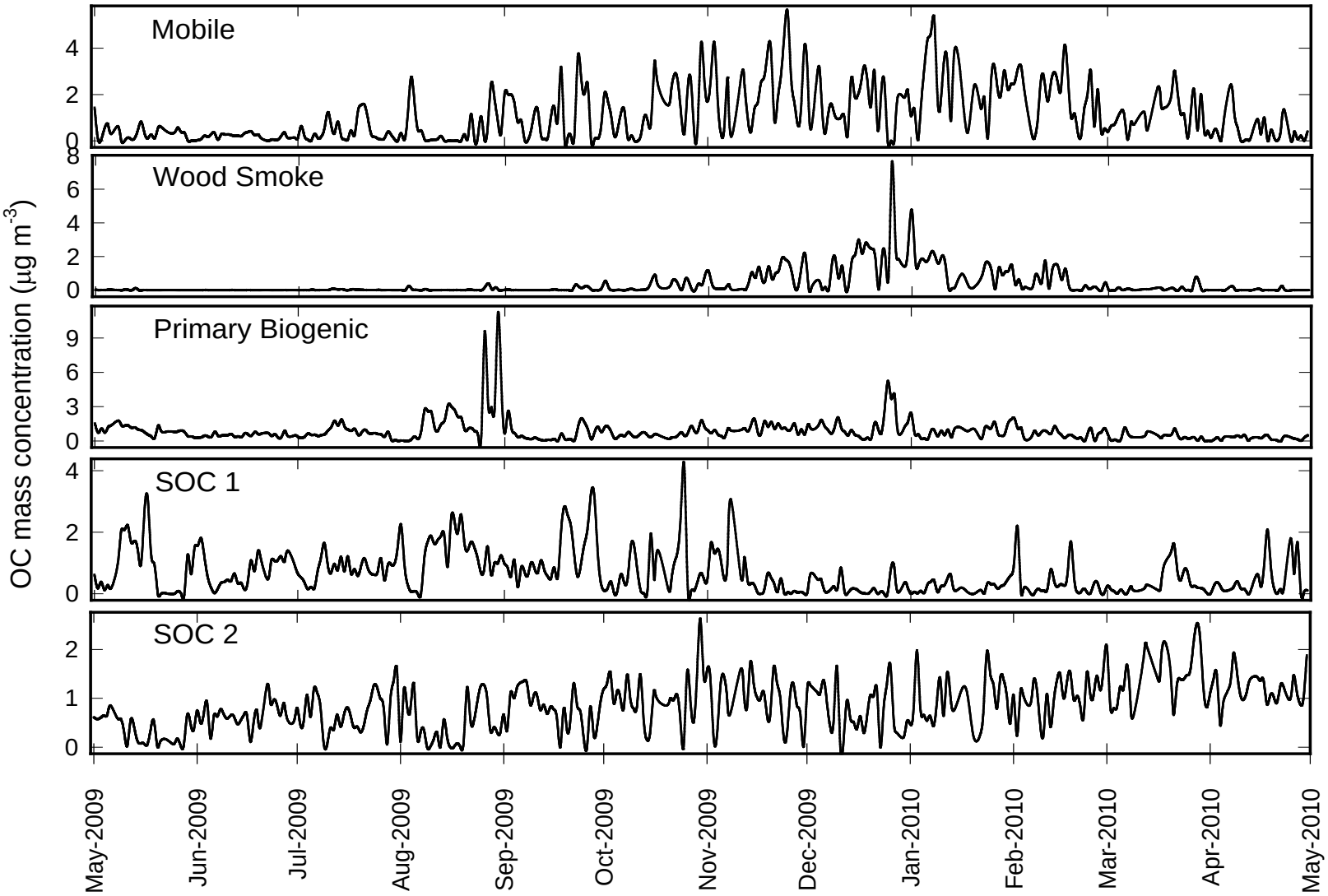

Figure 18– Molecular marker PMF source contributions to 5-factor model for Central LA

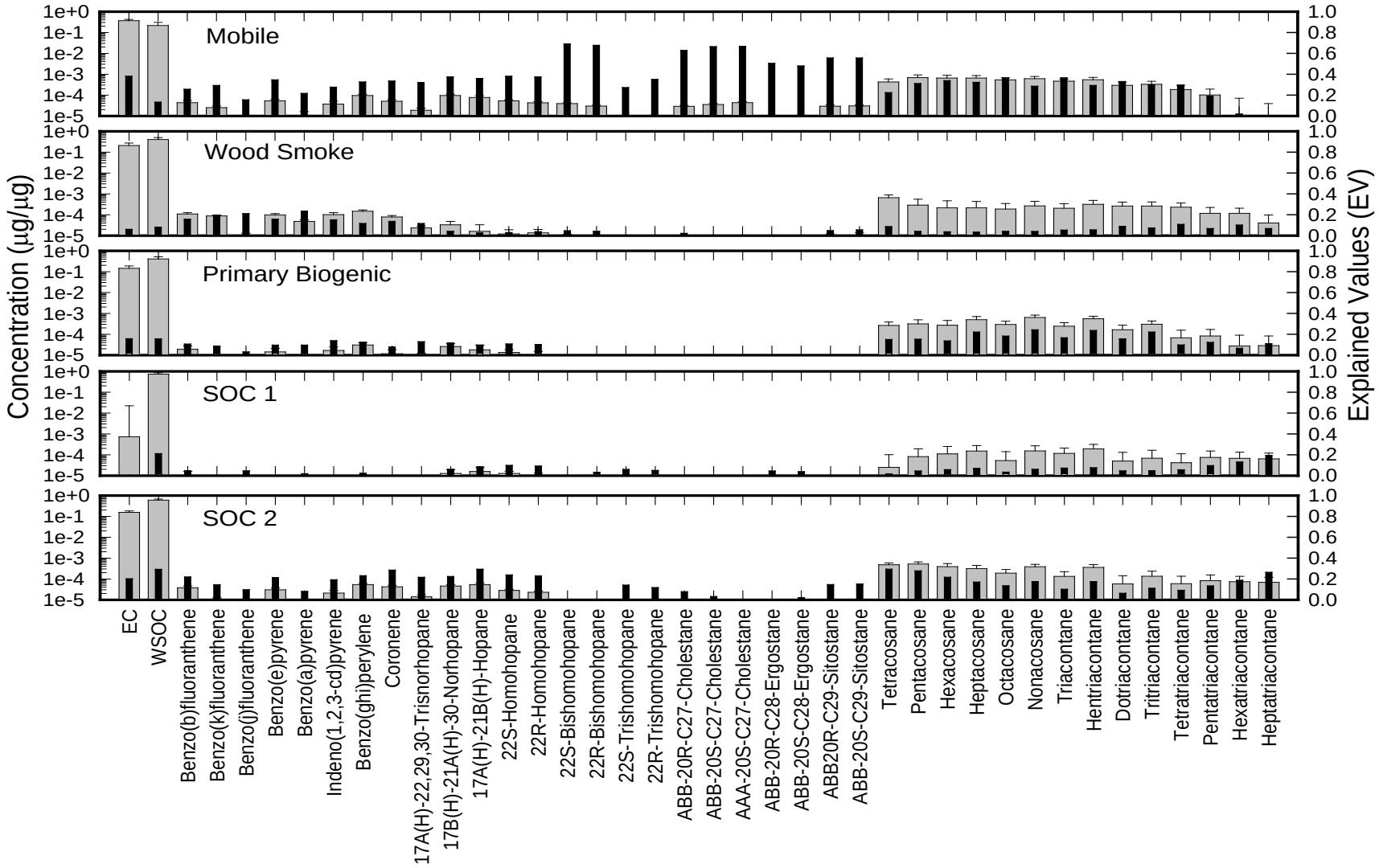

Figure 19– Molecular markers PM2.5 source profiles for 5-factor model in Central LA -Group 1

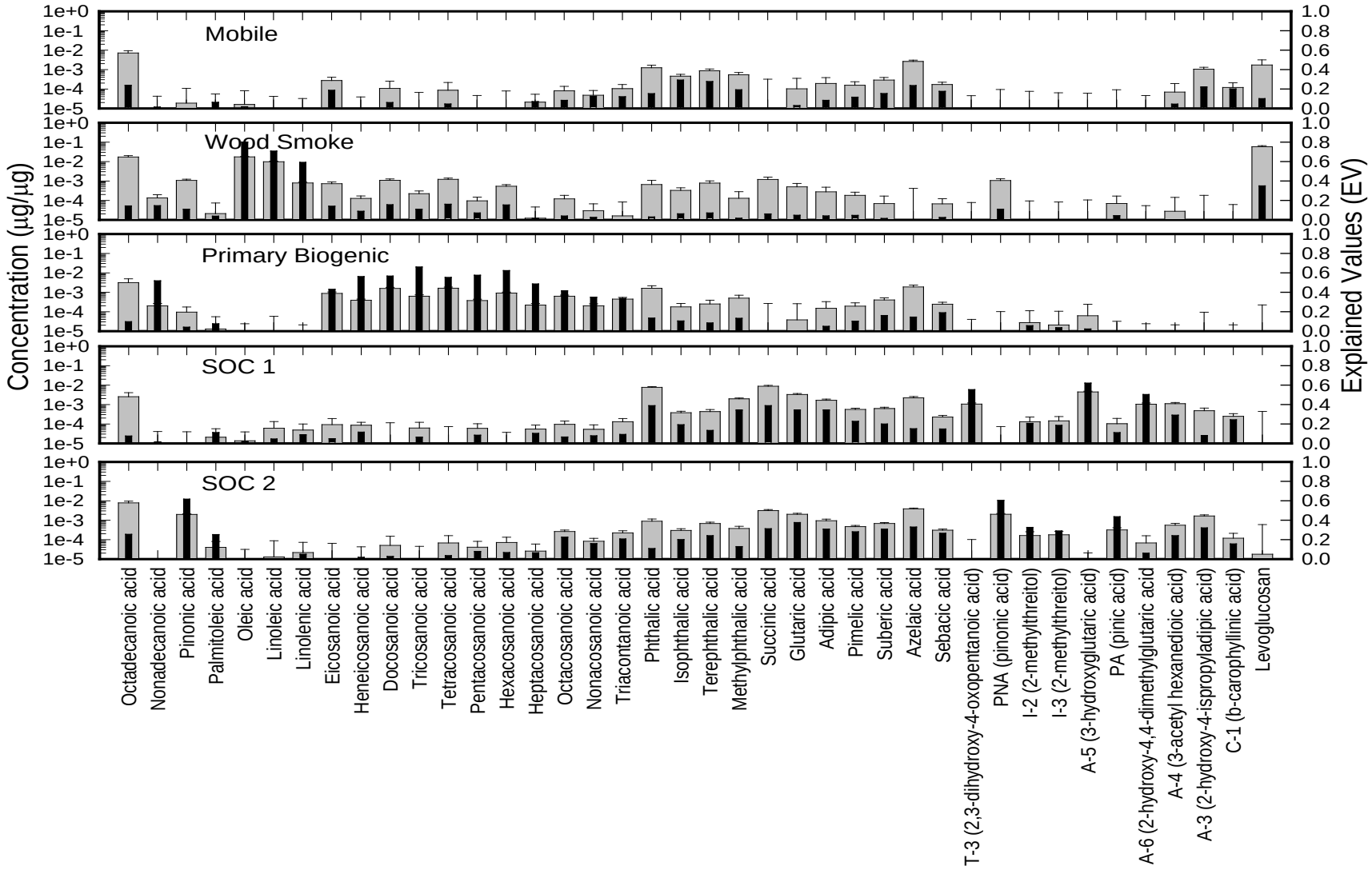

Figure 20– Molecular markers PM2.5 source profiles for 5-factor model in Central LA - Group 2

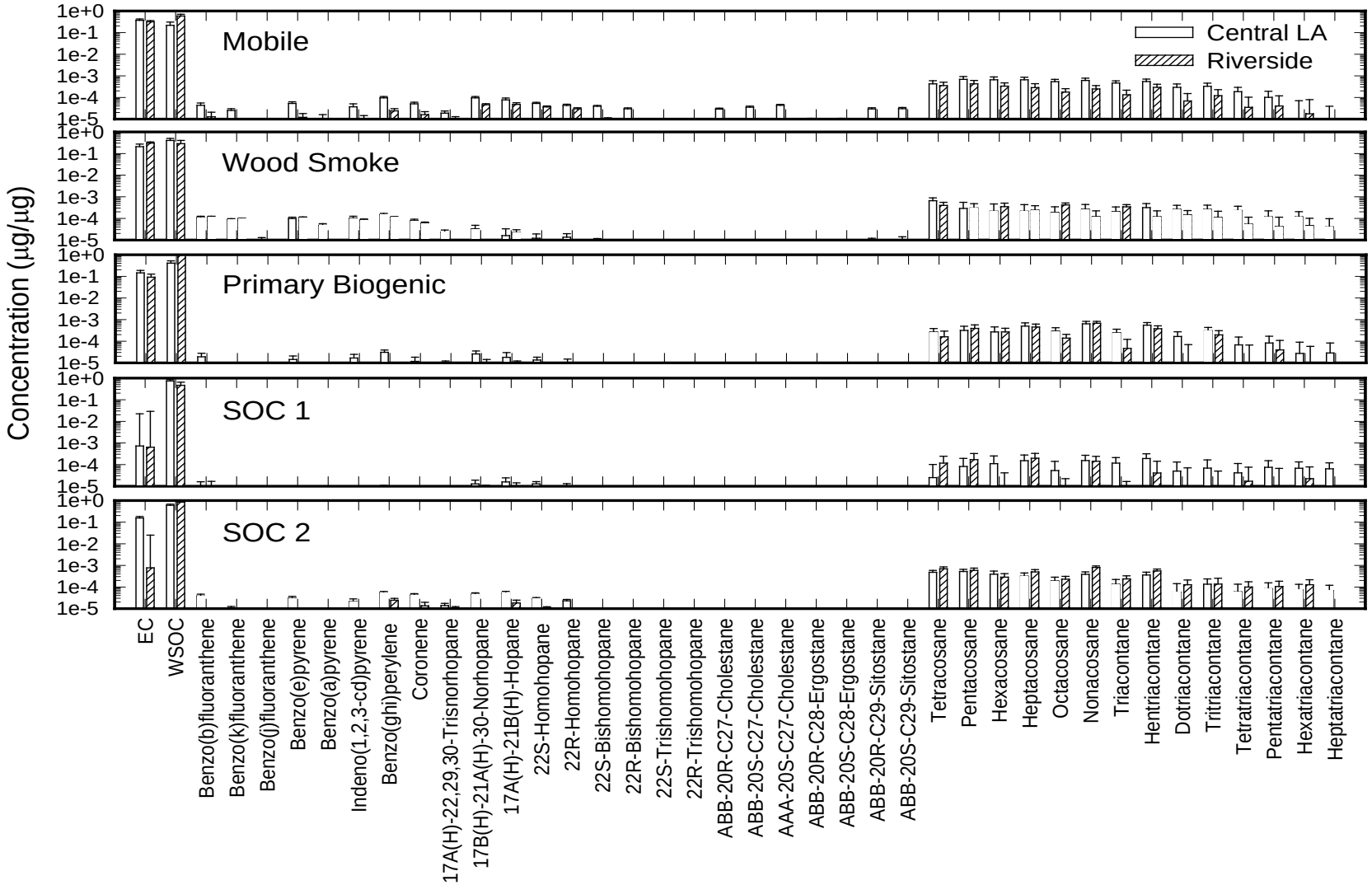

Figure 21– Comparison of molecular marker PMF source profiles for PM2.5 OC for Central LA and Riverside sites -Group 1

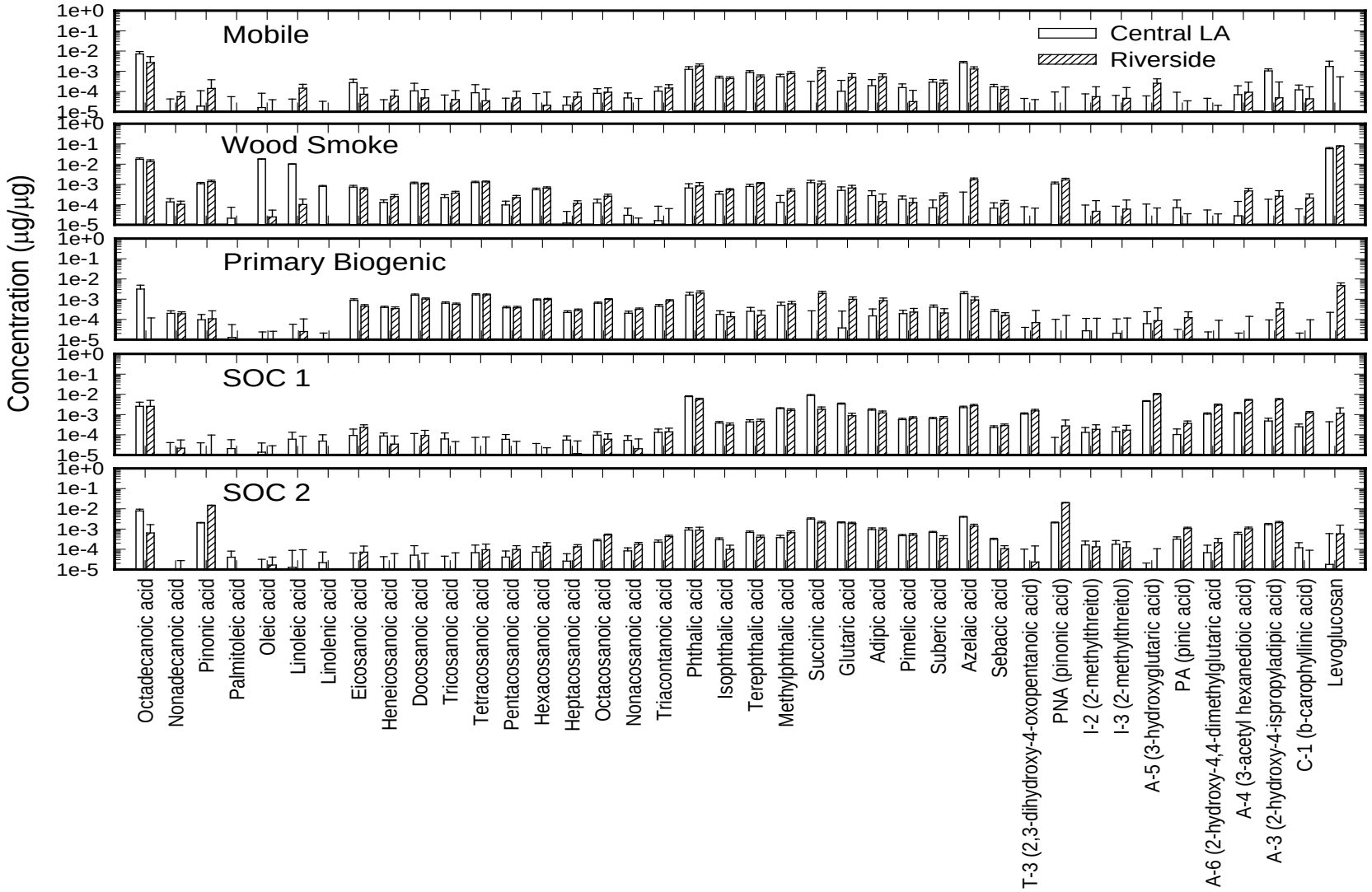

Figure 22– Comparison of molecular marker PMF source profiles for PM2.5 OC for Central LA and Riverside Sites - Group 2

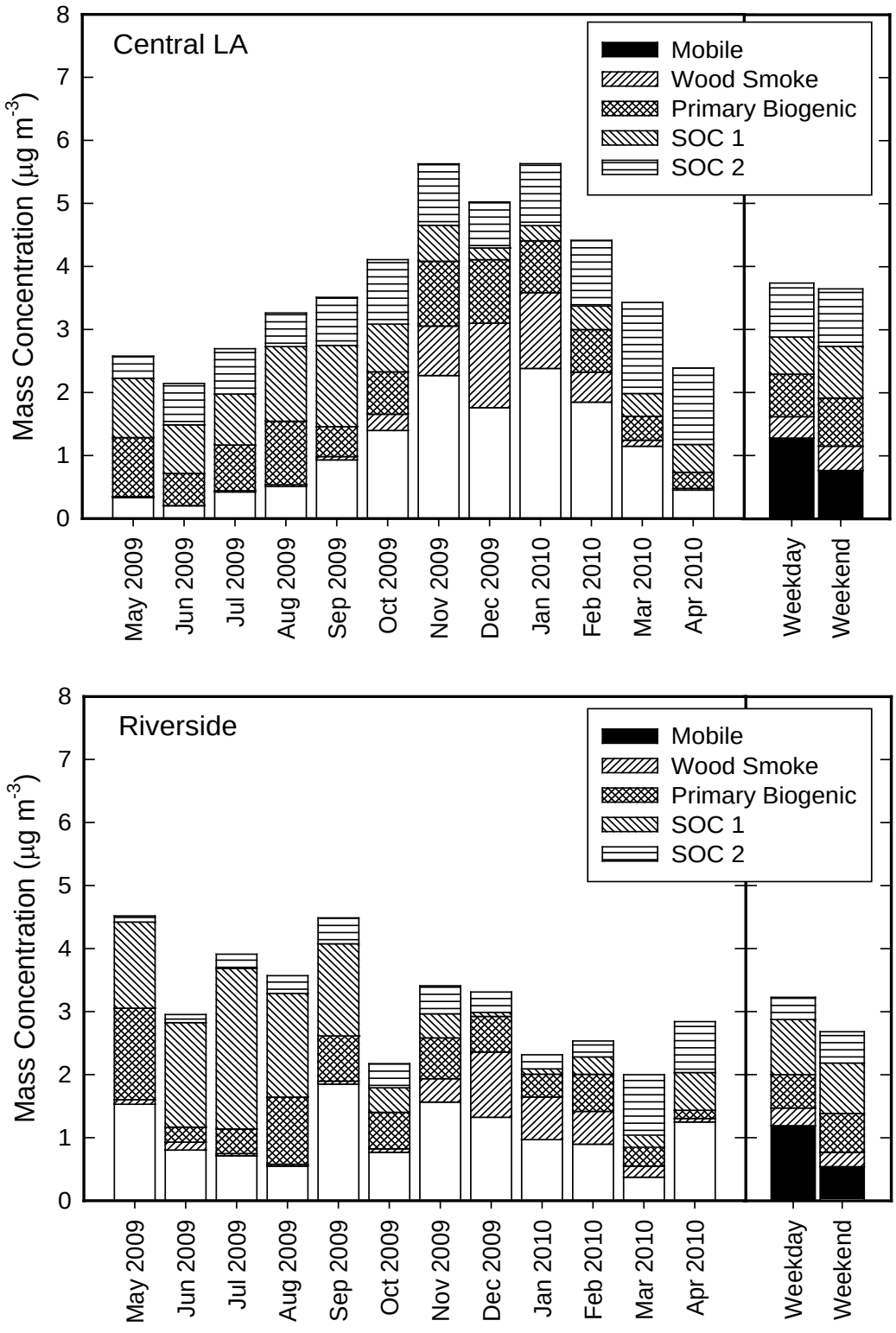

Figure 23– Monthly average molecular marker PMF model apportionment results for Central LA and Riverside

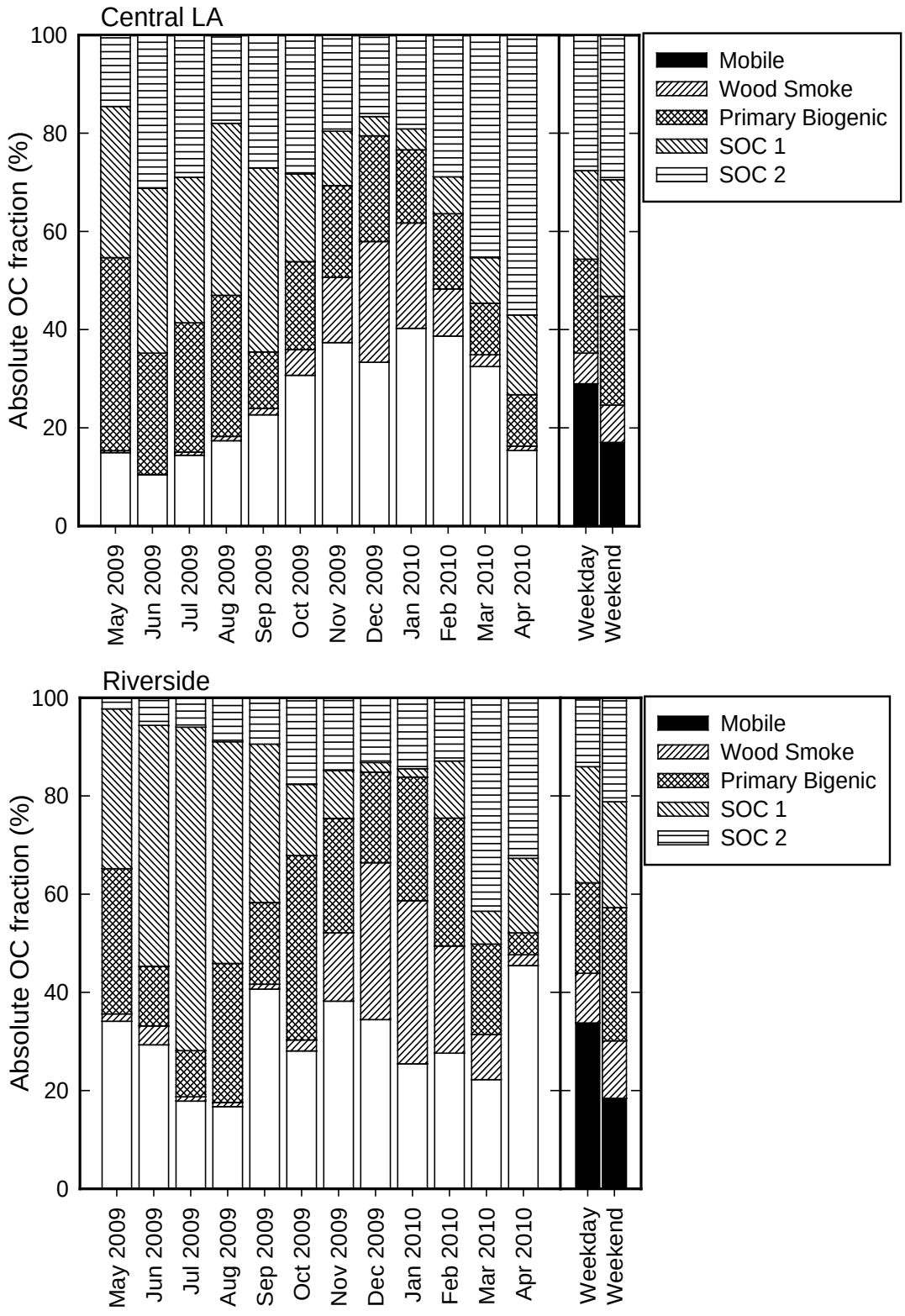

Figure 24– Relative monthly average molecular marker PMF model apportionment results for PM2.5 OC Central LA and Riverside

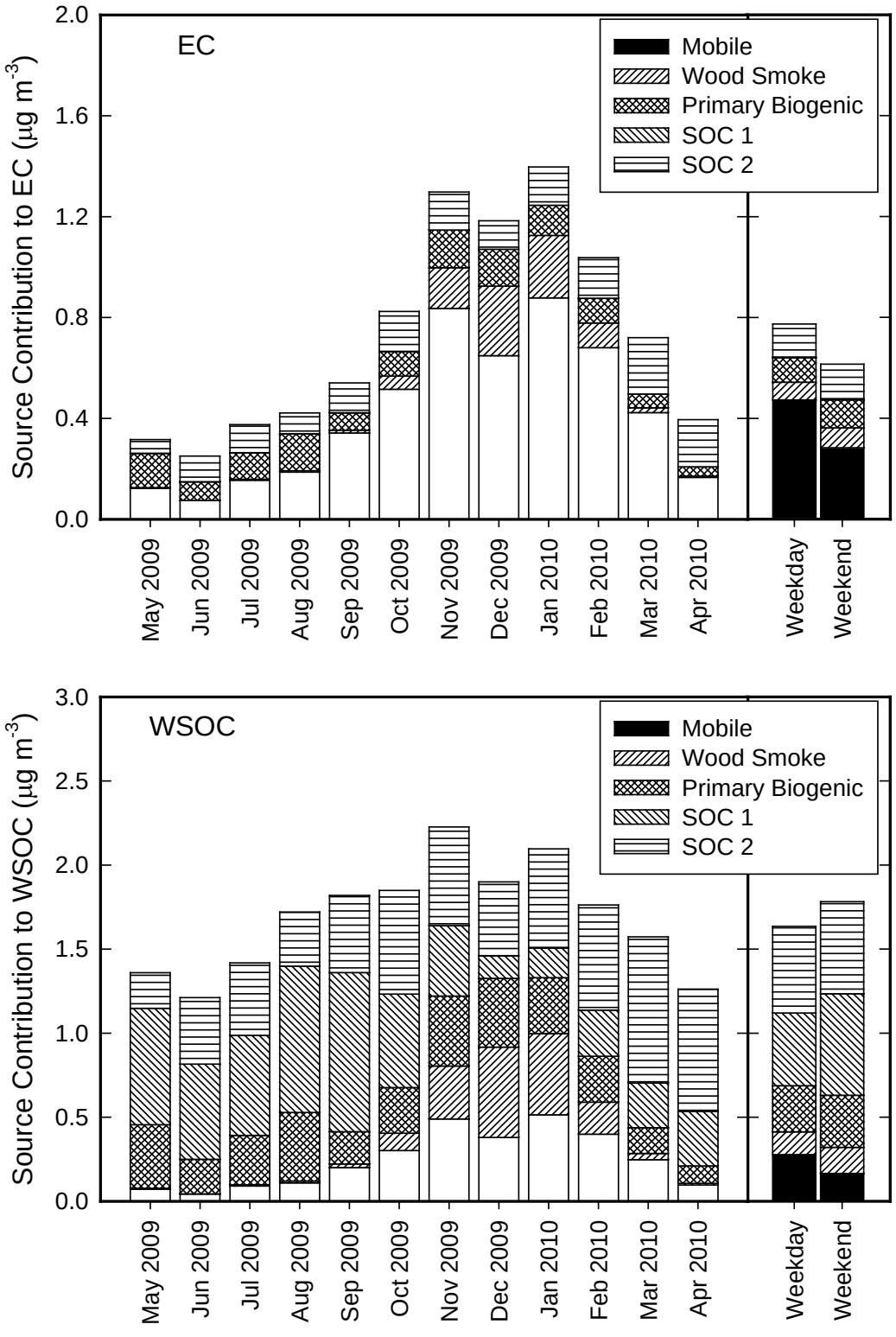

Figure 25– Relative monthly average molecular marker PMF model apportionment results for PM2.5 EC and WSOC Central LA and Riverside

Table 8.Monthly source contributions to PM2.5 OC deduced from PMF [(mean (+- standard error), unit; microgram per cubic meters]

Site	Month	Samples	Mobile	Wood Smoke	Primary Biogenic	SOC 1	SOC 2
Central LA	May-2009	28	0.33 (+- 0.06)	0.01 (+- 0.00)	0.93 (+- 0.08)	0.94 (+- 0.17)	0.35 (+- 0.05)
	Jun-2009	28	0.20 (+- 0.02)	0.00 (+- 0.00)	0.51 (+- 0.03)	0.77 (+- 0.09)	0.66 (+- 0.04)
	Jul-2009	31	0.42 (+- 0.08)	0.02 (+- 0.00)	0.72 (+- 0.08)	0.81 (+- 0.06)	0.72 (+- 0.07)
	Aug-2009	20[a)]	0.51 (+- 0.16)	0.03 (+- 0.01)	1.01 (+- 0.19)	1.18 (+- 0.17)	0.53 (+- 0.10)
	Sep-2009	26[a)]	0.93 (+- 0.21)	0.05 (+- 0.02)	0.47 (+- 0.10)	1.29 (+- 0.18)	0.76 (+- 0.08)
	Oct-2009	29	1.40 (+- 0.21)	0.26 (+- 0.05)	0.67 (+- 0.07)	0.76 (+- 0.17)	1.02 (+- 0.09)
	Nov-2009	28	2.27 (+- 0.27)	0.78 (+- 0.12)	1.03 (+- 0.08)	0.57 (+- 0.13)	0.98 (+- 0.09)
	Dec-2009	25[b)]	1.76 (+- 0.18)	1.34 (+- 0.20)	1.01 (+- 0.12)	0.18 (+- 0.04)	0.73 (+- 0.09)
	Jan-2010	26[b)]	2.38 (+- 0.26)	1.20 (+- 0.13)	0.82 (+- 0.09)	0.24 (+- 0.04)	0.98 (+- 0.09)
	Feb-2010	27	1.85 (+- 0.22)	0.47 (+- 0.10)	0.67 (+- 0.08)	0.37 (+- 0.10)	1.04 (+- 0.07)
	Mar-2010	26	1.15 (+- 0.15)	0.09 (+- 0.03)	0.38 (+- 0.06)	0.36 (+- 0.08)	1.44 (+- 0.10)
	Apr-2010	27	0.45 (+- 0.11)	0.02 (+- 0.01)	0.26 (+- 0.03)	0.44 (+- 0.11)	1.21 (+- 0.06)
	All study period	321	1.13 (+- 0.07)	0.35 (+- 0.04)	0.70 (+- 0.03)	0.65 (+- 0.04)	0.87 (+- 0.03)
Riverside	May-2009	4	1.53 (+- 0.37)	0.07 (+- 0.03)	1.45 (+- 0.60)	1.37 (+- 0.42)	0.10 (+- 0.02)
	Jun-2009	5	0.80 (+- 0.23)	0.12 (+- 0.09)	0.24 (+- 0.10)	1.66 (+- 0.52)	0.13 (+- 0.02)
	Jul-2009	5	0.71 (+- 0.16)	0.03 (+- 0.02)	0.39 (+- 0.13)	2.55 (+- 0.15)	0.22 (+- 0.06)
	Aug-2009	3[c)]	0.55 (+- 0.11)	0.03 (+- 0.02)	1.06 (+- 0.31)	1.65 (+- 0.48)	0.28 (+- 0.09)
	Sep-2009	4[c)]	1.85 (+- 0.35)	0.05 (+- 0.02)	0.71 (+- 0.06)	1.46 (+- 0.38)	0.41 (+- 0.10)
	Oct-2009	5	0.77 (+- 0.31)	0.05 (+- 0.03)	0.58 (+- 0.12)	0.39 (+- 0.24)	0.38 (+- 0.18)
	Nov-2009	5	1.56 (+- 0.63)	0.37 (+- 0.07)	0.64 (+- 0.16)	0.38 (+- 0.20)	0.44 (+- 0.07)
	Dec-2009	4[d)]	1.32 (+- 0.49)	1.04 (+- 0.29)	0.56 (+- 0.13)	0.06 (+- 0.04)	0.32 (+- 0.07)
	Jan-2010	5	0.97 (+- 0.58)	0.67 (+- 0.26)	0.36 (+- 0.10)	0.08 (+- 0.08)	0.22 (+- 0.09)
	Feb-2010	5	0.90 (+- 0.45)	0.52 (+- 0.11)	0.59 (+- 0.17)	0.27 (+- 0.07)	0.25 (+- 0.07)
	Mar-2010	5	0.37 (+- 0.11)	0.18 (+- 0.04)	0.30 (+- 0.10)	0.19 (+- 0.14)	0.96 (+- 0.36)
	Apr-2010	5	1.25 (+- 0.19)	0.06 (+- 0.01)	0.13 (+- 0.04)	0.60 (+- 0.43)	0.81 (+- 0.15)
	All study period	55	1.04 (+- 0.11)	0.27 (+- 0.05)	0.55 (+- 0.07)	0.86 (+- 0.13)	0.39 (+- 0.05)

a) averaged without possible forest fires events including from 8/15/2009 through 8/19/2009 and from 8/26/2009 through 9/4/2009
b) averaged without high wood smoke days including from 12/25/2009 through 12/27/2009, 12/31/2009 and 1/1/2010
c) averaged without possible forest events including 8/17/2009, 8/29/2009, and 9/4/2009
d) averaged without high wood smoke days including 12/27/2009

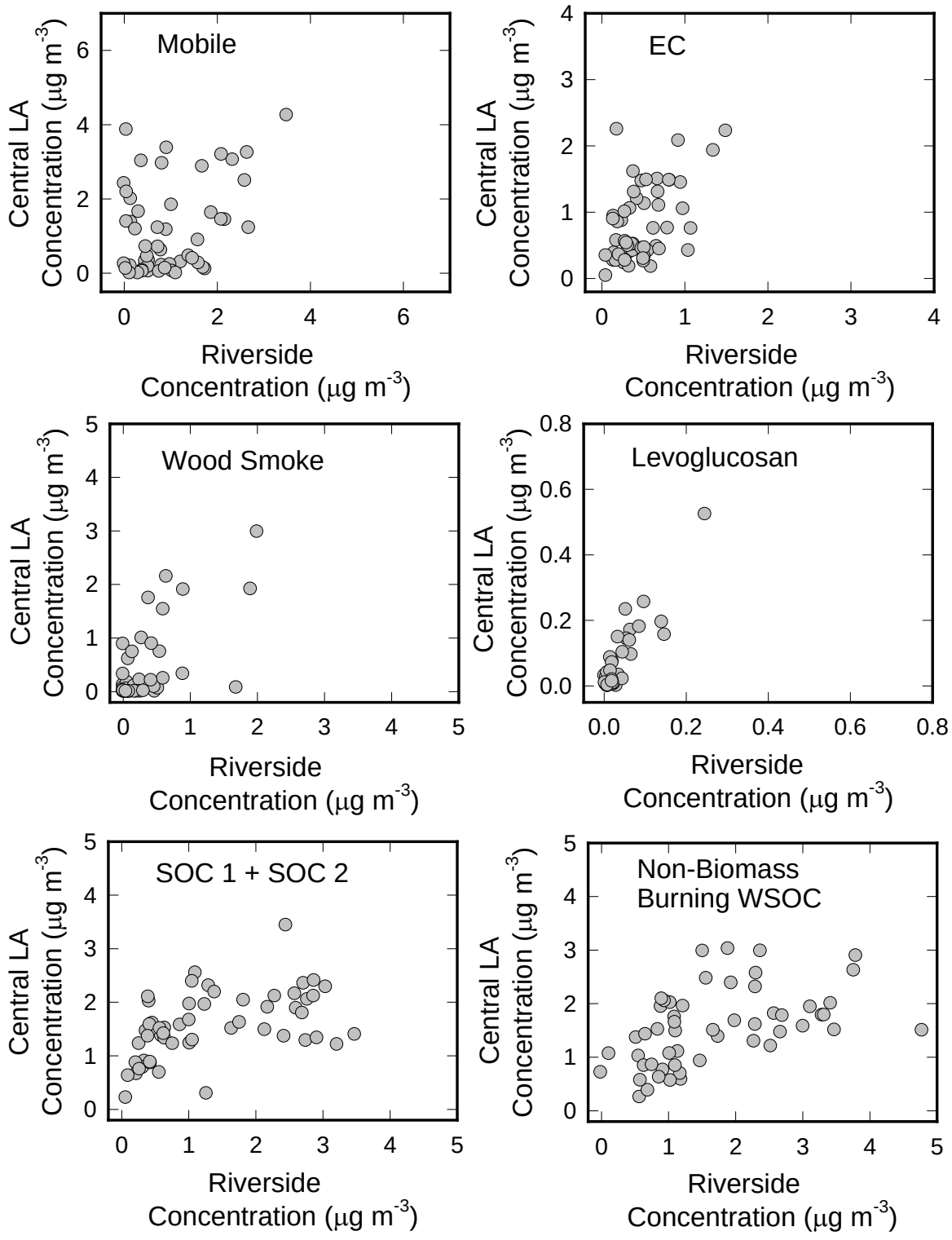

Figure 26– Comparison of OC source contributions from the molecular marker PMF model for Central LA and Riverside

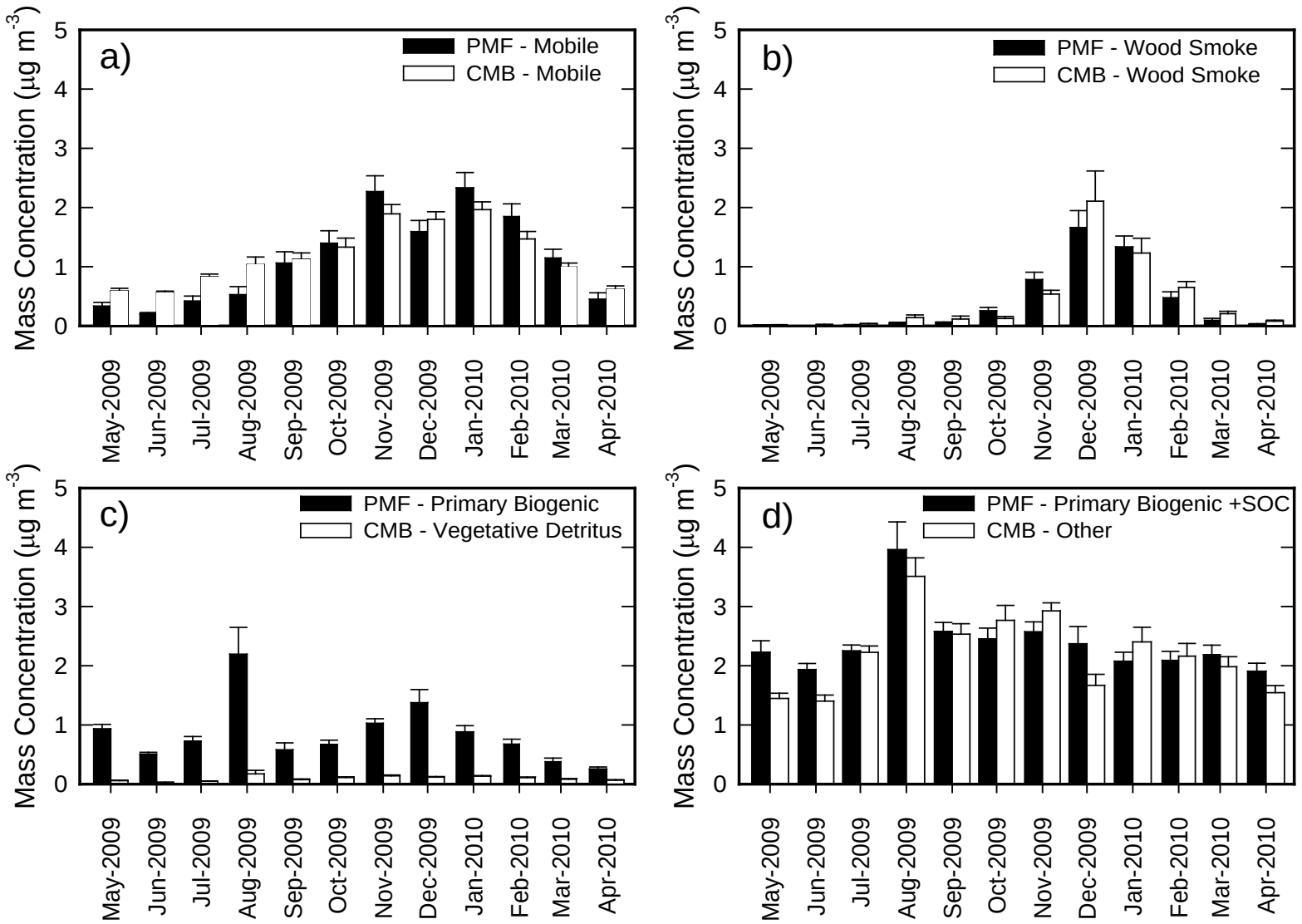

Figure 27adcd –Comparison of monthly apportionment from the molecular marker PMF and CMB for Central LA

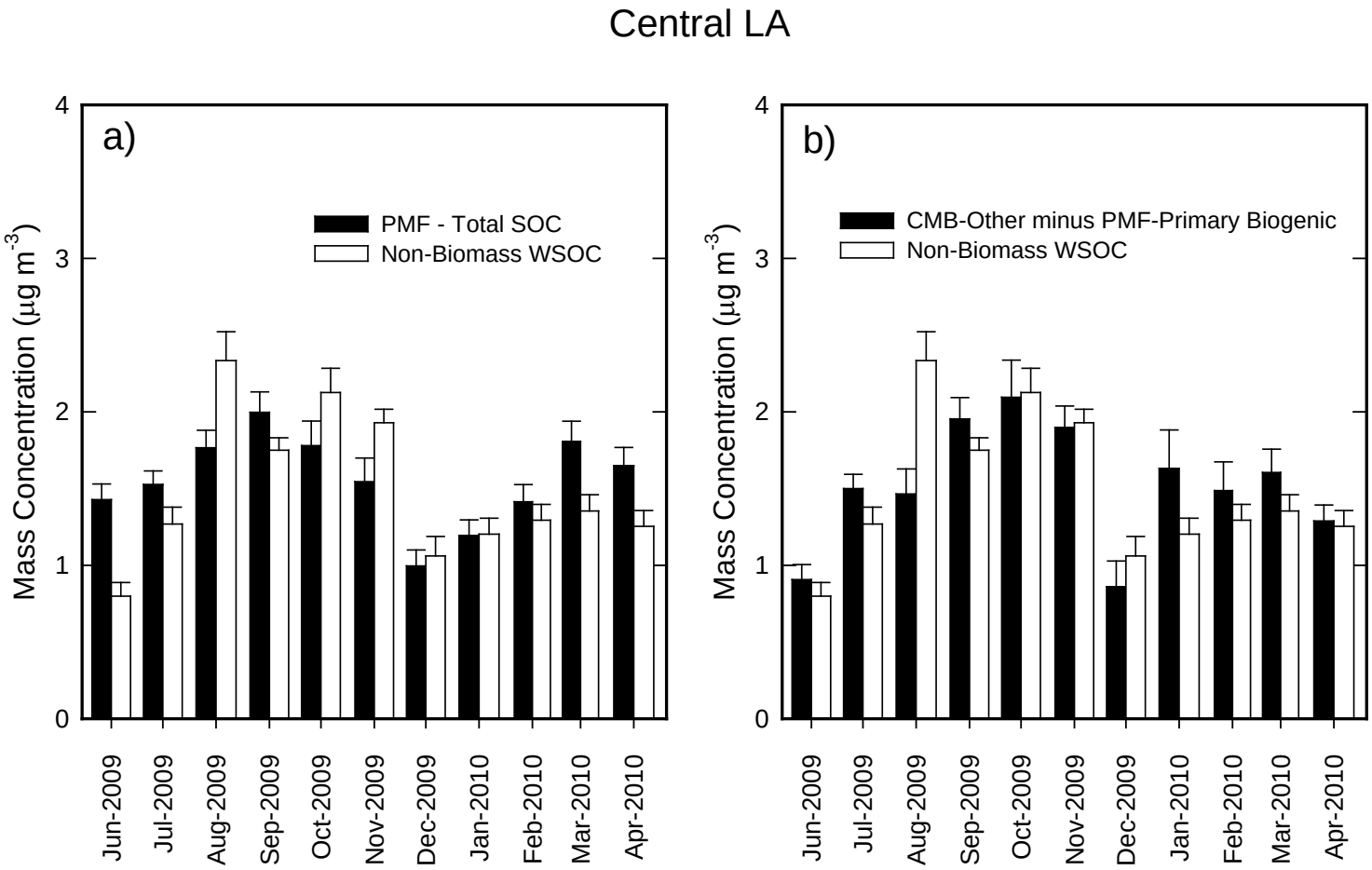

Figure 28ab –Comparison of monthly apportionment from the molecular marker PMF and CMB for Central LA

3.2.3 UNMIX method

For the UNMIX model, 341 observations and 32 key molecular markers were used to investigate source contributions to the PM2.5 OC at the Central LA, and a total of 59 samples and 28 key species were available at the Riverside site. The UNMIX model results indicate that similar source categories are obtained for both sites and each of the UNMIX deduced factors is the same as each of the PMF resolved source categories. Five source categories were identified providing reasonably stable profiles: 1) mobile with high composition of EC and hopanes; 2) wood smoke with high composition of levoglucosan; 3) primary biogenic with high composition of odd-numbered alkanes, especially nonacosane and hentriacontane, and n-alkanoic acids; 4) anthropogenic related SOC with high phthalic acid concentrations; and 5) biogenic related SOC with high pinonic acid concentrations. Annual average source contributions to the total PM2.5 OC mass at the Central LA were as follows: 24% mobile, 6% wood smoke, 17% primary biogenic emission, 34% anthropogenic SOC, and 19% biogenic SOC from the UNMIX. For the Riverside site, mobile, wood smoke, primary biogenic emission, anthropogenic SOC, and biogenic SOC contributed approximately 30%, 6%, 16%, 31%, and 16%, respectively. The UNMIX model is insufficient in separating mobile emission into gasoline and diesel vehicles. As shown in Figure 29, the daily temporal trends derived from the UNMIX and PMF models at the Central LA site are in good agreement with each other, but there are some days with poorer agreement. Due to the fact that the PMF model uses more organic molecular markers than the UNMIX model, the PMF model can do a better job addressing atmospheric aging represented by oxidized organic compounds.

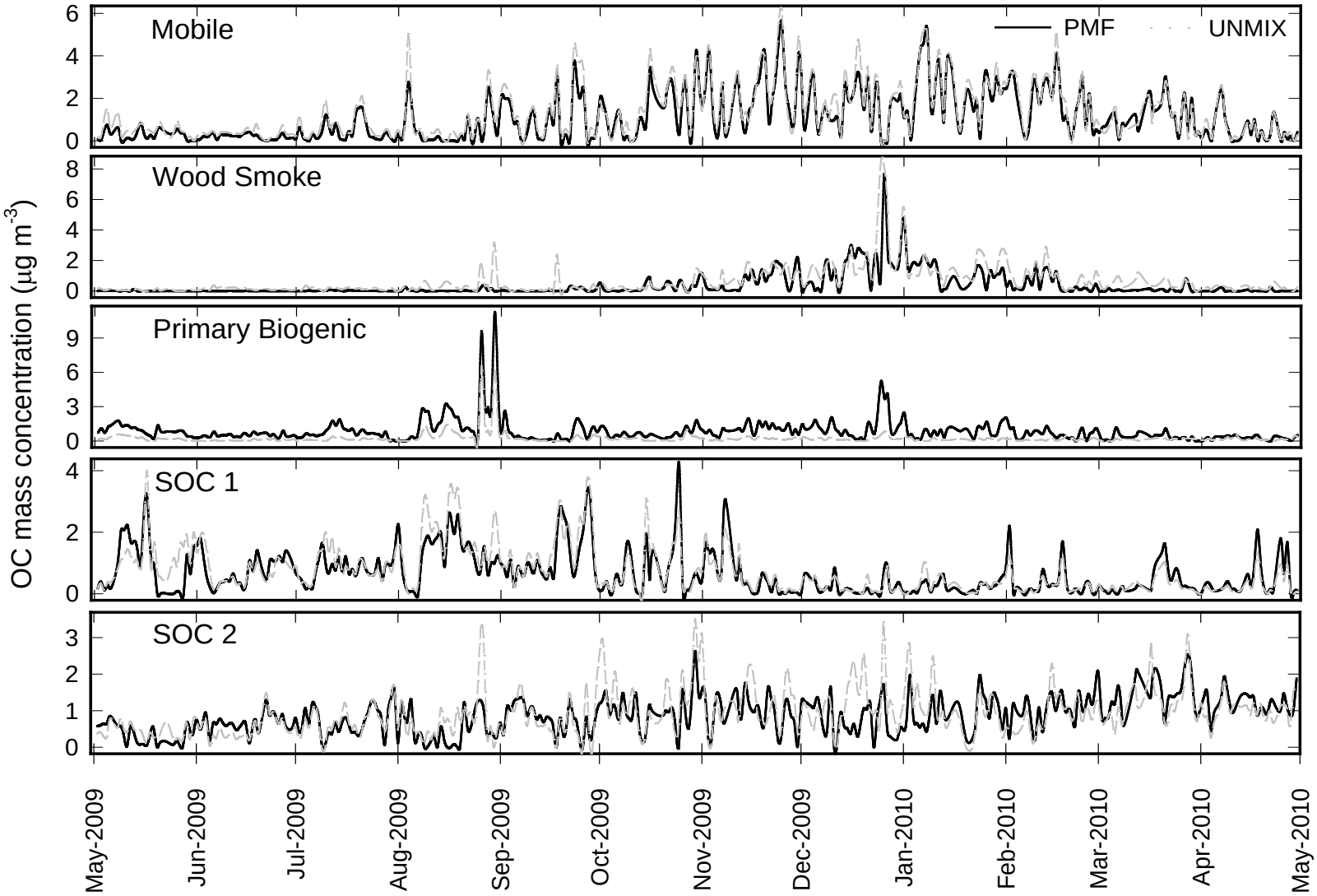

Figure 29– Comparison of molecular marker PMF and UNMIX source contributions to 5-factor model for Central LA

3.2.4 Iterated Confirmatory Factor Analysis

Two boundary scenarios, rigid boundaries with +/- 2 times uncertainty and looser boundaries with +/- 5 times uncertainty, were explored to constrain elements of source profiles for the Central LA data. The ICFA estimate of the species was often outside of the starting value of the boundaries when using relatively rigid boundaries, representing that this scenario could not provide a best model fit. By using looser boundaries for constraining the profiles, elements estimated from PMF and elements with no *a priori* information about the profile elements of CMB (e.g., the non-identified elements of the diesel, gasoline, and smoking vehicle profile) were more likely located within boundaries, indicating better model fit. For this reason, we used the ICFA based on the looser boundaries in this analysis.

Figure 30 shows the daily mobile source contributions to the total PM2.5 OC deduced from CMB, PMF, and ICFA. Although there are some days with poorer agreement, good agreement between the daily trends of total mobile source contributions for MM-ICFA, MM-CMB, and MM-PMF are observed. On an annual average, the MM-CMB and MM-PMF models show very good agreement for the contribution of total mobile sources to PM2.5 OC of 30%, and reasonable agreement with the MM-ICFA mobile source contributes to PM2.5 OC of 23%. Figure 31 shows comparison of daily source contributions for the MM-CMB, MM-PMF, and MM-ICFA. There is very good agreement between daily source contributions of wood smoke, SOC 1 and 2 from the MM-PMF and MM-ICFA. The split of mobile sources between gasoline, diesel, and smoking engines from the MM-CMB and MM-ICFA models exhibit different distributions. Given the uncertainty in the split between gasoline, diesel, and smoking vehicles in MM-CMB models, it is difficult to fully evaluate the accuracy of the MM-ICFA results, but the MM-ICFA results appear to agree with some previous estimates of the gasoline and diesel split. Future sensitivity analyses and application of multi-variant models are needed to better evaluate the accuracy and stability of the MM-ICFA results obtained in the current study. Nonetheless, the results demonstrate a viable pathway to further advance the relative understanding of gasoline and diesel engines source contributions in atmospheric aerosols.

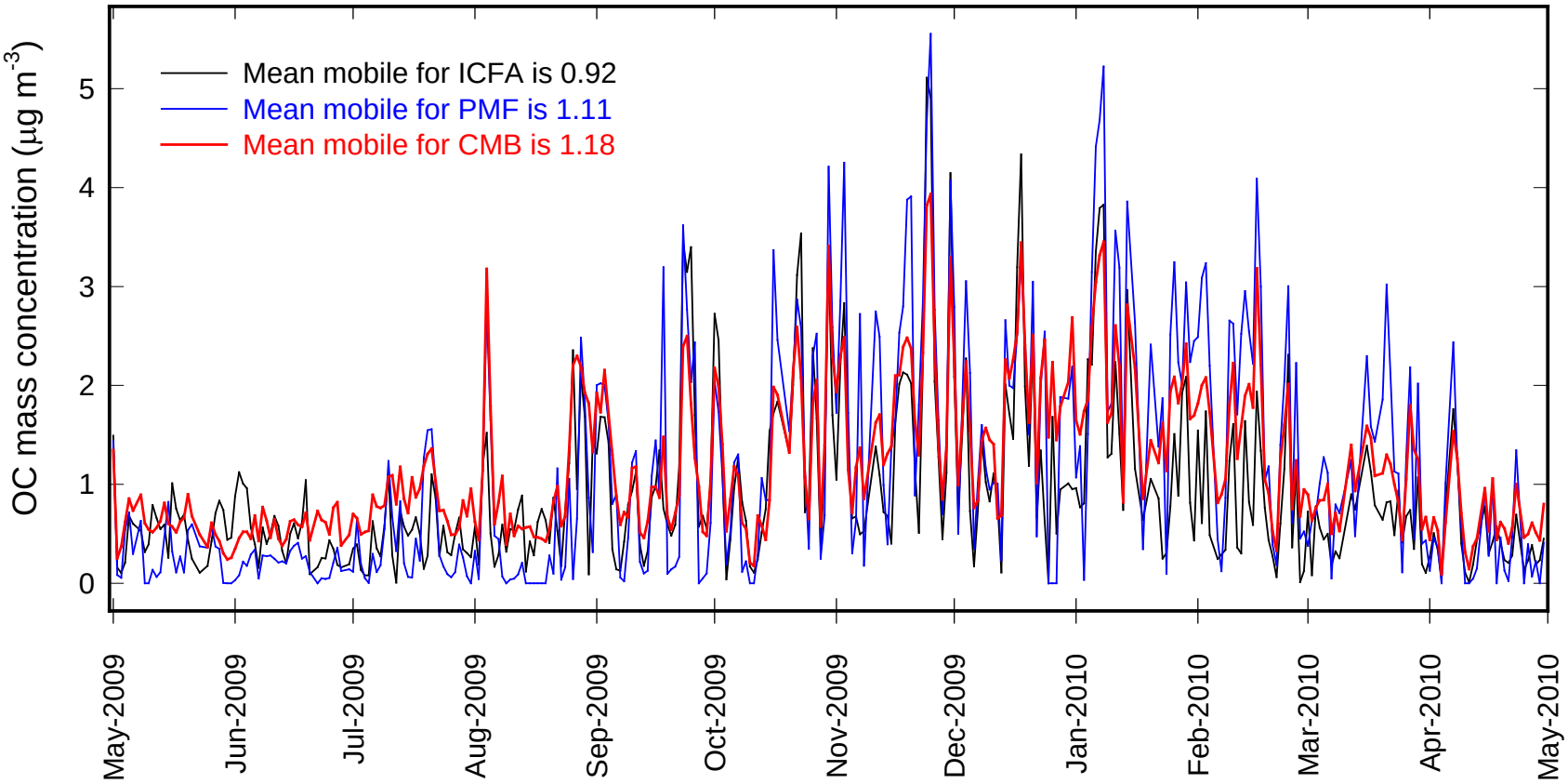

Figure 30– Mobile source comparison for molecular marker ICFA, PMF, and CMB (ICFA is black, PMF is blue, and CMB is red)

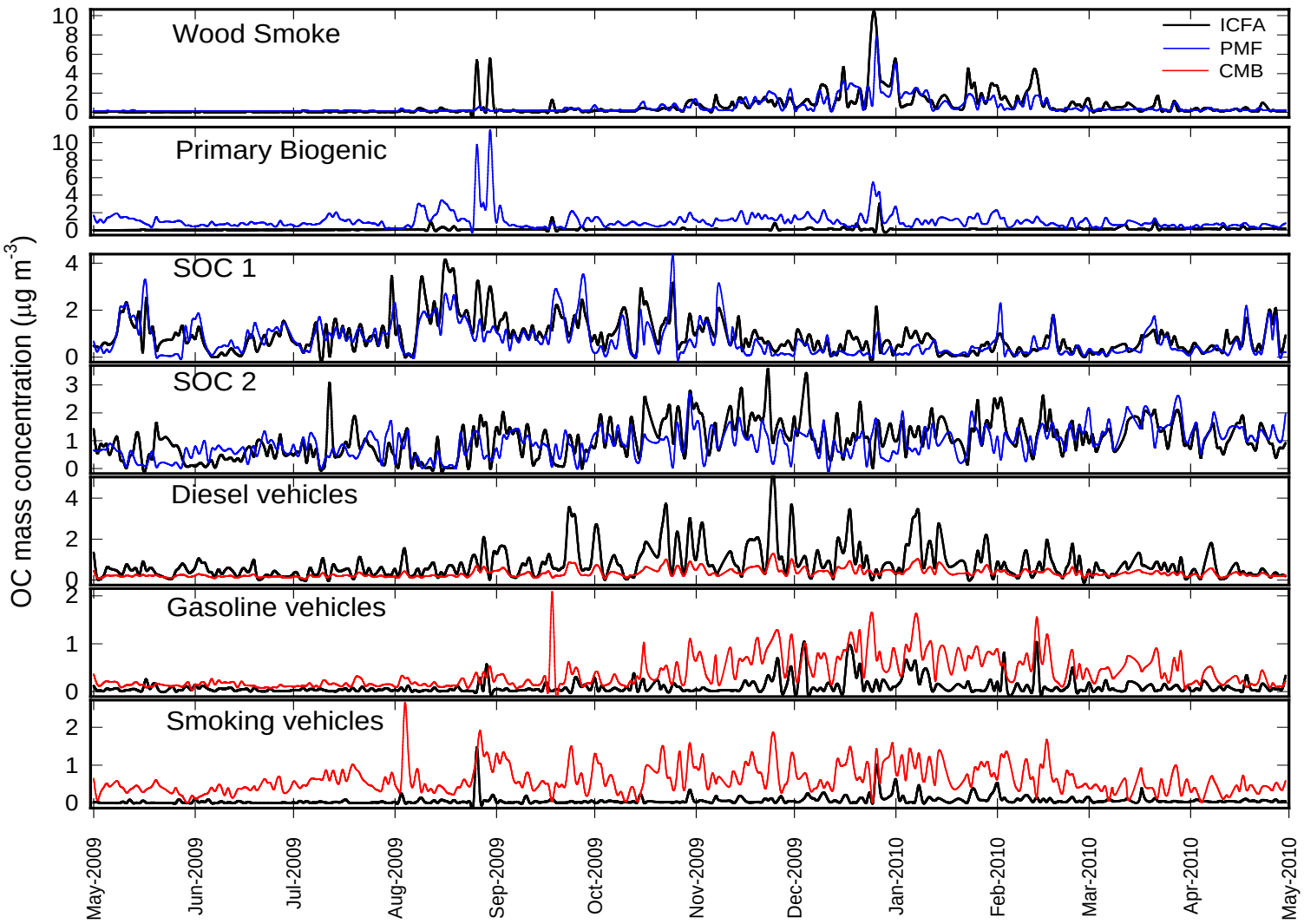

Figure 31– Comparison of molecular marker ICFA, PMF, and CMB source contribution (ICFA is black, PMF is blue, and CMB is red)

3.2.5 Potential Source Contribution Function

Figure32shows the sampling locations for this study using anelevation map of the southern US, and Figure 33 shows cluster mean results of the total trajectories arriving at the Central LA site during the entire study period. The main advection patterns of air masses are characterized at 500 m: local circulation of southeasterly flows with the relatively long air mass residence time (46%), westerly flows with the relatively long air mass residence time (31%), northeasterly flows of clockwise curvature with the relatively short air mass residence time (17%), and northwesterly flows with the long-range transported air masses (6%).

Areas of high probability for emissions of the anthropogenic SOC source, resolved by PSCF analysis appear to be located along the Central Valley and the South Coast Air Basin in California as seen in Figure 34. These indentified potential source regions are well matched with the high anthropogenic emission potentials, such as mobiles and stationary emission sources, in the area. In contrast, the PSCF plot for the biogenic SOC source indicates there is high probability of emissions from northeast of the sampling site. Northeast of the sampling site is a broad distribution from rural and forested areas (Figure 35). The PSCF map shows in Figure 36 a high density of primary biogenic emissions located in the Central Valley and the South Coast Air Basin. A primary biogenic hotspot area appears to be across the San Joaquin Valley and in the vicinity of the Central LA (i.e., the Angeles National Forest). These high potential source areas correspond to known wildfire regions and other primary biogenic emissions. These primary biogenic emissions include possible soil debris and vegetative detritus. When the PSCF model for the primary biogenic source was applied using threshold criterion of upper 10% of source contributions (i.e., approximately 34 days of the total samples), there is good agreement between forest fire activities detected by MODIS from January 2009 through December 2009, and the identified potential source locations as seen Figures37 and 40. The PSCF maps for the wood smoke source and mobile source show the potential source areas for both sources are located along the northwestern inlands areas, especially in and around Death Valley, as seen in Figures38 and 39. While these identified source locations can increase the source contributions to the PM2.5 OC at the Central LA site, it is more likely to be representing advection of air masses than the results of known emission areas, due to the fact that localized emission regions in the urban area are not captured by the PSCF maps. Since multi-day single trajectory techniques are too coarse to resolve the local scale emission sources including mobile and wood smoke, there is a need for applying a multiple-particle trajectories method such as FLEXPART [*Stohl et al.*, 2005] coupled with fine meteorological data (i.e., MM5 or WRF simulations).

Overall, while backward trajectories simulated by 40 kilometer gridded meteorological data could not show fine spatial resolution to identify localized emission sources, the identified source regions from the PSCF model support the conclusion that the PMF resolved source profiles for the $PM_{2.5}$ OC are properly separated in the present analysis.

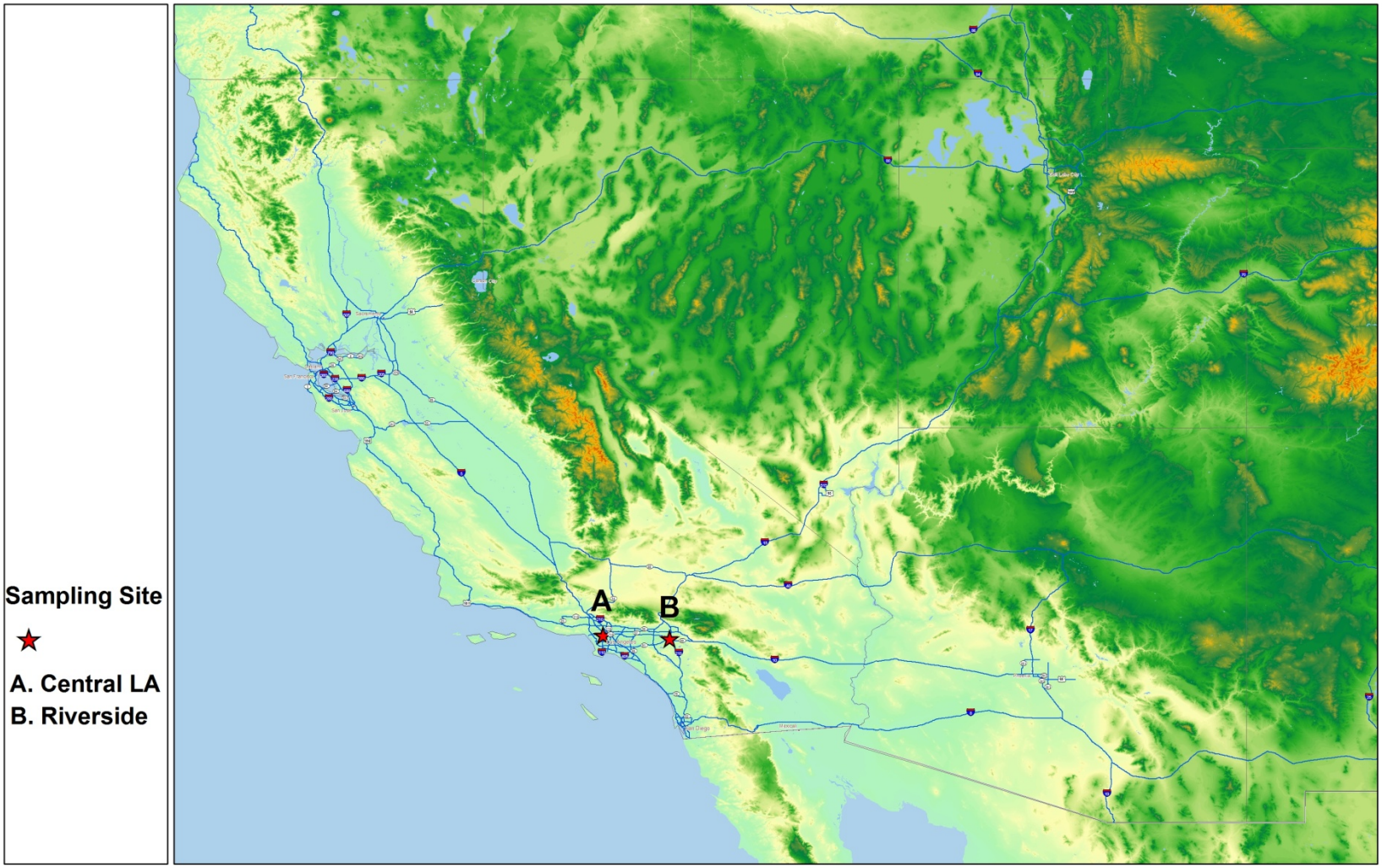

Figure 32– Sampling locations and elevation map of the southern US

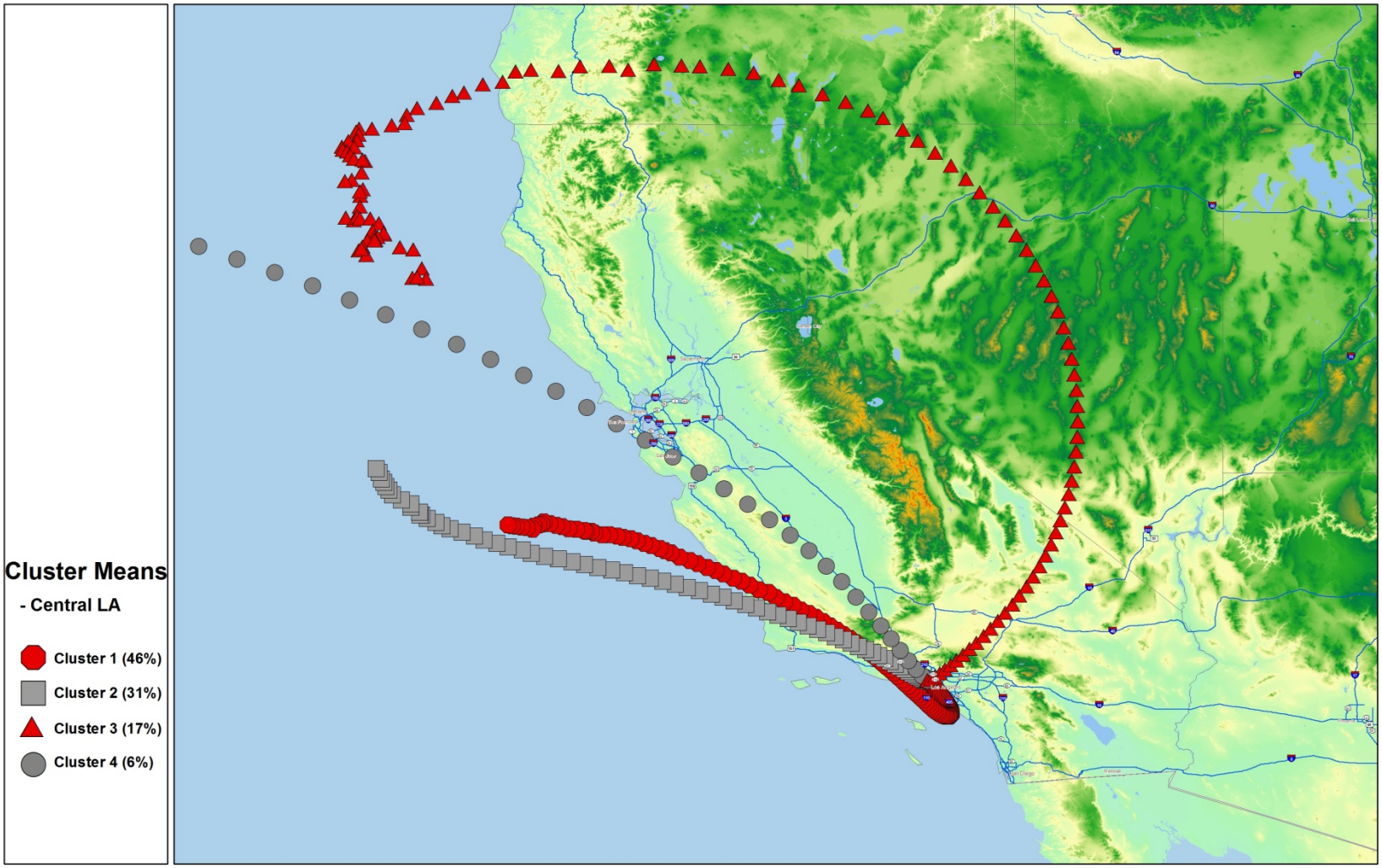

Figure 33– Cluster mean results for the total trajectories arriving at the Central LA site

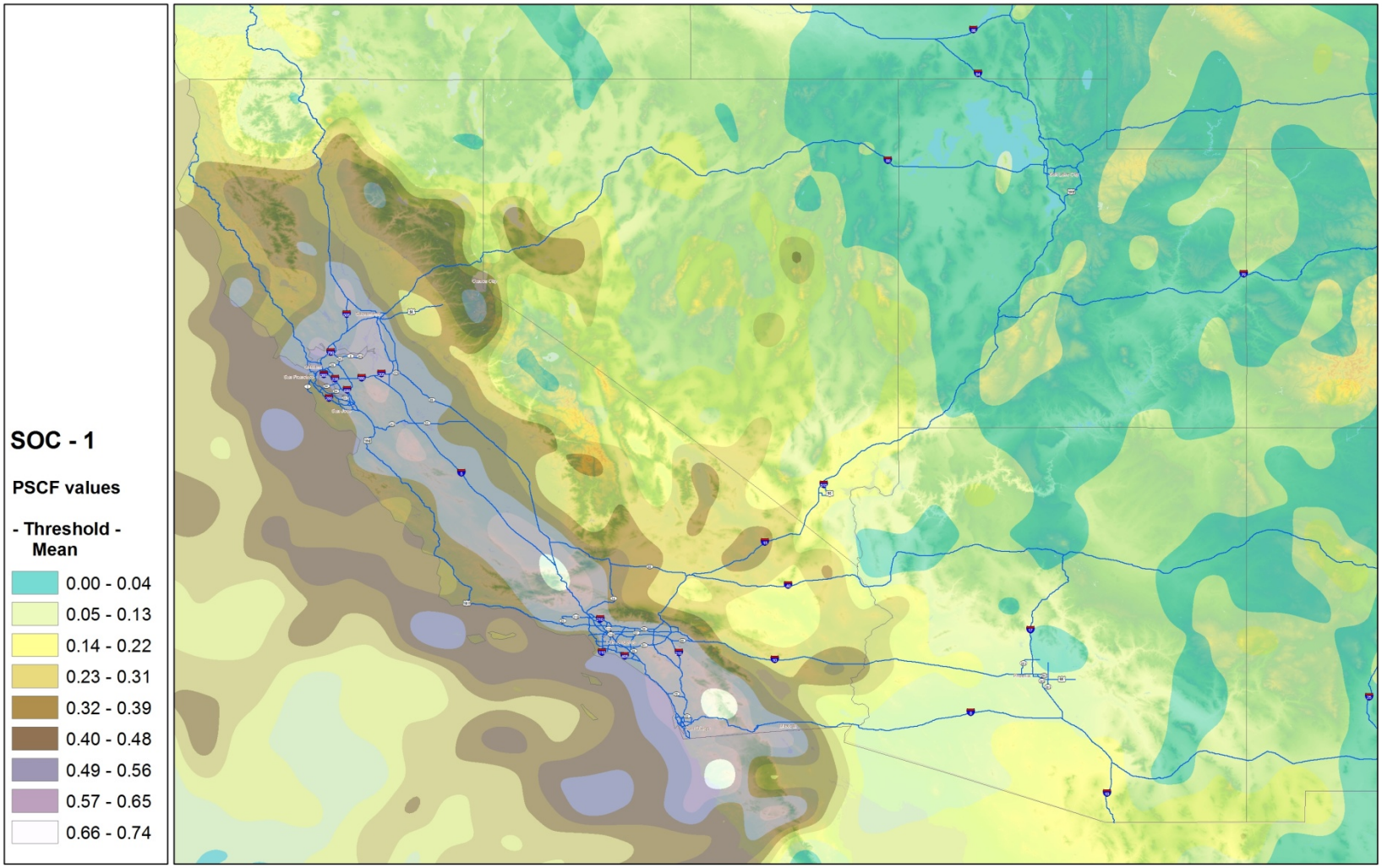

Figure 34– Areas of high probability of the anthropogenic SOC emissions as indentified in the potential source contribution function (PSCF) analysis for the Central LA

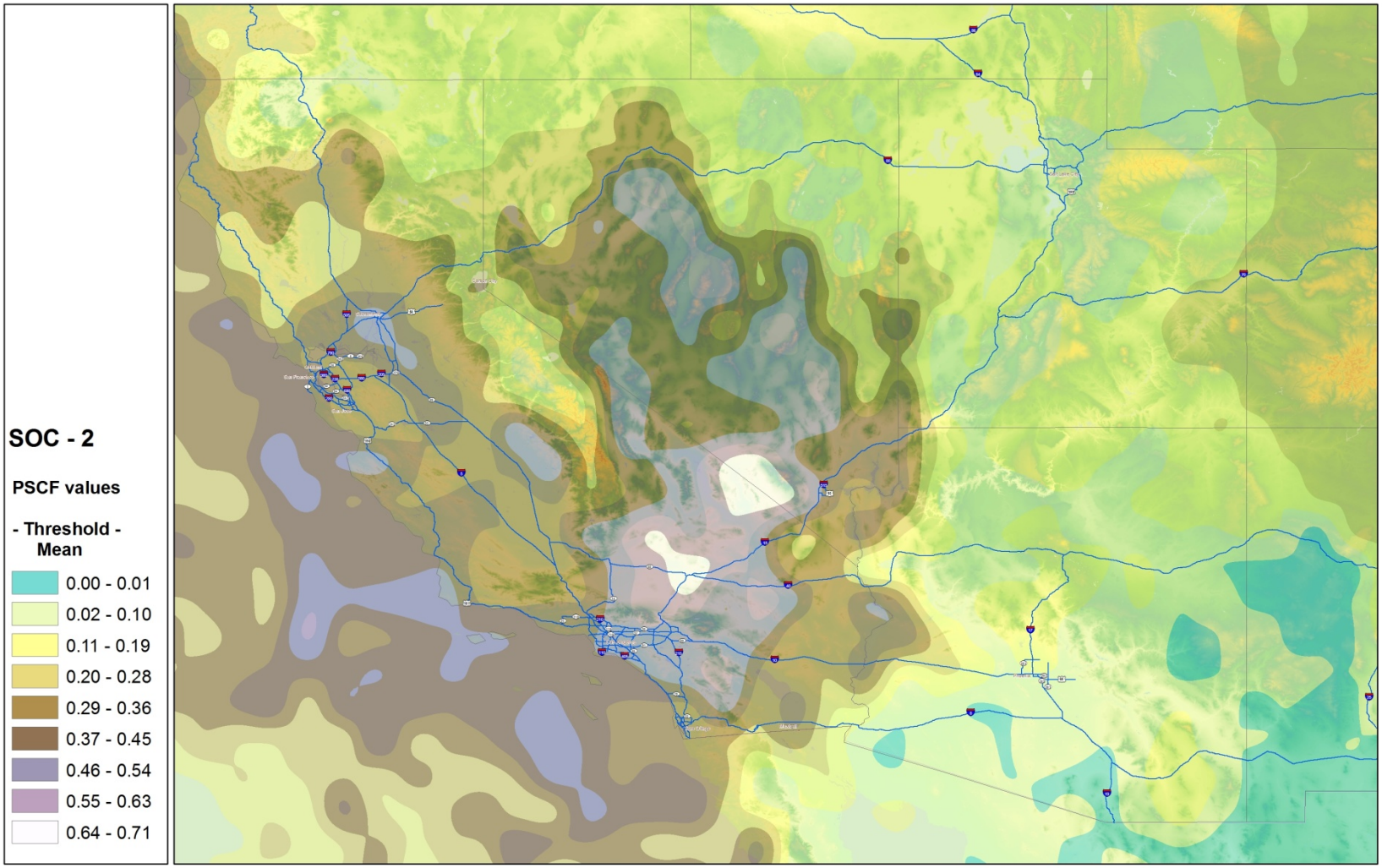

Figure 35– Areas of high probability of the biogenic SOC emissions as indentified in the PSCF analysis for the Central LA

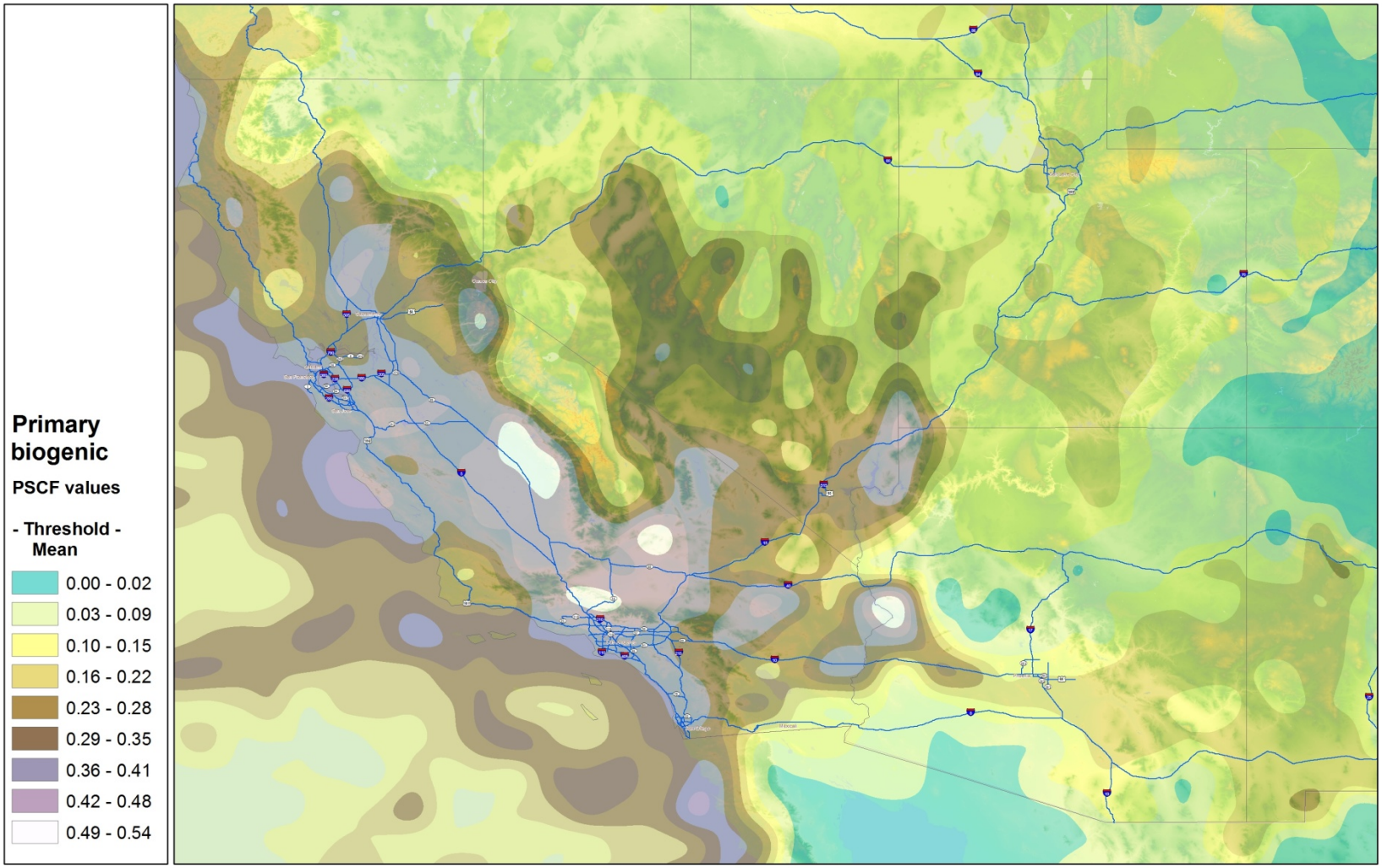

Figure 36– Areas of high probability of the primary biogenic source emissions as indentified in the PSCF analysis using threshold of average for the Central LA

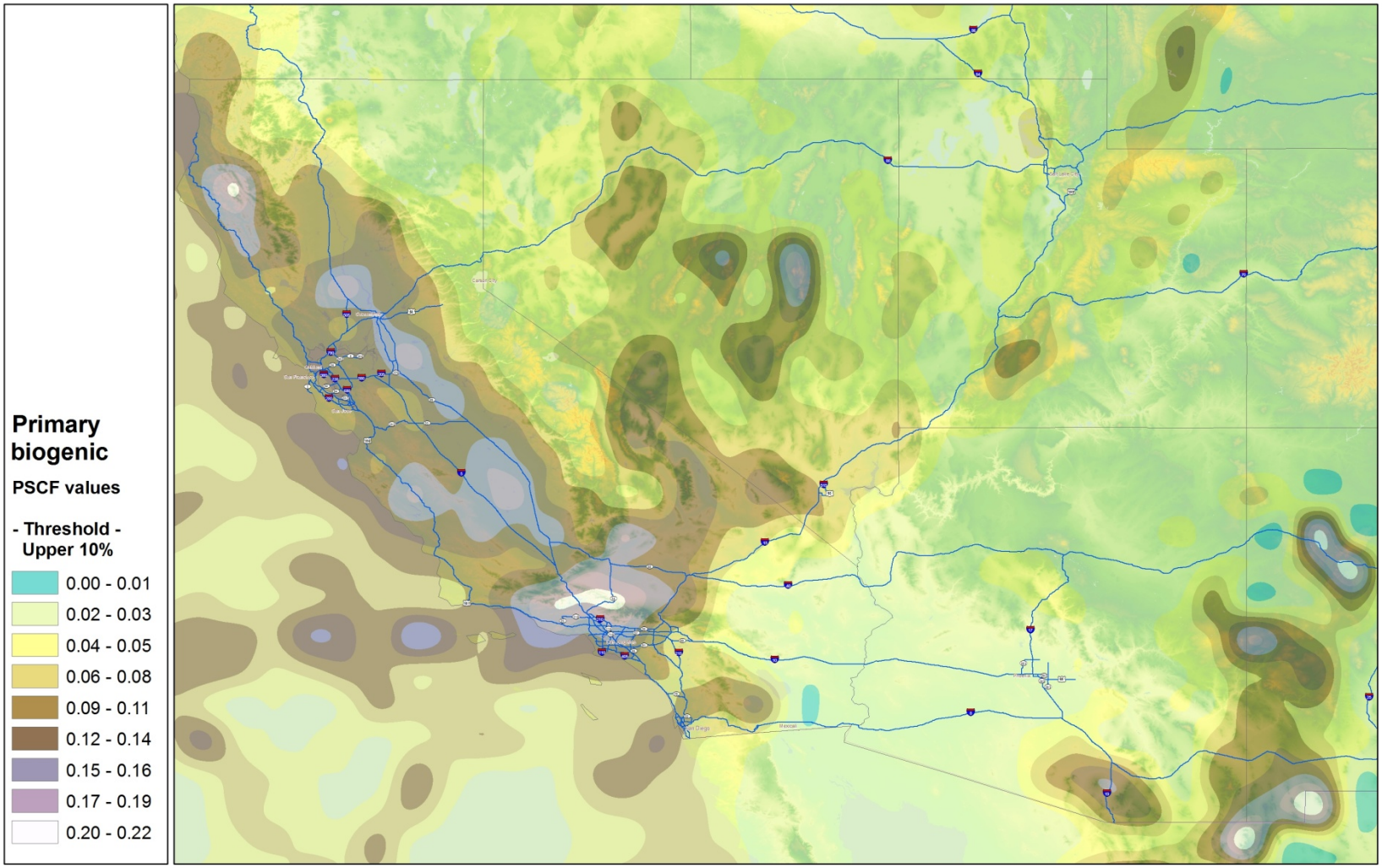

Figure 37– Areas of high probability of the primary biogenic source emissions as indentified in the PSCF analysis using threshold of upper 10% for the Central LA

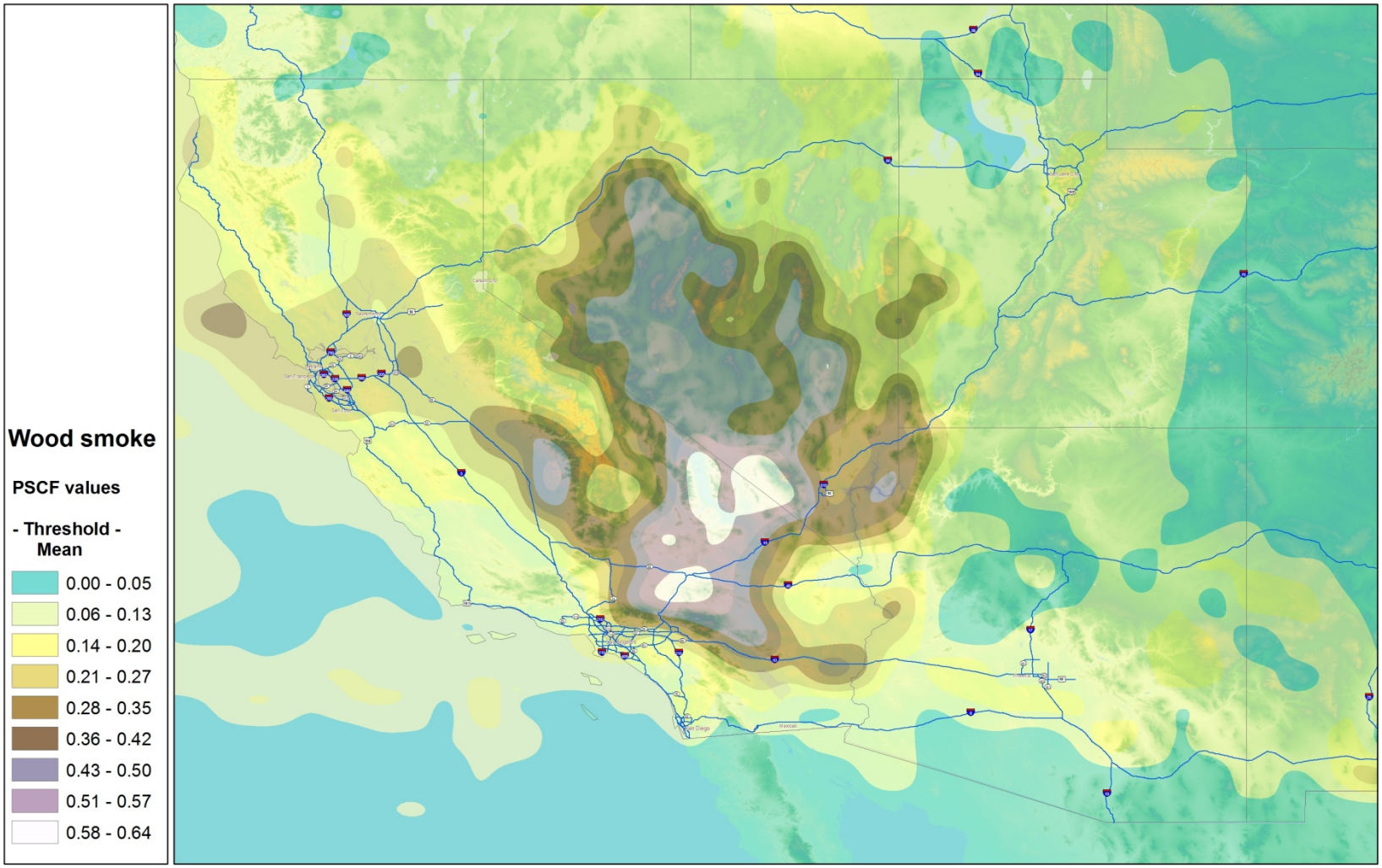

Figure 38– Areas of high probability of the wood smoke emissions as indentified in the PSCF analysis for the Central LA

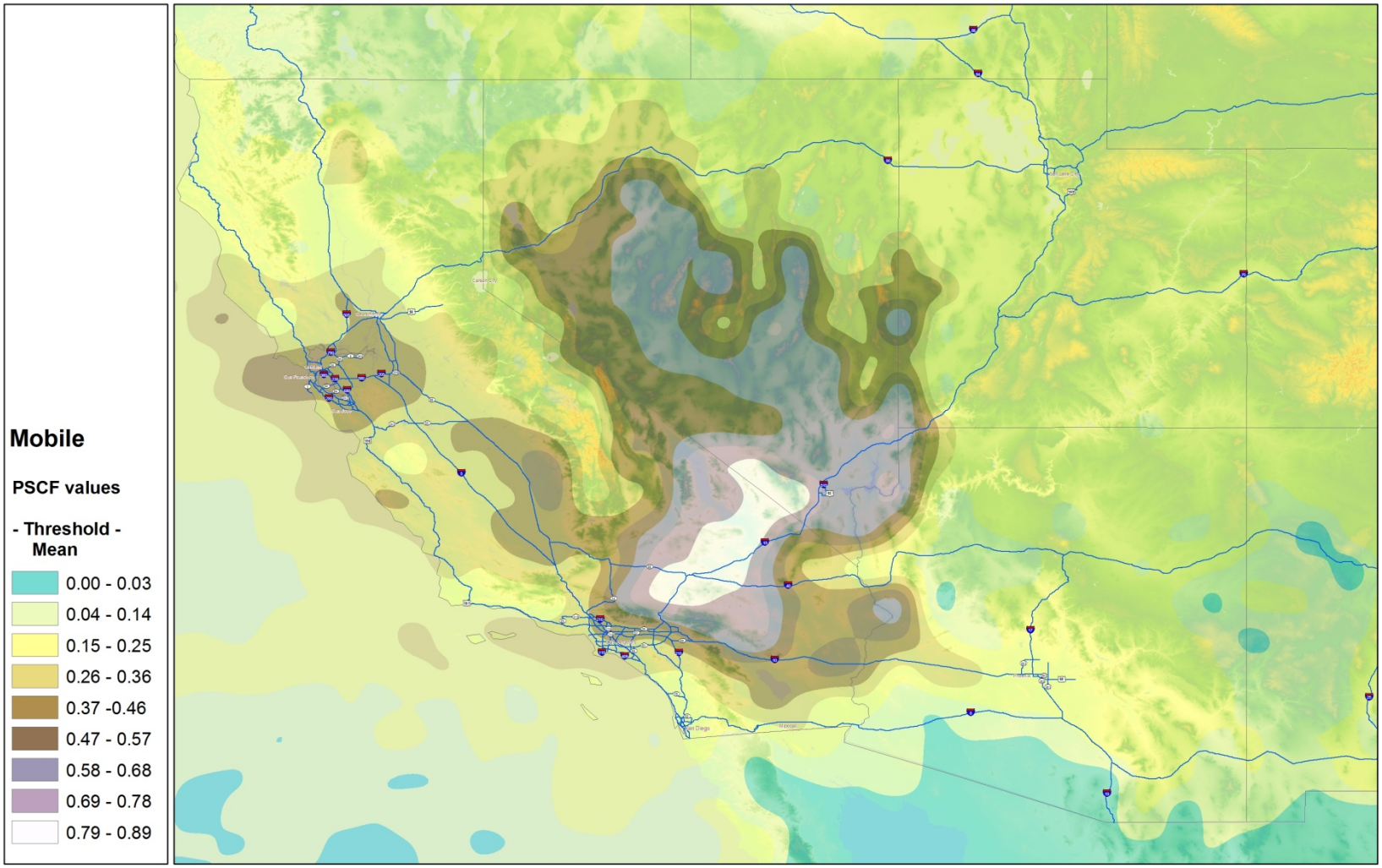

Figure 39– Areas of high probability of the mobile emissions as indentified in the PSCF analysis for the Central LA

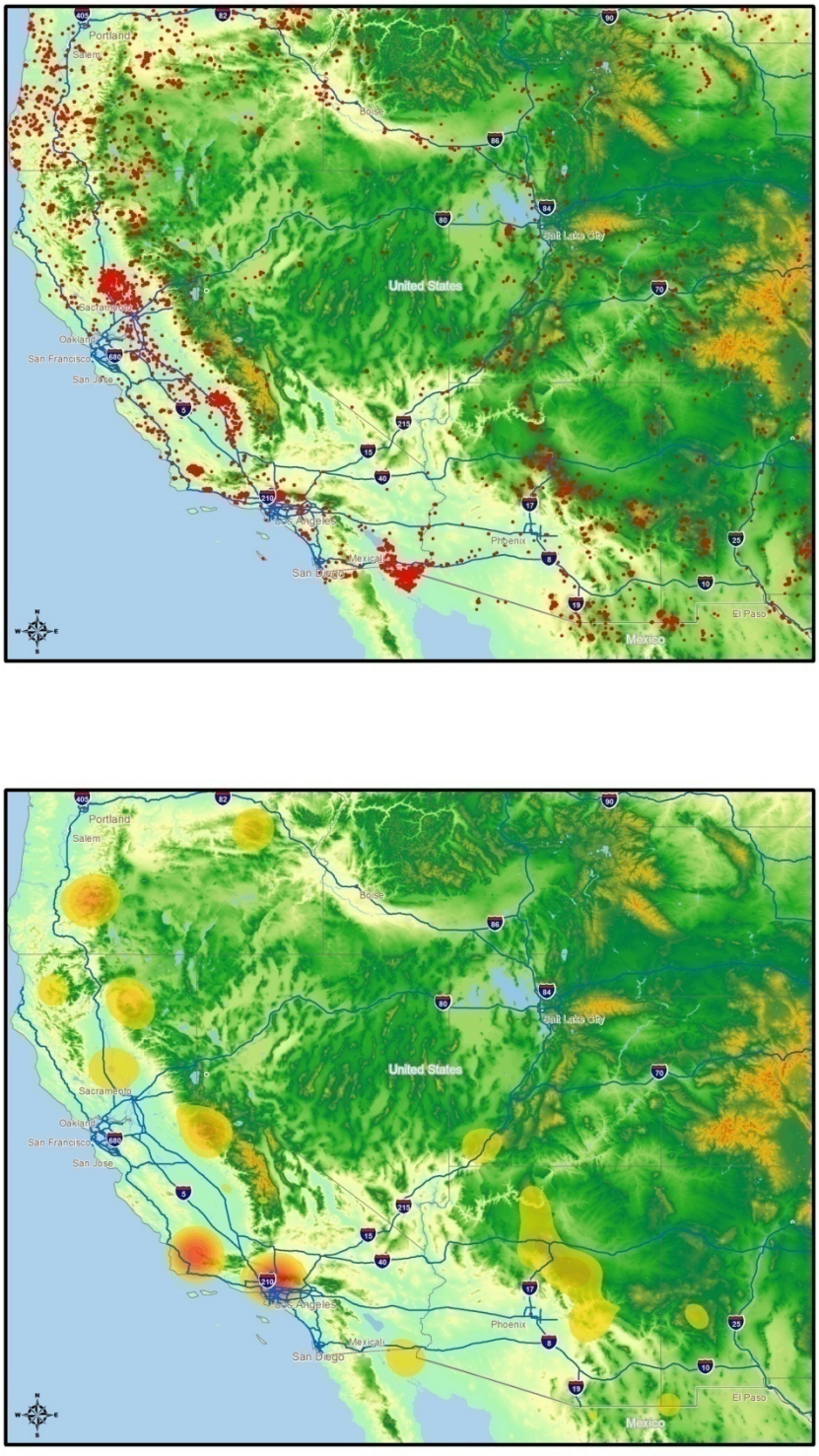

Figure 40– Fire counts (upper) and density mapping with temperature (bottom) detected by the moderate resolution imaging spectroradiometer (MODIS) from January 2009 through December 2010

3.3 Water Soluble Organic Nitrogen

As seen in Figures30 and 31, a significant amount of variability in total water soluble nitrogen (TN) was observed at the Central LA and Riverside study locations. Considerable variability in both water soluble inorganic nitrogen (Nx) and water soluble organic nitrogen (WSON) was observed at both sites. WSON constituted, on average, 21.7 % of TN observed at Riverside and comprised as much as 84.9 % and as little as 4.1 % of TN. Observed molar concentrations of WSON averaged 0.045 μmol m^{-3}. The maximum observed concentration of WSON at the Riverside site was 0.344 μmol m^{-3} (Table 9).

Concentrations of water-soluble nitrogen species at Riverside were generally higher than those observed in Central LA where WSON comprised 19.5% of TN. At the Central LA study site, WSON ranged from 0.090 to 0.001 μmol m^{-3} and comprised from 66.5% to 1.2% of TN (Table 10). While significant variability in the concentration of water-soluble nitrogen species was observed, with the exception of a few peak events, the organic fraction of water-soluble nitrogen at both sites remained fairly consistent and comparable to those observed in previous studies of nitrogenous aerosols.

A comparison between the temporal trends in WSON and those of bulk chemical species (Figure 32) for Riverside reveals a strong correlation between WSON and Nx ($r^2 = 0.86$) with no significant correlations observed between WSON and carbonaceous species WSOC and OC. Likewise, a strong correlation between WSON and Nx was observed at Central LA ($r^2 = 0.77$ excluding one outlier), a weak correlation between WSON and WSOC ($r^2 = 0.40$), and no correlation between WSON and OC (Figure 33).

Correlations between WSON and inorganic nitrogen species such as nitrate and ammonium have been observed previously in precipitation samples [*Cornell et al.*, 1995; *Jassby et al.*, 1994; *Knap et al.*, 1986; *Russell et al.*, 1998], and the correlations between WSON and Nx seen in these data suggest that the organic nitrogen observed at both sites may be the result of secondary organic aerosol formation, although no correlation between WSON and the OC/EC ratio (a general metric of secondary OC formation) was observed at either site (Figures32d and 33d).

A statistical analysis of organic carbon apportioned to source factors determined by the PMF analysis and WSON concentrations was performed. Pearson product-moment correlation coefficients were determined for annual and seasonal comparisons between WSON and OC attributed to the five source factors identified by the PMF model, designated as mobile source, wood smoke, forest fire, secondary organic aerosol 1 (SOC 1), and secondary organic aerosol 2 (SOC 2). Results of these analyses can be found in Tables 10 and 11. For comparison purposes, correlation coefficients were also determined between WSON, Nx, and WSOC.

Not surprisingly, WSON was most closely correlated with Nx at both Riverside ($r = 0.928$, $p < 0.001$) and Central LA ($r = 0.778$, $P < 0.001$). The correlations between WSON and the secondary aerosols factor SOC 1 were also significant at Riverside ($r = 0.495$, $p < 0.001$). This correlation was strongest in the summer ($r = 0.719$, $p = 0.003$) and winter months ($r = 0.882$, $p = 0.02$). WSON was also significantly correlated with SOC 2 during the winter months ($r = 0.823$, $p = 0.04$) and anti-correlated with SOC 2 during the summer months ($r = -0.592$, $p = 0.03$) in Riverside. WSON and SOC 1 were also most significantly correlated in summer ($r = 0.871$, $p < 0.001$) and winter months ($r = 0.758$, $p = 0.002$) in Central LA.

In addition to the secondary organic aerosol factors, some correlations between organic nitrogen and the forest fire factor were observed at Riverside in the winter ($r = 0.804$, $p = 0.009$) and at Central LA during both the winter ($r = 0.670$, $p = 0.009$) and the spring of 2010 ($r = 0.996$, $p = 0.004$), although the sample size for this spring period was small ($n = 4$). The California Department of Forestry and Fire Protection reported no significant wildfires in the Los Angeles Basin during these periods, suggesting this factor may characterize additional/alternate sources of organic aerosol.

The results of these analyses, while not conclusive, suggest that fine particulate water-soluble organic nitrogen in the Los Angeles Basin is primarily a result of the photo-oxidation of biogenic and/or anthropogenic emissions. Furthermore, the nature of the correlations between WSON and Nx and those between WSON and SOC appear to indicate that the photo-chemical processes which produce nitrate and ammonium are an important year-round source of organic nitrogen to the Basin, while those that produce SOC are a more seasonal contributor. The relative contribution of each source is currently unclear as water-soluble organic nitrogen is not necessarily elevated during periods in which SOC and WSON are significantly correlated.

This work represents an initial step in understanding how the sources of fine particulate organic matter influence the levels of organic nitrogen observed in the Los Angeles Basin. Additional studies will be required before organic nitrogen can be robustly apportioned. Critical steps along the path to a functional organic nitrogen source-apportionment model include obtaining a more thorough understanding of the primary sources of organic nitrogen and the sources of secondary organic nitrogen precursors. The focus of much current and past work on organic aerosols has been on understanding the sources of organic carbon; however, given the significance of nitrogen deposition to the eutrophication of soils and aquatic systems and concerns over the health impacts of nitrogenous organic compounds, a more thorough understanding of organic nitrogen sources are warranted.

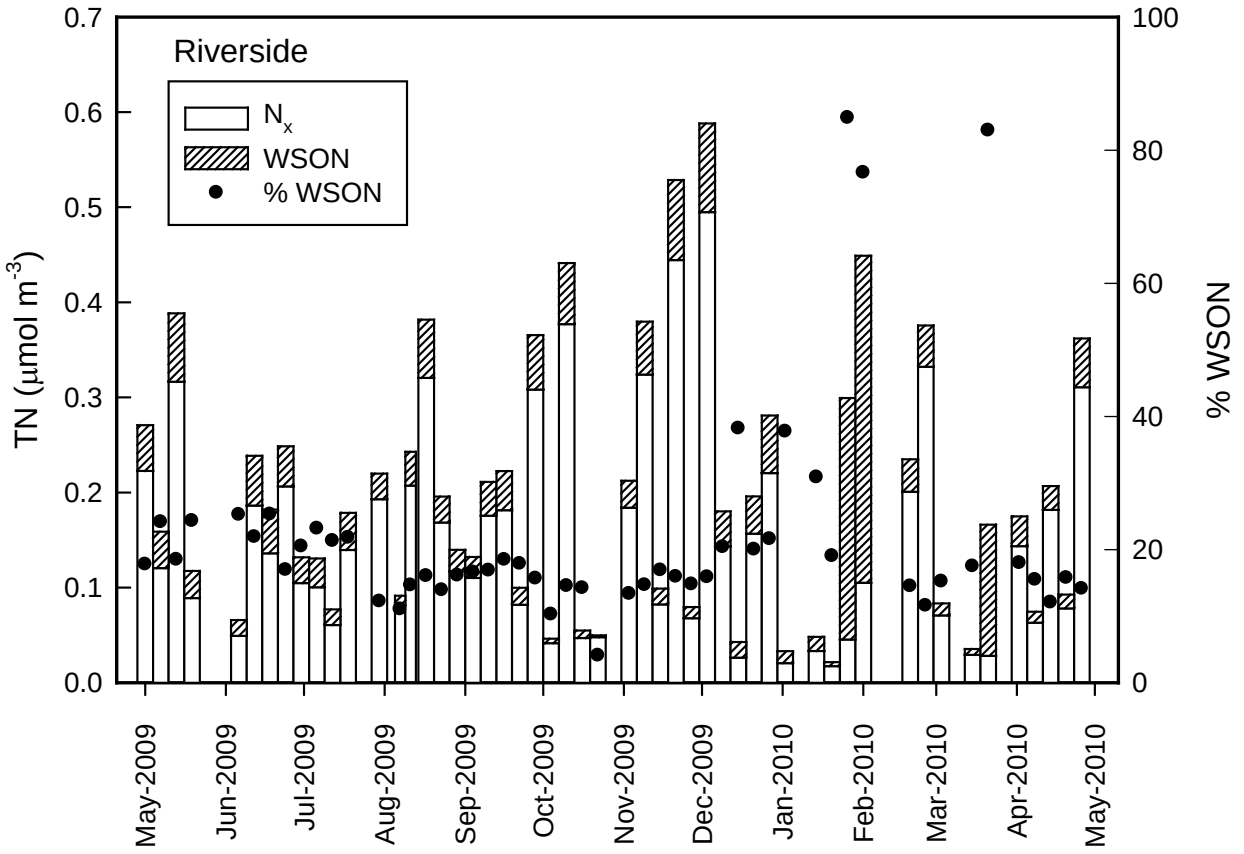

Figure 41– Concentrations of PM2.5 water soluble organic nitrogen (WSON) at the Riverside site

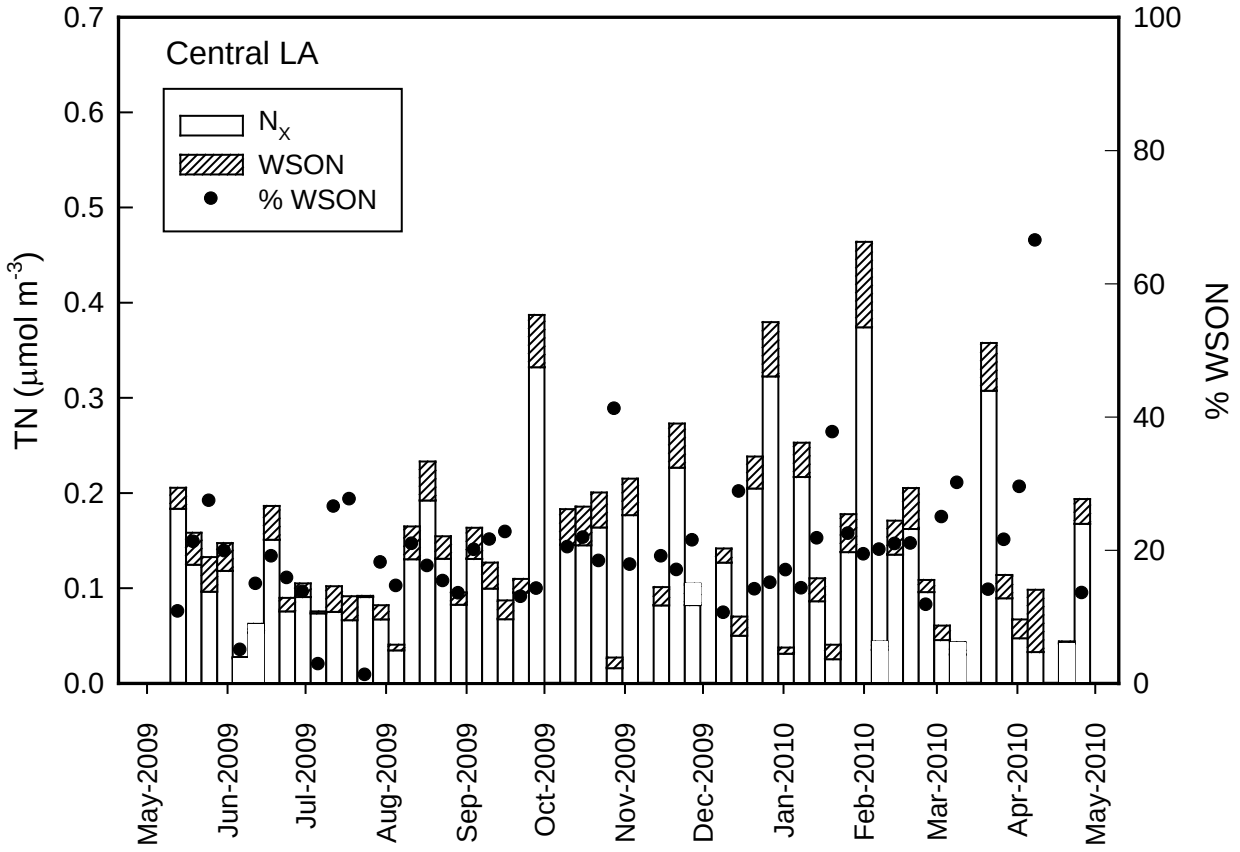

Figure 42– Concentrations of PM2.5 WSON at the Central LA site

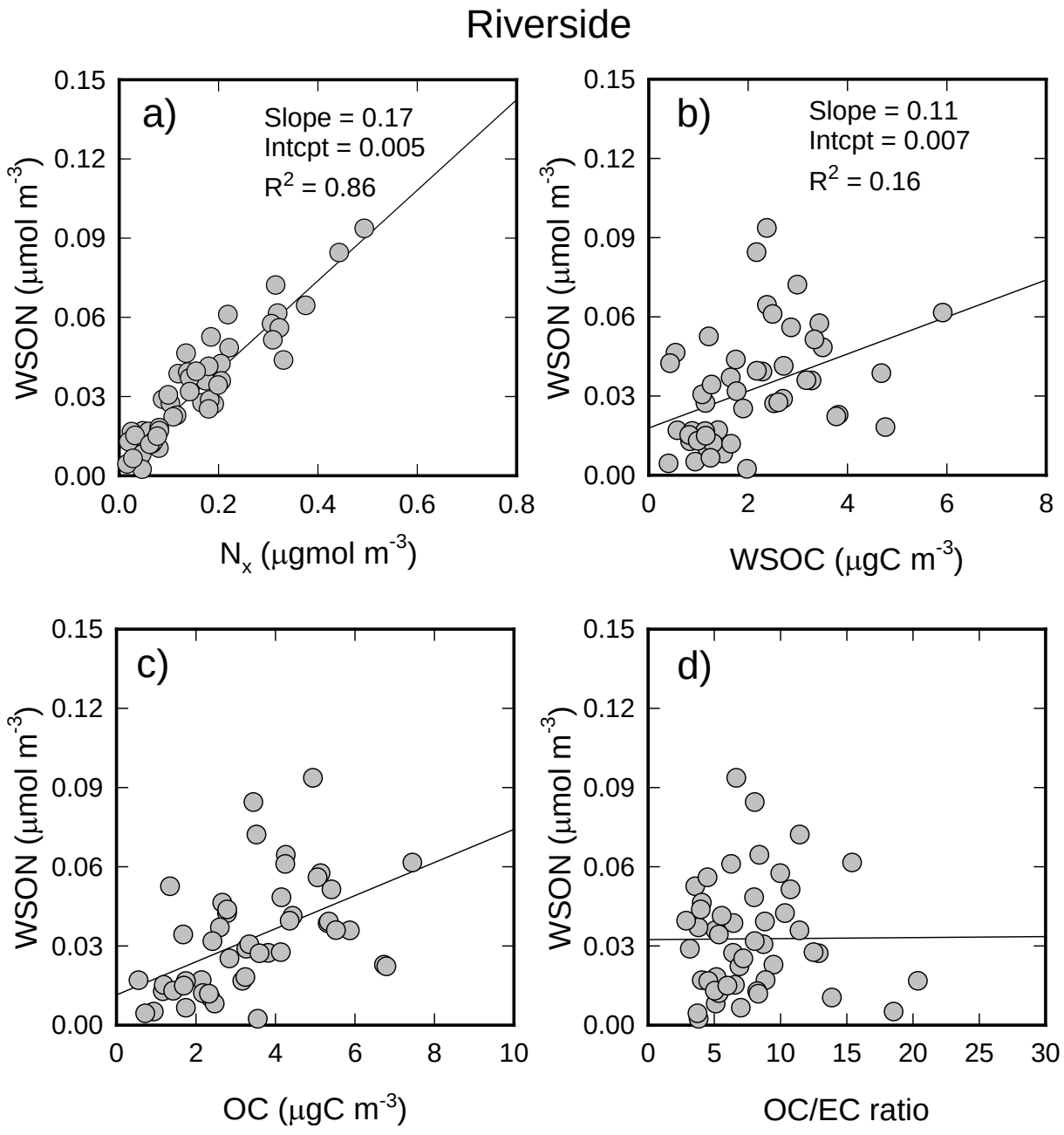

Figure 43– Relationship of PM2.5 WSON and PM2.5 N, WSOC, OC, and EC in Riverside

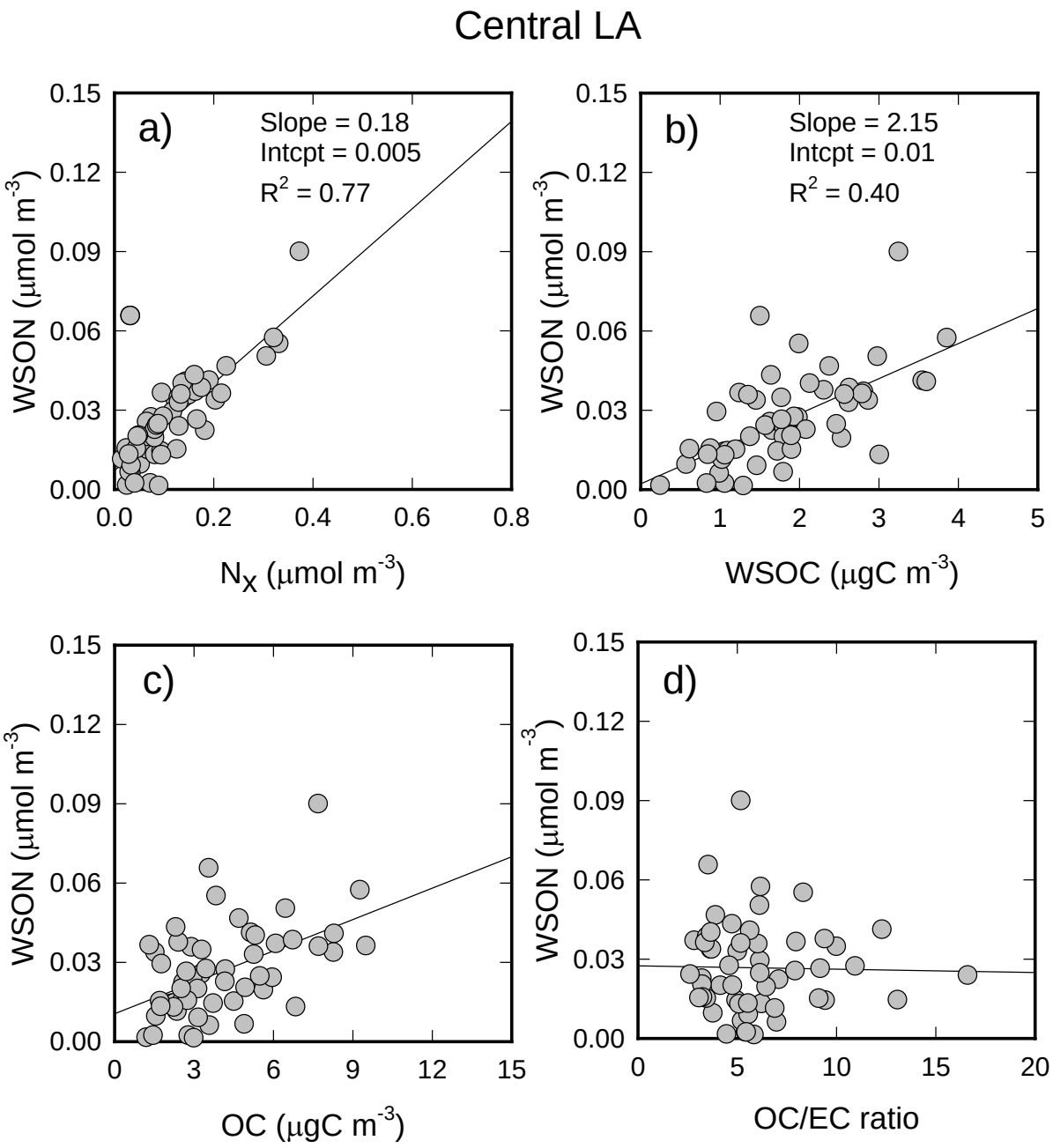

Figure 44– Relationship of PM2.5 WSON and PM2.5 N, WSON, OC, and EC in Central LA

Table 9.Speciation of water-soluble nitrogen contained in PM2.5 - Riverside and Central LA, CA based on 24-hour filter-based measurements. Numbers in parenthesis represent the percent of total water soluble nitrogen (TN) represented by the species

Site	Species	Arithmetic Mean (μmol m^{-3})	Max (μmol m^{-3})	Min (μmol m^{-3})
Riverside	TN	0.198	0.588	0.022
	Nx	0.154 (78.3)	0.495 (95.9)	0.017 (15.1)
	WSON	0.045 (21.7)	0.344 (84.9)	0.029 (4.1)
Central LA	TN	0.145	0.464	0.027
	Nx	0.118 (80.5)	0.374 (98.8)	0.016 (33.5)
	WSON	0.026 (19.5)	0.090 (66.5)	0.001 (1.2)

Table 10.Pearson correlations between observed WSON and NX, WSOC, and PMF source factors determined for Riverside CA. Bold values represent statistically significant correlations (value: Correlation Coefficients (p-value))

	All study period	Spring 2009	Summer 2009	Fall 2009	Winter 2009	Spring 2010
Number of Samples	46	7	14	12	9	4
Nx	**0.93 (<0.001)**	**0.94 (<0.001)**	**0.91 (<0.001)**	**0.97 (<0.001)**	**0.97 (<0.001)**	0.96 (0.010)
WSOC	**0.41 (0.004)**	**0.27 (0.500)**	0.48 (0.800)	**0.75 (0.003)**	**0.81 (0.004)**	**0.91 (0.020)**
Mobile	**-0.42 (0.005)**	-0.37 (0.400)	-0.41 (0.100)	-0.44 (0.200)	0.39 (0.300)	-0.36 (0.600)
Wood Smoke	0.08 (0.600)	0.74 (0.060)	-0.38 (0.200)	0.30 (0.300)	-0.19 (0.600)	-0.60 (0.400)
Primary Biogenic	0.23 (0.100)	0.48 (0.300)	0.23 (0.400)	0.36 (0.200)	**0.80 (0.009)**	-0.27 (0.700)
SOC 1	**0.50 (<0.001)**	0.74 (0.600)	**0.72 (0.003)**	0.30 (0.300)	**0.88 (0.020)***	0.91 (0.090)
SOC 2	-0.14 (0.400)	-0.19 (0.700)	**-0.59 (0.030)**	0.10 (0.700)	**0.82 (0.040)***	-0.11 (0.900)

*Excludes extreme WSON events

Table 11. Pearson correlations between observed WSON and NX, WSOC, and PMF source factors determined for Central LA CA. Bold values represent statistically significant correlations (value: Correlation Coefficients (p-value))

	All study period	Spring 2009	Summer 2009	Fall 2009	Winter 2009	Spring 2010
Number of Samples	54	9	15	12	14	4
Nx	**0.78 (<0.001)**	**0.70 (0.030)**	**0.81 (<0.001)**	**0.90 (<0.001)**	**0.94 (<0.001)**	-0.13 (0.800)
WSOC	**0.66 (<0.001)**	**0.75 (0.020)**	**0.55 (0.030)**	**0.82 (0.001)**	**0.76 (0.002)**	0.57 (0.400)
Mobile	0.29 (0.030)	-0.08 (0.800)	-0.24 (0.400)	0.07 (0.800)	0.43 (0.100)	**0.99 (0.010)**
Wood Smoke	0.14 (0.300)	0.01 (1.000)	-0.24 (0.400)	0.27 (0.400)	-0.14 (0.600)	0.91 (0.900)
Primary Biogenic	**0.35 (0.010)**	-0.03 (1.000)	0.25 (0.400)	0.37 (0.200)	**0.67 (0.009)**	**1.00 (0.004)**
SOC 1	**0.39 (0.030)**	0.16 (0.700)	**0.87 (<0.001)**	0.56 (0.060)	**0.76 (0.002)**	0.06 (0.900)
SOC 2	-0.02 (0.900)	-0.59 (0.100)	**-0.72 (0.003)**	0.14 (0.700)	0.06 (0.800)	**0.99 (0.010)**

4. Summary and Conclusions

This study advances the scientific tools used to understand the sources of organic aerosols and applies these tools to understand the trends in sources of organic aerosol in Southern California. The results have important implications to air quality management in four key areas: 1) source allocation of organic aerosols, 2) reducing concentrations of organic aerosols during high particulate matter days in Southern California, 3) reducing the annual average organic aerosol concentrations in Southern California, and 4) the design of atmospheric chemistry and health effects studies that seek to understand the sources and impacts of SOC. These results should be used to design better monitoring efforts to understand the sources of organic aerosols that lead to unacceptable short term and long term human exposures to organic aerosols such that better control strategies can be developed to protect public health and for accountability of air quality management interventions.

The study shows that the apportionment of mobile source emissions and biomass burning with molecular marker chemical mass balance models are accurate and should be used more routinely to study the sources of organic aerosols during short-term and long-term conditions of unacceptable air quality. The molecular marker based CMB models, however, do not accurately quantify SOC. Therefore, alternative methods such as non-biomass burning water soluble organic carbon (WSOC)or molecular marker PMF models should be used to determine SOC concentrations. Although some studies in the past suggested the ability to accurately distinguish gasoline and diesel vehicle emissions and other subsets of mobile source tailpipe emissions with organic tracers, the current study further demonstrates that the apportionment of mobile source subcategories is highly uncertain. Finally, the study clearly demonstrates that forest fire emissions are chemically very different from wood burning and the source profiles from wood burning should not be used to represent forest fires when assessing the impact of forest fire on particulate matter emissions.

Southern California experiences a number of days with very high organic carbon concentrations that result from local biomass burning, forest fires, and secondary organic aerosols. During the one year sampling program, thirteen days had OC concentrations greater than 8.0 µg per cubic meter of OC, which is approximately14-15 µg per cubic meter of organic compound mass. Of these 13 days, five were the very high wood smoke days, three had high wood smoke concentrations, three were impacted by forest fires, and only two of these days were not impacted by forest fires or high wood smoke events. Although forest fires can be considered outside the scope of local air quality regulation, the extreme events due to local wood smoke needs to be better tracked and mitigated in Southern California.

On an annual average, the CMB and PMF models show good agreement for the contribution of mobile sources and biomass smoke to PM2.5 OC of 30% and 10%, respectively. However, the remaining 60% of the OC from the CMB model, which has historically been assumed to be

dominated by SOC, was much larger than the SOC estimated from the PMF model. PMF estimated the remaining OC to be approximately40% SOC and 20% primary biogenic material from sources that include forest fires and is believed to include food cooking emissions. The SOC estimates from the PMF model were in good agreement with non-biomass burning WSOC, which has been shown in the past as a robust estimate of SOC. SOC concentrations have a seasonal trend that reach a maximum in late spring and early summer of about 60%, and a minimum in December of around 20%. It is important to note that the primary biogenic source, which peaks in days with large forest fires, is very different from the biomass burning source. In addition, the CMB model was able to quantify vegetative detritus, which was only a very small component of the primary biogenic source.

The study demonstrates that the relative composition and sources of SOC varies with season and the short intensive studies that seek to study the chemistry of SOC formation are unlikely to be representative of all periods when SOC is important to OC concentrations in Southern California. Future studies that seek to characterize the chemistry, precursors, and impacts of SOC in Southern California need to examine seasonal differences in SOC to assure future control strategies to mitigate SOC and organic aerosol concentrations are effective at all times of the year.

5. Recommendations

1) The measurement of molecular markers in Southern California and other regions in California that do not comply with fine particle regulations should be conducted as part of routine monitoring programs to better quantify the impacts of wood smoke and mobile sources during extreme events and to characterize the year to year trends as a means of accountability.

2) Effort should be directed at mitigating extreme wood smoke events in winter periods that lead to very high exposures to organic aerosols.

3) Given the emerging evidence concerning the health effect of carbonaceous aerosols, more emphasis should be directed at reducing the sources of organic aerosols in the context of reducing fine particulate matter concentrations and protecting human health.

4) Future efforts to study SOC should not only focus on summer SOC as SOC is an important contributor in spring and fall and is shown to have different composition and sources across seasons.

6. References

Bae, M.-S., K. L. Demerjian, and J. J. Schwab (2006), Seasonal estimation of organic mass to organic carbon in PM2.5 at rural and urban locations in New York state, *Atmospheric Environment*, *40*(39), 7467–7479.

Bhave, P. V., G. A. Pouliot, and M. Zheng (2007), Diagnostic model evaluation for carbonaceous PM2. 5 using organic markers measured in the southeastern US, *Environmental science & technology*, *41*(5), 1577–1583.

Christensen, W. F., and J. J. Schauer (2008), Impact of species uncertainty perturbation on the solution stability of positive matrix factorization of atmospheric particulate matter data, *Environmental science & technology*, *42*(16), 6015–6021.

Christensen, W. F., J. J. Schauer, and J. W. Lingwall (2006), Iterated confirmatory factor analysis for pollution source apportionment, *Environmetrics*, *17*(6), 663–681, doi:10.1002/env.782.

Cornell, S., A. Randell, and T. Jickells (1995), Atmospheric inputs of dissolved organic nitrogen to the oceans, *Nature*, *376*(6537), 243–246.

Delfino, R. J., N. Staimer, T. Tjoa, M. Arhami, A. Polidori, D. L. Gillen, M. T. Kleinman, J. J. Schauer, and C. Sioutas (2010a), Association of biomarkers of systemic inflammation with organic components and source tracers in quasi-ultrafine particles, *Environmental health perspectives*, *118*(6), 756.

Delfino, R. J., N. Staimer, T. Tjoa, M. Arhami, A. Polidori, D. L. Gillen, S. C. George, M. M. Shafer, J. J. Schauer, and C. Sioutas (2010b), Associations of primary and secondary organic aerosols with airway and systemic inflammation in an elderly panel cohort, *Epidemiology*, *21*(6), 892.

Docherty, K. S. et al. (2008), Apportionment of primary and secondary organic aerosols in Southern California during the 2005 Study of Organic Aerosols in Riverside (SOAR-1), *Environmental science & technology*, *42*(20), 7655–7662.

Draxler, R.R. and Rolph, G.D., (2012). HYSPLIT (Hybrid Single-Particle Lagrangian Integrated Trajectory) Model access via NOAA ARL READY Website (http://ready.arl.noaa.gov/HYSPLIT.php). NOAA Air Resource Laboratory, Silver Spring, MD.

Dutton, S. J., S. Vedal, R. Piedrahita, J. B. Milford, S. L. Miller, and M. P. Hannigan (2010), Source apportionment using positive matrix factorization on daily measurements of inorganic and organic speciated PM2.5, *Atmospheric Environment*, *44*(23), 2731–2741, doi:10.1016/j.atmosenv.2010.04.038.

Henry, R. C. (2003), Multivariate receptor modeling by N-dimensional edge detection, *Chemometrics and intelligent laboratory systems*, *65*(2), 179–189.

Heo, J., P. Hopke, and S. Yi (2009), Source apportionment of PM2. 5 in Seoul, Korea, *Atmos. Chem. Phys*, *9*, 4957–4971.

Hopke, P. K. (2010), Discussion of "Sensitivity of a molecular marker based model to the number of receptor observations" by YuanXun Zhang, Rebeccca J. Sheesley, Min-Suk Bae and James J. Schauer, *Atmospheric Environment*, *44*(8), 1138–1138.

Jaeckels, J. M., M. S. Bae, and J. J. Schauer (2007), Positive matrix factorization (PMF) analysis of molecular marker measurements to quantify the sources of organic aerosols, *Environmental science & technology*, *41*(16), 5763–5769.

Janssen, N. et al. (2011), Black carbon as an Additional Indicator of the Adverse Health Effects of Airborne Particles Compared to PM10 and PM2. 5., *Environmental health perspectives*.

Jassby, A. D., J. E. Reuter, R. P. Axler, C. R. Goldman, and S. H. Hackley (1994), Atmospheric deposition of nitrogen and phosphorus in the annual nutrient load of Lake Tahoe (California-Nevada), *Water Resources Research*, *30*(7), 2207–2216.

Kim, E., P. K. Hopke, D. M. Kenski, and M. Koerber (2005), Sources of fine particles in a rural midwestern US area, *Environmental science & technology*, *39*(13), 4953–4960.

Kim, E., K. Turkiewicz, S. A. Zulawnick, and K. L. Magliano (2010), Sources of fine particles in the South Coast area, California, *Atmospheric Environment*, *44*(26), 3095–3100.

Kleindienst, T. E., M. Jaoui, M. Lewandowski, J. H. Offenberg, C. W. Lewis, P. V. Bhave, and E. O. Edney (2007), Estimates of the contributions of biogenic and anthropogenic hydrocarbons to secondary organic aerosol at a southeastern US location, *Atmospheric Environment*, *41*(37), 8288–8300.

Knap, A., T. Jickells, A. Pszenny, and J. Galloway (1986), Significance of atmospheric-derived fixed nitrogen on productivity of the Sargasso Sea,

Lee, J. H., and P. K. Hopke (2006), Apportioning sources of PM2. 5 in St. Louis, MO using speciation trends network data, *Atmospheric Environment*, *40*, 360–377.

Lingwall, J. W., W. F. Christensen, and C. S. Reese (2008), Dirichlet based Bayesian multivariate receptor modeling, *Environmetrics*, *19*(6), 618–629, doi:10.1002/env.902.

Lough, G. C., and J. J. Schauer (2007), Sensitivity of source apportionment of urban particulate matter to uncertainty in motor vehicle emissions profiles, *Journal of the Air & Waste Management Association*, *57*(10), 1200–1213.

Lough, G. C., C. G. Christensen, J. J. Schauer, J. Tortorelli, E. Mani, D. R. Lawson, N. N. Clark, and P. A. Gabele (2007), Development of molecular marker source profiles for emissions from on-road gasoline and diesel vehicle fleets, *Journal of the Air & Waste Management Association*, *57*(10), 1190–1199.

Miller, S. L., M. J. Anderson, E. P. Daly, and J. B. Milford (2002), Source apportionment of exposures to volatile organic compounds. I. Evaluation of receptor models using simulated exposure data, *Atmospheric Environment*, *36*(22), 3629–3641.

Moussaoui, S., D. Brie, O. Caspary, and et al (2004), A Bayesian Method For Positive Source Separation, in *IN PROCEEDINGS OF IEEE INTERNATIONAL CONFERENCE ON ACOUSTICS, SPEECH, AND SIGNAL PROCESSING (ICASSP'2004*, pp. 485–488.

Paatero, P., and P. K. Hopke (2003), Discarding or downweighting high-noise variables in factor analytic models, *Analytica Chimica Acta*, *490*(1-2), 277–289.

Paatero, P., and P. K. Hopke (2009), Rotational tools for factor analytic models, *Journal of Chemometrics*, *23*(2), 91–100.

Paatero, P., and U. Tapper (1994), Positive matrix factorization: A non-negative factor model with optimal utilization of error estimates of data values, *Environmetrics*, *5*(2), 111–126.

Paatero, P., P. K. Hopke, X. H. Song, and Z. Ramadan (2002), Understanding and controlling rotations in factor analytic models, *Chemometrics and intelligent laboratory systems*, *60*(1-2), 253–264.

Polissar, A. V., P. K. Hopke, P. Paatero, W. C. Malm, and J. F. Sisler (1998), Atmospheric aerosol over Alaska 2. Elemental composition and sources, *Journal of Geophysical Research. D. Atmospheres*, *103*, 19–045.

Polissar, A. V., P. K. Hopke, and R. L. Poirot (2001), Atmospheric aerosol over Vermont: chemical composition and sources, *Environmental science & technology*, *35*(23), 4604–4621.

Robinson, A. L., R. Subramanian, N. M. Donahue, A. Bernardo-Bricke, and W. F. Rogge (2006a), Source apportionment of molecular markers and organic aerosol 1. Polycyclic aromatic hydrocarbons and methodology for data visualization, *Environmental science & technology*, *40*(24), 7803–7810.

Robinson, A. L., R. Subramanian, N. M. Donahue, A. Bernardo-Bricker, and W. F. Rogge (2006b), Source apportionment of molecular markers and organic aerosol. 2. Biomass smoke, *Environmental science & technology*, *40*(24), 7811–7819.

Robinson, A. L., R. Subramanian, N. M. Donahue, A. Bernardo-Bricker, and W. F. Rogge (2006c), Source apportionment of molecular markers and organic aerosol. 3. Food cooking emissions, *Environmental science & technology*, *40*(24), 7820–7827.

Rogge, W. F., L. M. Hildemann, M. A. Mazurek, G. R. Cass, and B. R. . Simoneit (1993a), Sources of fine organic aerosol. 4. Particulate abrasion products from leaf surfaces of urban plants, *Environmental Science & Technology*, *27*(13), 2700–2711.

Rogge, W. F., L. M. Hildemann, M. A. Mazurek, G. R. Cass, and B. R. T. Simoneit (1993b), Sources of fine organic aerosol. 5. Natural gas home appliances, *Environmental science & technology*, *27*(13), 2736–2744.

Rogge, W. F., L. M. Hildemann, M. A. Mazurek, G. R. Cass, and B. R. T. Simoneit (1998), Sources of fine organic aerosol. 9. Pine, oak, and synthetic log combustion in residential fireplaces, *Environmental Science & Technology*, *32*(1), 13–22.

Russell, K. M., J. N. Galloway, S. A. Macko, J. L. Moody, and J. R. Scudlark (1998), Sources of nitrogen in wet deposition to the Chesapeake Bay region, *Atmospheric Environment*, *32*(14-15), 2453–2465.

Rutter, A. P., D. C. Snyder, J. J. Schauer, R. J. Sheesley, M. R. Olson, and J. DeMinter (2011), Contributions of resuspended soil and road dust to organic carbon in fine particulate matter in the Midwestern US, *Atmospheric Environment*, *45*(2), 514–518, doi:10.1016/j.atmosenv.2010.10.014.

SCAQMD (2008), SCAQMD-final report, Multiple Air Toxics Exposure Study in the South Coast Air Basin: http://www.aqmd.gov/prdas/matesIII/MATESIIIFinalReportSept2008.html (Accessed 15 January 2012)

Schauer, J.J., Rogge, W.F., Hildemann, L.M., Mazurek, M.A., Cass, G.R (1996).Source apportionment of airborne particulate matter using organic compounds as tracers, *Atmospheric Environment*, 30(22),3837-3855.

Schauer, J. J., M. P. Fraser, G. R. Cass, and B. R. T. Simoneit (2002), Source reconciliation of atmospheric gas-phase and particle-phase pollutants during a severe photochemical smog episode, *Environmental science & technology*, *36*(17), 3806–3814.

Schauer, J. J. et al. (2003), ACE-Asia intercomparison of a thermal-optical method for the determination of particle-phase organic and elemental carbon, *Environmental science & technology*, *37*(5), 993–1001.

Sheesley, R. J., J. J. Schauer, E. Bean, and D. Kenski (2004), Trends in secondary organic aerosol at a remote site in Michigan's upper peninsula, *Environmental science & technology*, *38*(24), 6491–6500.

Sheesley, R. J., J. J. Schauer, M. Zheng, and B. Wang (2007), Sensitivity of molecular marker-based CMB models to biomass burning source profiles, *Atmospheric Environment*, *41*(39), 9050–9063, doi:10.1016/j.atmosenv.2007.08.011.

Shrivastava, M. K., R. Subramanian, W. F. Rogge, and A. L. Robinson (2007), Sources of organic aerosol: Positive matrix factorization of molecular marker data and comparison of results from different source apportionment models, *Atmospheric Environment*, *41*(40), 9353–9369.

Simoneit, B. R. T., J. J. Schauer, C. Nolte, D. R. Oros, V. O. Elias, M. Fraser, W. Rogge, and G. R. Cass (1999), Levoglucosan, a tracer for cellulose in biomass burning and atmospheric particles, *Atmospheric Environment*, *33*(2), 173–182.

Snyder, D. C., A. P. Rutter, R. Collins, C. Worley, and J. J. Schauer (2009), Insights into the origin of water soluble organic carbon in atmospheric fine particulate matter, *Aerosol Science and Technology*, *43*(11), 1099–1107.

Spira-Cohen, A., L. C. Chen, M. Kendall, R. Lall, and G. D. Thurston (2011), Personal exposures to traffic-related air pollution and acute respiratory health among Bronx schoolchildren with asthma, *Environmental health perspectives*, *119*(4), 559.

Stohl, A., C. Forster, A. Frank, P. Seibert, and G. Wotawa (2005), Technical note: The Lagrangian particle dispersion model FLEXPART version 6.2, *Atmos. Chem. Phys.*, *5*(9), 2461–2474, doi:10.5194/acp-5-2461-2005.

Stone, E. A., C. J. Hedman, J. Zhou, M. Mieritz, and J. J. Schauer (2010), Insights into the nature of secondary organic aerosol in Mexico City during the MILAGRO experiment 2006, *Atmospheric Environment*, *44*(3), 312–319, doi:10.1016/j.atmosenv.2009.10.036.

Subramanian, R., N. M. Donahue, A. Bernardo-Bricker, W. F. Rogge, and A. L. Robinson (2006), Contribution of motor vehicle emissions to organic carbon and fine particle mass in Pittsburgh, Pennsylvania: Effects of varying source profiles and seasonal trends in ambient marker concentrations, *Atmospheric Environment*, *40*(40), 8002–8019.

Wangersky, P. J. (1993), Dissolved organic carbon methods: a critical review, *Marine chemistry*, *41*(1-3), 61–74.

Watson, J. G., J. A. Cooper, and J. J. Huntzicker (1984), The effective variance weighting for least squares calculations applied to the mass balance receptor model, *Atmospheric Environment (1967)*, *18*(7), 1347–1355.

Wonaschütz, A., S. P. Hersey, A. Sorooshian, J. S. Craven, A. R. Metcalf, R. C. Flagan, and J. H. Seinfeld (2011), Impact of a large wildfire on water-soluble organic aerosol in a major urban area: the 2009 Station Fire in Los Angeles County, *Atmos. Chem. Phys.*, *11*(16), 8257–8270, doi:10.5194/acp-11-8257-2011.

Zhang, Y. X., R. J. Sheesley, M. S. Bae, and J. J. Schauer (2009), Sensitivity of a molecular marker based positive matrix factorization model to the number of receptor observations, *Atmospheric Environment*, *43*(32), 4951–4958.

Zhao, W., and P. K. Hopke (2006), Source investigation for ambient PM 2.5 in Indianapolis, IN, *Aerosol science and technology*, *40*(10), 898–909.